E.T.S. de Ingeniería Industrial,
Informática y de Telecomunicación

RESONANT POWER CONVERTER FOR FUEL CELLS: ANALYSIS, DESIGN AND SIMULATION

Grado en Ingeniería
en Tecnologías Industriales

Trabajo Fin de Grado

AUTOR: María Garcés Quílez

DIRECTOR: Pablo Sanchis Gúrpide

SUBDIRECTOR: Ernesto Barrios Rípodas

Pamplona, 27 / 06 / 2014

upna Universidad Pública de Navarra
Nafarroako Unibertsitate Publikoa

TABLE OF CONTENTS

INDEX OF FIGURES

INDEX OF TABLES

CHAPTER 1

INTRODUCTION

The objective of this project is to analyze a power generation system based on hydrogen, connected to the electricity grid.

The power generator system consists of four fuel cells of the model Nexa 1200 and a power inverter.

The fuel cells are available at the Renewable Energies Laboratory located in the Public University of Navarra and each of them can deliver a nominal power of 1.2 kW.

On the other hand, the mentioned inverter comprises a Boost, a resonant converter and an H-Bridge inverter. It is a photovoltaic converter provided by the enterprise Ingeteam, and it will be adapted to be connected to fuel cells.

Firstly, a theoretical study about the different possible technologies for fuel cells is carried out. For their fast response and their low operation temperature and pressure, the PEMFC has been proved as a good option for residential applications. The different phenomena that take place in the inner part of the cells are going to be analyzed. Based on their electrochemical model, the PEMFC equivalent electric circuit is studied and validated by means of its simulation using the PSIM software.

The fuel cell simulation shows the voltage, power and efficiency of the cells for different delivered currents. Moreover, special attention is paid to the factors that affect the fuel cell efficiency, being the operation temperature fundamental.

Afterwards, the different connection configurations for fuel cells are explained. In the actual system available at the university, each fuel cell gives approximately 20 V at full load. Since the system will be connected to the electric grid, it is important to find a connection configuration capable to increase the given voltage of the system. For that the Series

Connection is the most adequate. The principal advantage of this configuration is its simplicity and low price. However, it needs an extra protection for when one of the connected cells suffers a fault, because otherwise the whole system would be invalidated.

The proposed protection consists on connecting a diode in parallel to each fuel cell, and so when there is a fault and a cell operates deficiently, a switch disconnects the cell and enables the flow of current through the diode.

The next part of this document consists on doing a study from empirical data taken in the laboratory. Based on this data, an analysis similar to the one developed via the simulation is carried out. Furthermore, the fuel cell consumption is taken into consideration.

Provided that the real system comprises four fuel cells, the efficiency of the system will be evaluated as a function of the number of operative fuel cells at any time.

The following step will be orientated to describe the power conversion stage. First of all, a Boost converter is connected to the fuel cells. The aim of this first power converter is to increase the output voltage of the fuel cells. Afterwards, a resonant DC/DC converter is added. This kind of converter is chosen because the transistors can be switched when the current is zero due to the resonance created, minimizing the commutation losses. Furthermore, this intermediate structure includes a high frequency transformer to isolate electrically the system and increase the output voltage from the Boost. Finally, since the power is injected to the grid, the voltage and current waves must be adapted to the grid's characteristics. For this purpose, an H-Bridge inverter is added to the system.

Finally, the parameters of the conversion stage are analyzed and calculated before being simulated in PSIM. With this simulation, the correct operation of the system is checked and it can be seen that the power delivered to the grid fulfills the required properties.

The final aim of this project is finding the optimal operation point for the system. For that, a power control loop has been implemented. The operation of this control is based on determining the optimal number of fuel cells connected at any time in order to work with the highest efficiency possible.

CHAPTER 2

FUEL CELLS FOUNDATIONS AND ELECTROCHEMICAL MODELING

2.1. INTRODUCTION

A fuel cell is a device that transforms chemical energy into electric power, heat and water. This chemical energy is obtained from the reaction for the recombination of hydrogen (fuel) and oxygen (oxidizing agent) to water with the aid of a catalyst.

They can be used as electric power sources for portable electric appliances, as well as for power plants in the automotive industry, or even as small cogeneration units producing low-potential heat [1]. They are also used in stationary applications, especially within the system for decentralized production of electric power or heat.

Fuel cells can be also used for energy storage for renewable resources and u hard-to-predict production of electric power.

The most common way of classifying FC technologies is according to the electrolyte's type, therefore distinguishing among:

- PEMFC: Proton Exchange Membrane
- DMFC: Direct Methanol
- AFC: Alkaline
- PAFC: Phosphoric Acid
- MCFC: Molten Carbonate
- SOFC: Solid oxides

The main parameters of these technologies are stored in Table 2.1.

Type	Operating tempera-ture (°C)	Off-load voltage (V DC)	Power	Used fuel
AFC	65 - 220	1,1 - 1,2	to 20 kW	$H_2 + O_2$
PEMFC	50 - 120	1,1	kW	H_2/methanol + O_2/air
DMFC	130	1,1	to 10 kW	Methanol/ethanol + O_2/air
PAFC	150 - 210	1,1	hundreds kW	H_2/hydrogenous gas + air
MCFC	600 - 700	0,7 - 1,0	MW	H_2/hydrogenous gas/CO + air
SOFC	650 - 1000	0,8 - 1,0	to 10 MW	H_2 /hydrogenous gas/CO + air

Table 2.1. *Main parameters of Fuel Cells [1]*

It has been found that for low power applications the PEM technology is a good solution [2], especially for its low operation temperature that enables a shorter connection time than the rest of the technologies. This is why they can be used for applications where there are fast load variations, such us vehicles, distributed generation and stand-alone systems.

The low pressure at which they can work allows safety conditions and high efficiency. Furthermore, their low power enables a lot of modularity.

Another advantage of this technology is the use of a dry solid electrolyte, which reduces corrosion and improves the live span of cells. It is also characterized for having low emission.

It is predictable that for their good characteristics, a potential cost reduction will be achieved due to a scale economy.

As shown in Figure 2.1, the fuel cell must be supplied simultaneously by hydrogen on the anode side and oxygen on the cathode side. Between them there is a proton exchange membrane covered at each side with a catalyst.

When the oxygen reaches the catalyst in the cathode side, it is separated into ions.

On the other hand, when the hydrogen reaches the catalyst in the anode side, it is separated into protons and electrons. The protons will go through the membrane to the

catalyst in the cathode side, while the electrons will create an electric current through an external electric circuit.

At the cathode's catalyst the hydrogen protons will react with the oxygen ions to form water.

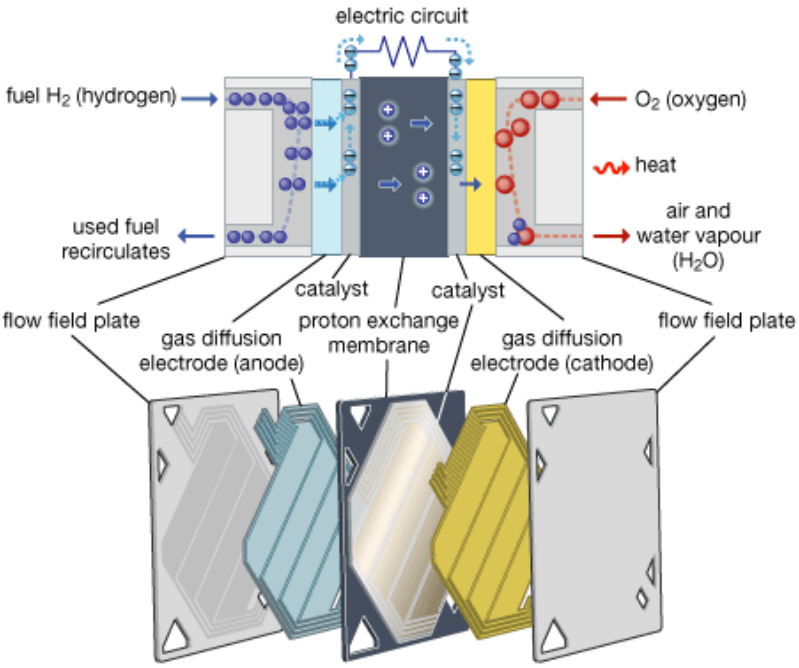

Figure 2.1. *Diagram of a PEM Fuel Cell [3]*

Therefore, the chemical reactions that take place in a PEMFC are:

- Anode: $2\,H_2 \rightarrow 4H^+ + 4e^-$
- Cathode: $O_2 + 4e^- + 4H^+ \rightarrow 2H_2O$
- Overall reaction: $2H_2 + O_2 \rightarrow 2H_2O$

2.2. ELECTROCHEMICAL MODEL

2.2.1. POLARIZATION CURVE

For a temperature of 25 °C and a pressure of 101,325 kPa, the voltage generated in a fuel cell can be obtained [4]:

$$\varepsilon_{cell} = -\frac{\Delta G°}{n \cdot F} = \frac{-229kJ}{mol_{water}} \cdot \frac{1000J}{kJ} \cdot \frac{mol_{water}}{2 \cdot mol\ e^-} \cdot \frac{mol\ e^-}{96500C} = 1.187\ V \qquad (2.1)$$

Where ε_{cell} is the voltage in every cell, related to the Gibbs free energy.

n refers to the number of electrons involved in the reaction.

$mol\ e^-$= 6,023·10^{23} electrons; 2 $mol\ e^-$ for every newly formed mol_{water} .

F is the Faraday´s constant, whose value is 96500 C / $mol\ e^-$.

In the ideal situation, the electric output of a fuel cell would achieve the theoretical voltage of 1,187 V under any operating current. Actually, the fuel cells achieve their highest output voltage during off-load periods. However, as the current increase, the cell voltage will decrease, as shown in Figure 2.2.This effect is called polarization, and it is caused by chemical and physical agents that limit the process of reaction with the flow of current through the cell, provoking energy losses.

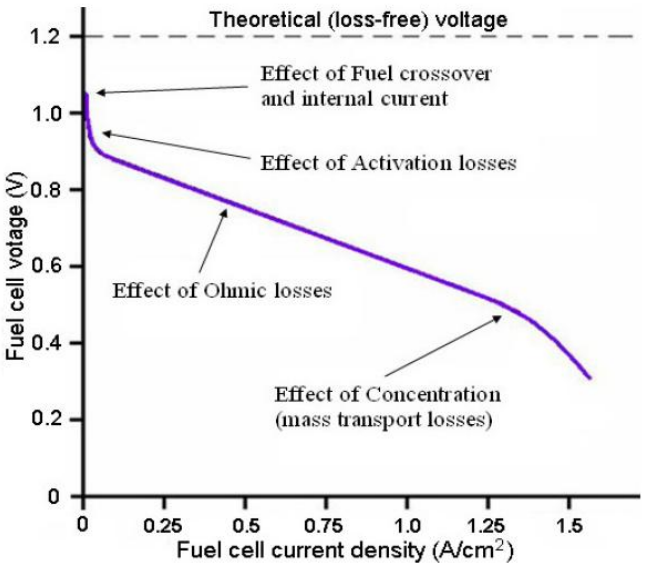

Figure 2.2. Polarization curve of a PEM fuel cell [1]

There are three basic fields of action affecting the overall polarization:

i. Activation Losses
ii. Ohmic Losses
iii. Concentration Losses

The polarization curve depends on the operating temperature, pressure and humidity of particular components of the fuel cell. The changes on these parameters can cause a rise or decline of the V-I Characteristic, and the efficiency of the fuel cell can respectively increase or decrease.

2.2.2. ELECTRIC MODEL

In the following lines the phenomena taking place during the operation of the fuel cell are described from the point of view of the electrochemistry [5]. These phenomena are responsible of the formation of the polarization curve presented in Figure 2.2.

2.2.2.1. Thermodynamic phenomena

When the hydrogen and oxygen react to produce water, a reversible voltage is generated in every fuel cell:

$$V_{rev} = 1.229 - 8.45 \cdot 10^{-4}\big((T + 273.15) - 298.15\big) + 4.31 \cdot 10^{-5}(T + 273.15)ln\big(p_{H2}\sqrt{p_{O2}}\big) \quad (2.2.)$$

Where:

T is the operation temperature of the cell, in Celsius

p_{H2} is the hydrogen pressure in bar

$$p_{H2} = p_0 + p_1 \cdot i_{FC} \quad (2.3)$$

p_{O2} is the oxygen pressure in bar

The fuel cells are connected in series forming a stack, whose voltage will be proportional to the number of cells comprising the stack, Ns.

Therefore the total voltage generated can be expressed as:

$$V_{rev,s} = V_{rev} \cdot N_s \quad (2.4)$$

2.2.2.2. Activation phenomena

There is an energy barrier called Activation Energy that the charge must overcome to pass from the reactants to the electrodes. This energy is shown as a voltage Vact, which can be obtained experimentally with the following equation:

$$v_{act} = a + b \cdot ln(i_{act}) , \tag{2.5}$$

where:

$$a = a_0 + a_1(T + 273.25) \tag{2.6}$$

$$b = b_0 + b_1(T + 273.25) \tag{2.7}$$

Therefore, as seen in (2.6) and (2.7), Vact is dependant to the temperature.

Taking into account that all the cells comprising a stack are series connected, the same current will flow though all of them:

$$Iact, s = Iact = e^{\left(\frac{v_{act} - a}{b}\right)} \tag{2.8}$$

The total overvoltage of a stack can be expressed as:

$$v_{act\,,s} = v_{act} \cdot N_s \tag{2.9}$$

2.2.2.3. Concentration phenomena

The concentration phenomena are related to the mass transport in the fuel cell, which is due to convection and diffusion. When the fuel cell is working, it is necessary to constantly feed the electrodes with oxygen and hydrogen, as well as to remove the water generated. Consequently, these phenomena will be greater as the fuel cell current increases.

The Concentration Voltage of one cell can be obtained with the following empirical equation:

$$v_{con} = m \cdot e^{(n \cdot i_{act})}, \tag{2.10}$$

Where:

$$m = m_0 + m_1(T + 273.25) \tag{2.11}$$

For a stack comprising Ns fuel cells:

$$v_{con,s} = v_{con} \cdot N_s \tag{2.12}$$

2.2.2.4. Double-Layer phenomena

At the electrode-electrolyte interfaces of every cell, a capacitive effect called the Double-Layer Effect takes place. This effect is based on the charge transfer that occurs during the oxidation and reduction half-reactions. To model these phenomena a capacitor Cdl (double-layer capacitor) is included because it simulates the accumulation of ionic and electronic charges.

For a stack of Ns series-connected cells:

$$C_{dl,s} = \frac{C_{dl}}{Ns} \tag{2.13}$$

2.2.2.5. Ohmic phenomena

These phenomena occur because of the resistance of the fuel cell elements to the flow of ions and electrons, provoking voltage losses in the cells. The voltage drop in one cell is:

$$v_{ohm} = R_{ohm} \cdot i_s \ , \tag{2.14}$$

where:

i_s is the current through the fuel cell stack

$$R_{ohm} = R_{ohm,0} + R_{ohm,1}(T + 273.15) \tag{2.15}$$

As the total number of cells connected in series in a stack is Ns:

$$v_{ohm,s} = v_{ohm} \cdot N_s \tag{2.16}$$

2.2.2.6. Peripheral energy consumption

Some of the energy previously generated is used to power the peripherals, such us the control board and purge valve. It is modeled as a current source in parallel to the stack, and can be obtained as follows:

$$i_{per} = k_2 \cdot i_{FC}^2 + k_1 \cdot i_{FC} + k_0 \tag{2.17}$$

Finally, the fuel cell can be approximated to the electrochemical model shown in Figure 2.3. This model will represent the fuel cell electric performance, both in steady and dynamic state. It includes some elements that stand for the thermodynamic and electrochemical phenomena, as well as the consumption of the peripherals.

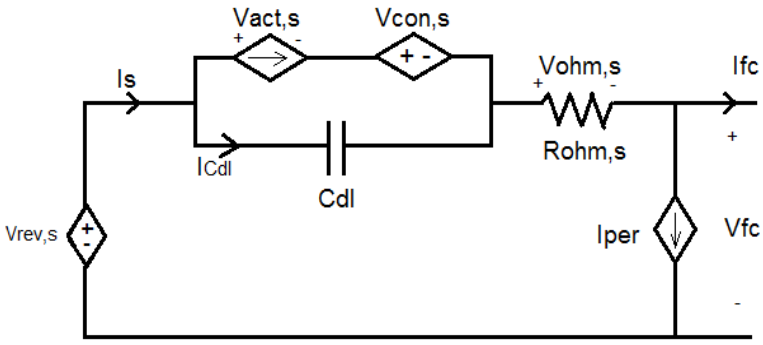

Figure 2.3. *Electrical model of the fuel cell*

2.3. REAL SYSTEM DESCRIPTION AND CHARACTERISTICS

The Renewable Energies Laboratory situated in the Public University of Navarra (UPNA) is equipped with a hydrogen system comprising four PEM fuel cells, fed with a hydrogen supply system. These fuel cells, which will be simulated in this project, correspond to the model Nexa®1200 shown in Figure 2.4.

This fuel cell model is characterized for having a DC voltage range between 20 and 36 V, a maximum current of 60 A, and a nominal power generation of 1200 W.

As the system comprises four series-connected FCs, the maximum power produced will be 4800 W.

(a) Front view *(b) Back view*

Figure 2.4. *Fuel cell Nexa®1200 [6]*

Each Nexa®1200 comprises a Ballard stack of 36 series-connected cells. Each cell comprises a membrane-electrode assembly and two flow channels. The assembly consists of two electrodes, the anode and the cathode, covered with a platinum catalyst, and separated by a polymeric membrane electrolyte.

The gases are supplied to the electrodes at each side of the membrane. The hydrogen will flow to the anode while the oxygen will flow to the cathode.

The system also includes some auxiliary systems that enable an efficient operation, namely:

- Hydrogen supply system (Figure 2.5)
- Air supply system
- External voltage source
- Relay and reverse diode
- Remote Control Software (RCS)
- Control valves and sensors

As seen in Figure 2.4 (b), a connection panel (1) as well as the hydrogen supply and voltage output (2) can be found in the backside of the device.

2.3.1. HYDROGEN SUPPLY SYSTEM

For a correct operation of the fuel cell, it is necessary to supply hydrogen with a minimum purity of 4.0 (99.99%), and pressure between 1 and 15 bar.

***Figure 2.5**. Hydrogen supply system [6]*

The FC has a pressure regulation system, which replaces the hydrogen at the same rate than it is consumed.

This system includes a purge valve that expulses periodically the inert gases (water steam and nitrogen) accumulated in the anode during the operation of the fuel cell. The frequency of the purges depends on the reaction velocity, that is, on the current delivered by the fuel cell.

2.3.2. AIR SUPPLY SYSTEM

The fuel cell is fed with air through a ventilator situated in its backside. This air provides the needed oxygen for the electrochemical reaction, cools the cell and dilutes the purged hydrogen.

The ventilator velocity is set by the control software depending on the generated current; a higher current implies an increase in the generated heat.

2.3.3. EXTERNAL VOLTAGE SOURCE

During the switching on and off of the fuel cell, an external voltage source is needed to feed the peripherals. However, during normal operation the working fuel cell is capable of feeding the auxiliary systems.

2.3.4. RELAY AND REVERSE DIODE

In order to disconnect automatically the fuel cell during faults, a relay is used.

Furthermore, a reverse diode is included in the system to protect the cells when there is an unwanted current, normally provoked by the electronic charge connected to the system.

2.3.5. REMOTE CONTROL SOFTWARE (RCS)

The fuel cell parameters are monitored and controlled by an electronic system. The controller regulates a safe operation of the system, its switching, and shows error messages. It also controls the purge valve, the ventilator velocity and the trigger signal for the relay.

2.4. ELECTRIC MODEL SIMULATION

Finally, using the electric model explained in Section 2.2, one of the fuel cells available in the laboratory has been simulated. For that, voltage and current sources has been used, as seen in Figure 2.6.

It can be noted that the output of the fuel cell consists on a current source which represents the delivered current. Trough this current, the power delivered by the device can be controlled, and so depending on the asked current it will be working for more or less load.

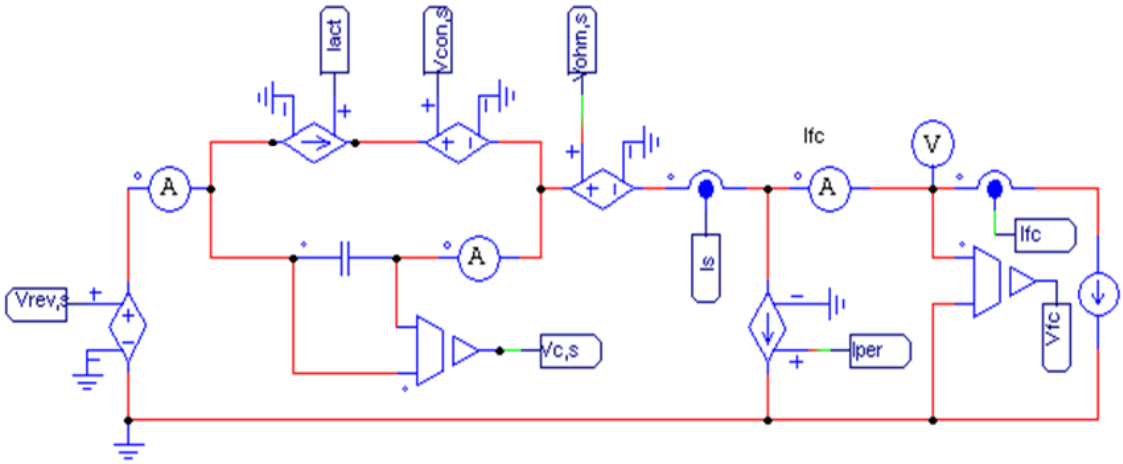

Figure 2.6. *Electric model in PSIM*

It is also necessary to introduce in PSIM the fuel cell parameters shown in the equations of the electric model, used to approximate the internal phenomena of the fuel cells. These parameters are stored in the following table:

DESCRIPTION	PARAMETER	VALUE
Peripheral consumption	K_0 (A)	1.534
	K_1	$-1.208 \cdot 10^{-3}$
	K_2 (A^{-1})	$4.118 \cdot 10^{-4}$
Thermodynamic phenomena	P_0 (bar)	1.324
	P_1 ($bar \cdot A^{-1}$)	$-1.305 \cdot 10^{-4}$
Activation phenomena	A_0 (V)	0.6259
	A_1 ($V \cdot ºC^{-1}$)	$-1.1128 \cdot 10^{-3}$
	b_0 (V)	$9.1487 \cdot 10^{-2}$
	b_1 ($V \cdot ºC^{-1}$)	$-1.4866 \cdot 10^{-4}$
Concentration phenomena	m_0 (V)	$1.8250 \cdot 10^{-2}$
	m_1 ($V \cdot ºC^{-1}$)	$-3.328 \cdot 10^{-5}$
	N (A^{-1})	$4.5 \cdot 10^{-2}$
Ohmic phenomena	$R_{ohm,0}$ (Ω)	$2.8959 \cdot 10^{-3}$
	$R_{ohm,1}$ ($Ω \cdot ºC^{-1}$)	$-4.8479 \cdot 10^{-6}$
Double layer phenomena	C_{dl}(F)	4.9183

Table 2.2. *Parameters of the electric model*

The parameters will be introduced in PSIM using voltage sources:

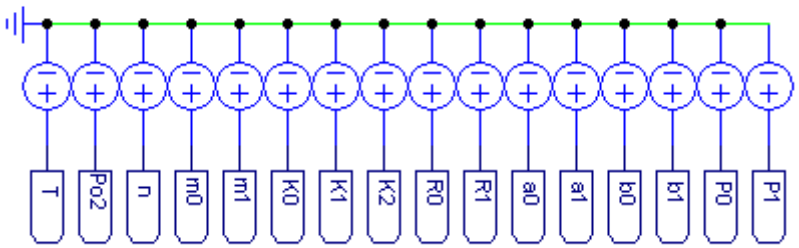

Figure 2.7. *Parameters introduced in PSIM*

Furthermore, the different phenomena occurring in the fuel cell, modeled by equations (2.2) to (2.17), are implemented in PSIM via voltage sources and operation blocks:

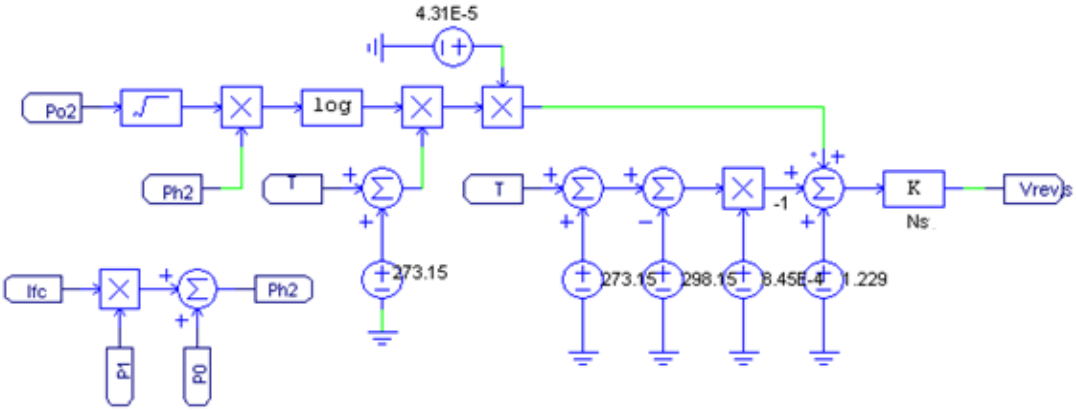

(a) Reversible Voltage

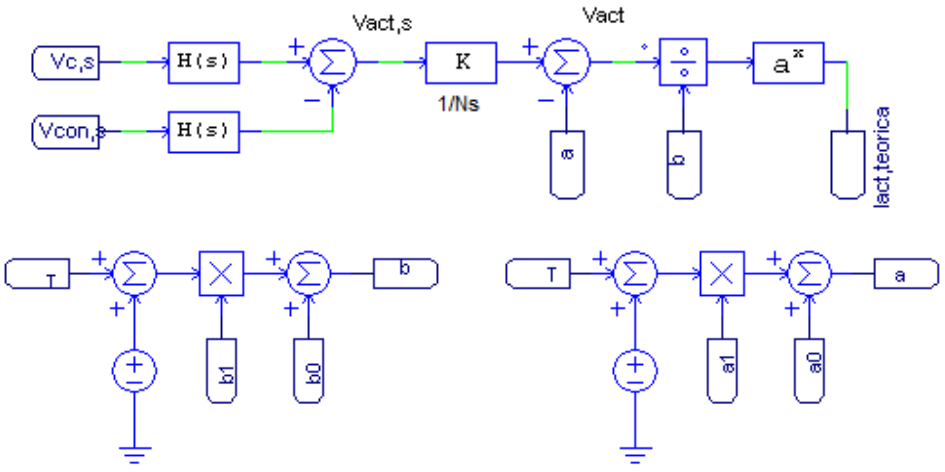

(b) Activation Current

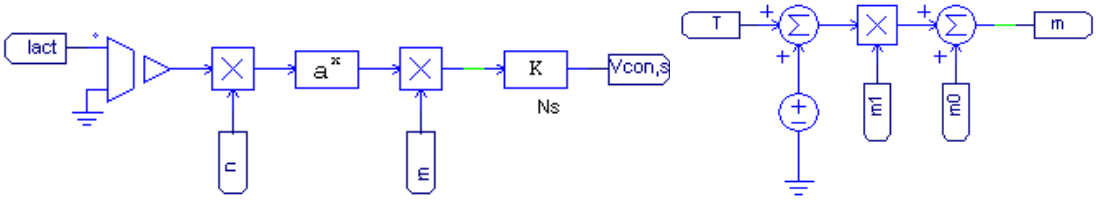

(c) Concentration Voltage

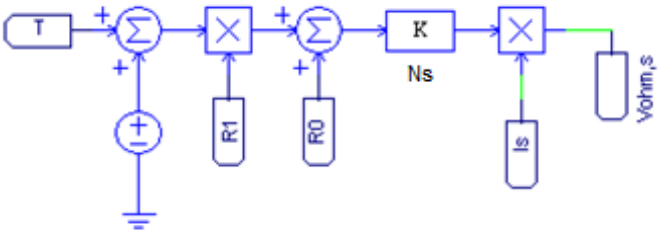

(d) Ohmic Voltage

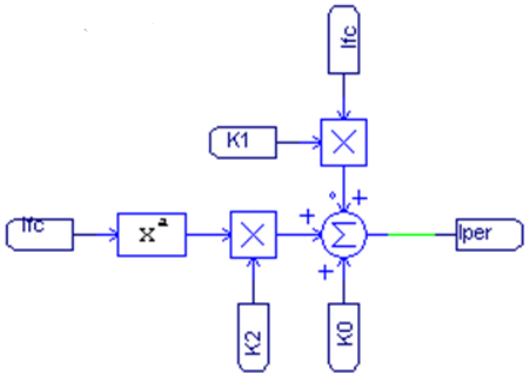

(e) Peripheral Current

***Figure 2.8**. Implementation of the phenomena of the FC in PSIM*

The value for the activation current obtained before is the theoretical one, which corresponds to the fuel cell model. Nevertheless, the value of this current must be initialized in our simulation since if not, it would be zero, and the current and voltage of the fuel cell would be zero too.

As a solution a switch has been added, shown in Figure 2.9, to change Iact from the chosen value at the beginning (30 A) to the theoretical one after 10 ms. That way, during those 10 ms, there is a voltage $V_{con,s}$ and the capacitor starts charging.

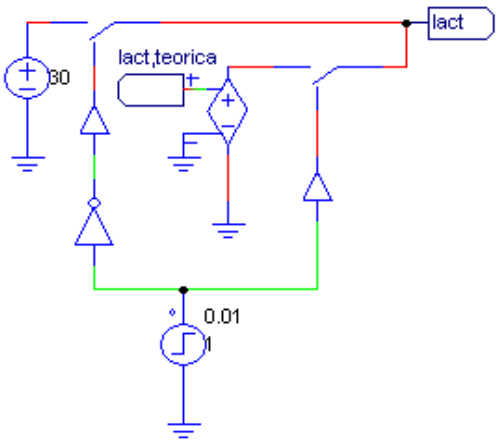

Figure 2.9. *Initialization and switching of the activation current*

After performing the electrical model in PSIM, it has been simulated for an output DC current of 60 A and a temperature of 55 ℃, since they have been considered as nominal values.

In the following figure, the values of currents and voltages, measured when the system is stable, are shown:

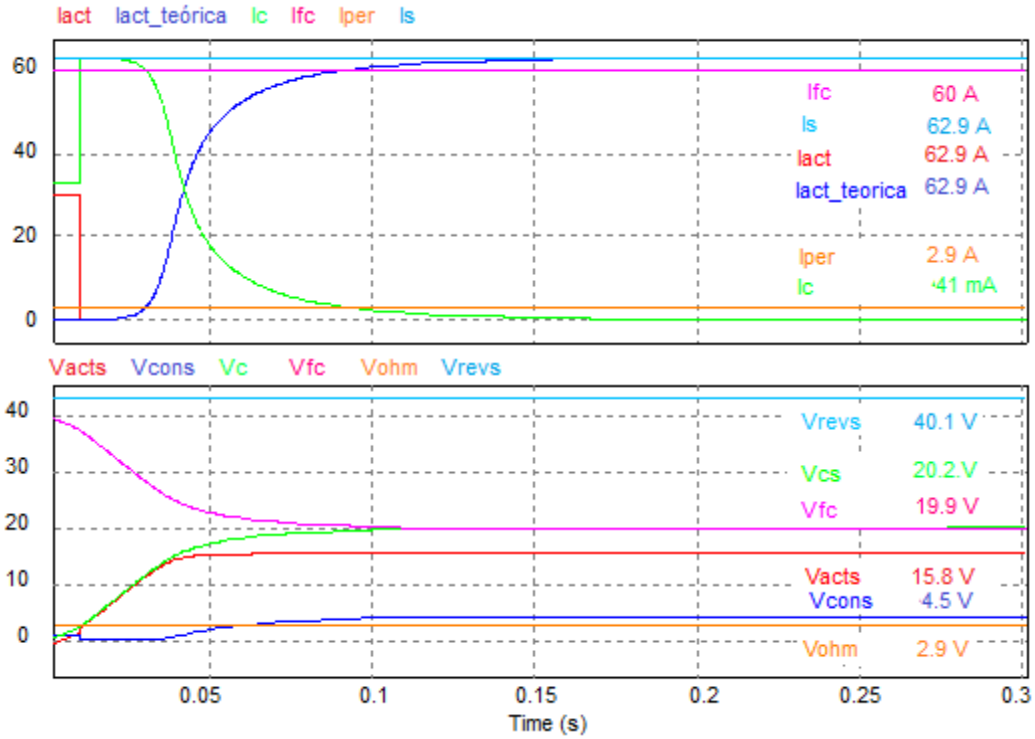

Figure 2.10. *Voltages and Currents for T= 55 ℃ and Ifc=60A*

Three different stages are distinguished:

- Before 0.01 s :

The first part of the simulation consists on the inicialization of Iact. This inicialization is justified seeing the real value of Iact, Iact_teorica, which is obtained whith equation (2.8). As seen, the value of this current remains zero, and consequently the activation voltage and the voltage in the capacitor would be zero too.

The value manually introduced for the inicialization has been chosen as 30 A. Paying attention to the voltages, $V_{act,s}$ is also initialized, and the capacitor starts to charge. This first stage can be more closely observed below:

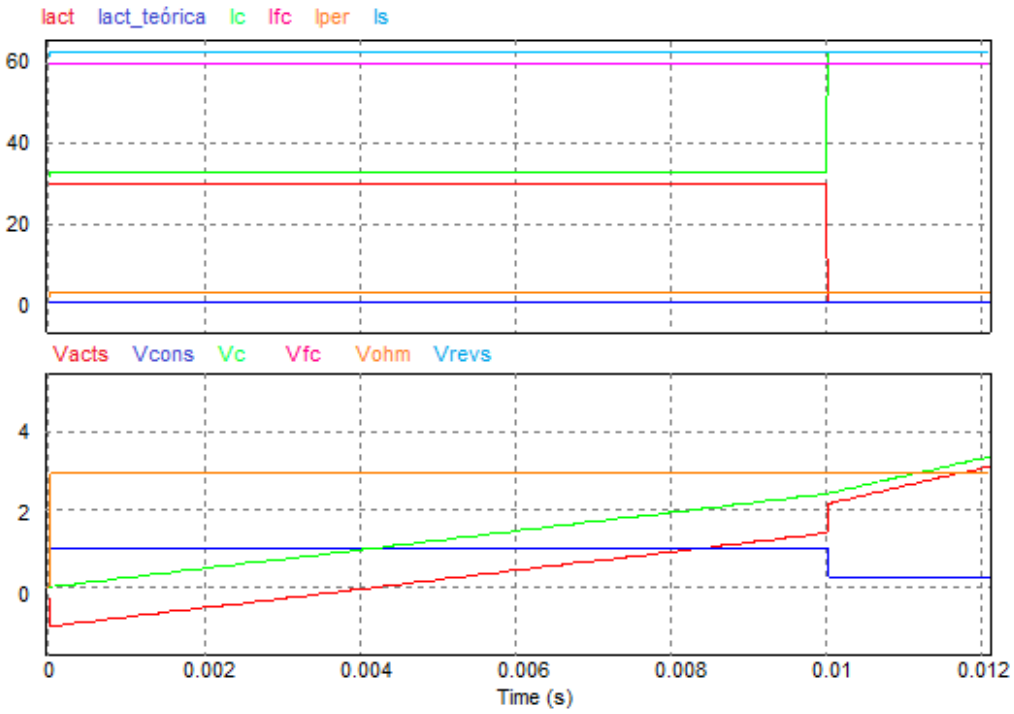

Figure 2.11. *Switching of the activation current at t=10ms*

- 0.01 s- 0.18 s :

When the real value of the activation current is switched on, the system needs some time to pass from the transient to the the steady state.

This stabilization period can vary depending on the current delivered by the cell, I_{FC}. Particularly, it will be maximized for low currents.

- After 0.18 s :

The stack has achieved the steady state, and gives constant values of voltage and current, included in Figure 2.10.

2.5. EFFICIENCY OF A FUEL CELL

The efficiency is a very important parameter to define an energy generator system, since it represents the quantity of useful energy is obtained from the net primary energy used.

Consequently, the efficiency of a fuel cell is defined as the ratio of useful output power P_{FC} to the power that is supplied to the system, P_{H_2} :

$$\eta_{FC} = \frac{P_{FC}}{P_{H_2}} = \frac{V_{FC} \cdot I_{FC}}{P_{H_2}} \tag{2.18}$$

2.5.1. SIMULATION FOR DIFFERENT CURRENTS

We are interested in obtaining the polarization curve of the system. For that, the voltage Vfc is measured for different output currents. The power given by the stack at its output, Pfc, as well as the net power generated in the electrochemical reaction, Prev,s , have been measured too. The efficiency of the system can be obtained with the ratio of the delivered power Pfc to the total power generated Prev,s. The values obtained for a Temperature of 55 ºC are stored in Table 2.3 and plotted in Figure 2.12.

IFC (A)	VFC (A)	Prev (W)	PFC (W)	Losses (W)	Efficiency (%)
0	32.71	65.5	0	65.5	0
5	30.1075	281	150.525	130.475	53.57
10	28.9	497.5	289	208.5	58.09
20	27.25	933.225	544.9	388.325	58.39
30	25.715	1372.315	771.435	600.88	56.21
40	24.16	1815	966.4	848.6	53.25
50	22.325	2261.1	1116.625	1144.475	49.38
60	19.825	2710	1189.5	1520.5	43.89

Table 2.3. *Output values of the fuel cell when T=55 ℃*

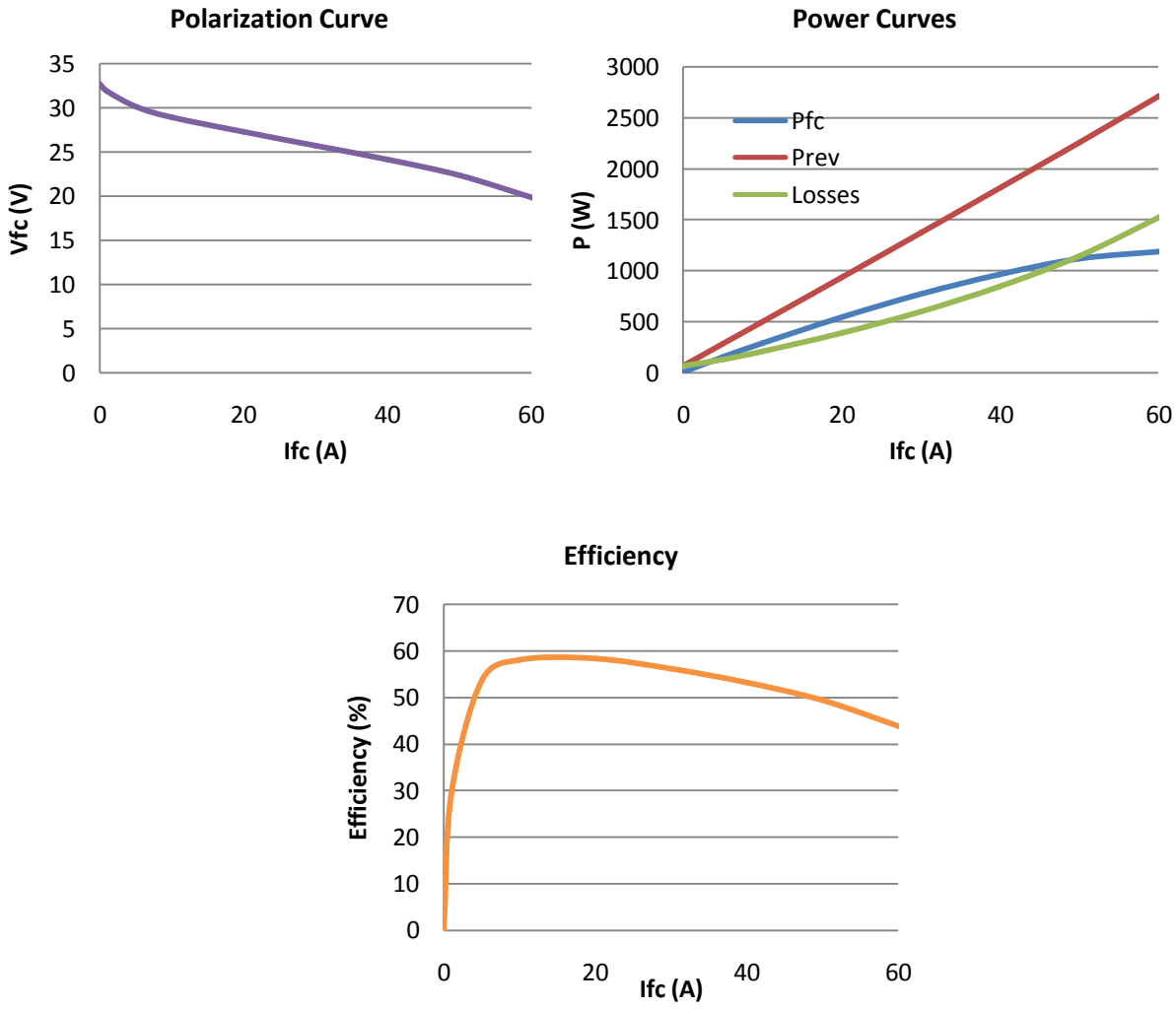

Figure 2.12. *Output values of the system when T=55 ℃*

- *The temperature effect*

An increase in the operation temperature will raise the polarization curve of a fuel cell, and therefore its efficiency [7]. The reason for that is the increase of kinetic energy of the molecules of the reacting gases, accelerating transmission of mass inside the fuel cell.

As deduced from Figure 2.13, the optimal temperature of the fuel cell is around 80 °C.

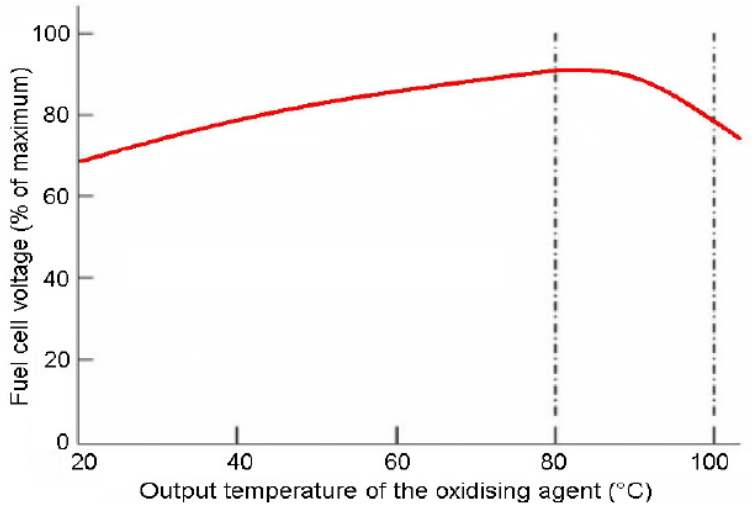

Figure 2.13. *Effect of the temperature on the Fuel Cell output voltage [7]*

In order to check this variation with the operating temperature, the fuel cell has been simulated for two different temperatures. Measuring the output values of the voltage and power it can be noted that lower temperatures decline the polarization curves and therefore the power delivered by the fuel cell stack and its efficiency is smaller.

The comparison of Voltage, Power and efficiency for 55 ℃ and 25 ℃, is shown in Figure 2.14.

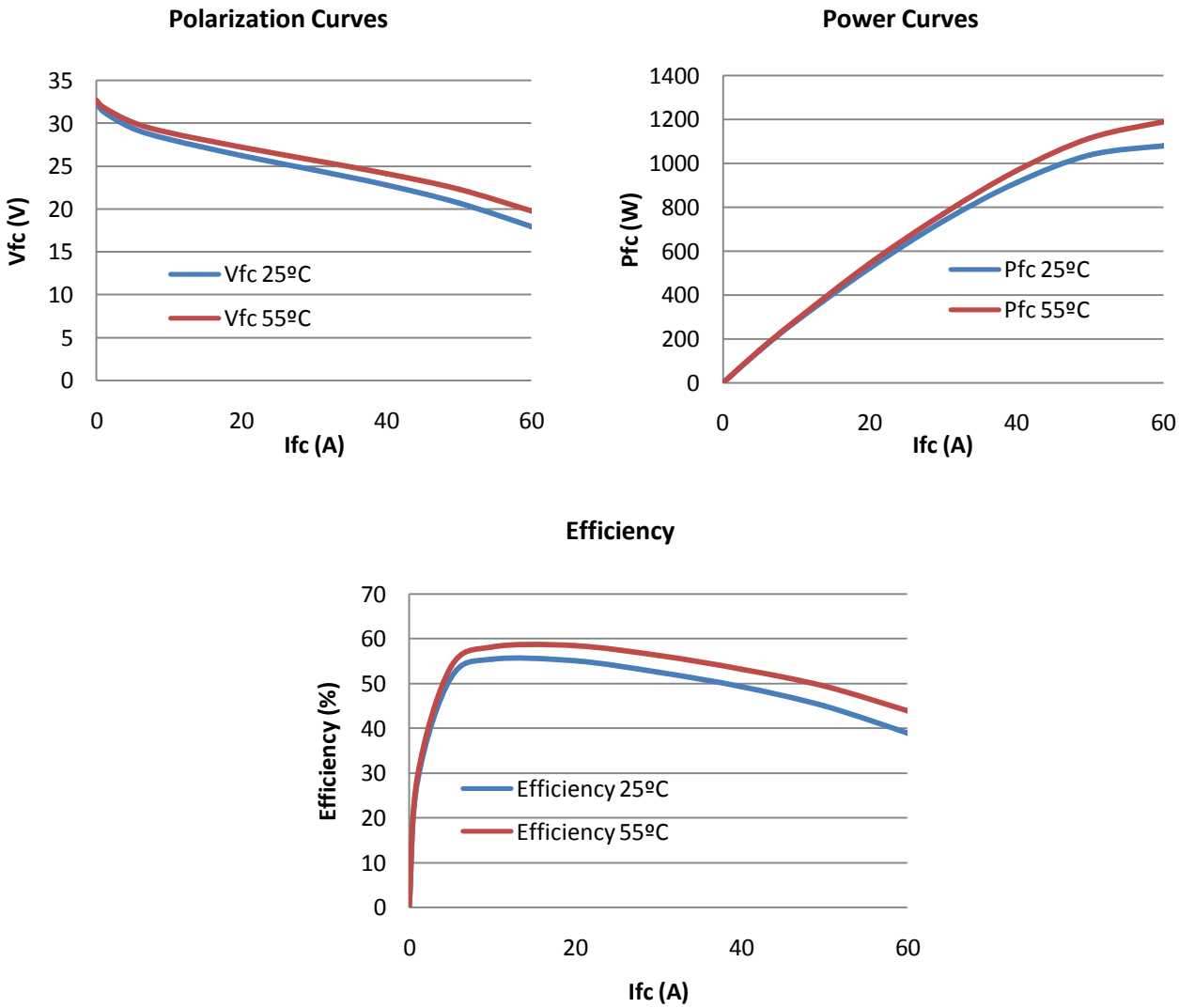

Figure 2.14. *Comparison of Vfc ,Pfc and efficiency for different temperatures*

2.5.2. STUDY OF A FC FROM EMPIRICAL DATA

In a previous project [5] accomplished in the Public University of Navarra, the fuel cells available in the laboratory were tested for five different operation temperatures. The results of this empirical experiment consist on the voltages and fuel consumption of a fuel cell for the different possible currents delivered.

The selected operation temperatures are: 31.5°C, 41°C, 52.8°C, 56.5°C and 58.7°C. Furthermore, the maximum current delivered by the fuel cell will be 60 A.

This empirically obtained data has been employed to obtain different graphs in Matlab, which will demonstrate the real behavior of a fuel cell stack, in contrast to the graphs obtained in the simulation, shown in the previous section.

- Polarization, power and efficiency curves

First of all, the fact that the fuel cell operation is affected by the temperature, as simulated in the previous section, has been checked:

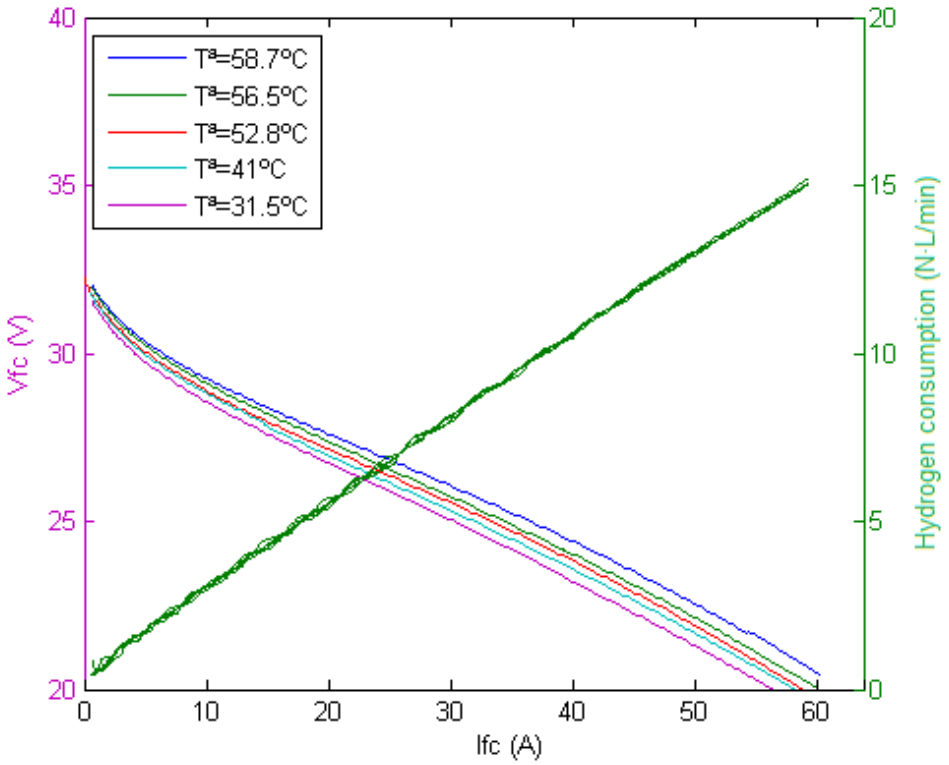

Figure 2.15. *Polarization Curve and hydrogen consumption*

For higher temperatures, the value of the output voltage for a certain current is bigger.

Having the voltages correspondent to the FC currents, the electric power Pfc delivered can be obtained.

From the fuel consumption data (NL/min), the total power available in the fuel, P_{H2}, can be obtained using its low calorific value:

$$\mathrm{LCV} = 3\ \frac{\mathrm{kWh}}{\mathrm{N}\cdot\mathrm{m}^3}$$

$$\mathrm{P_{H2}} = \mathrm{fuel}\left(\frac{\mathrm{N}\cdot\mathrm{L}}{\mathrm{min}}\right)\cdot\frac{\mathrm{m}^3}{1000\ \mathrm{L}}\frac{60\ \mathrm{min}}{\mathrm{h}}\cdot\mathrm{LCV}\left(\frac{\mathrm{kWh}}{\mathrm{N}\cdot\mathrm{m}^3}\right)\cdot 1000\quad[\mathrm{W}] \tag{2.19}$$

Once this power is obtained, the efficiency of the fuel cell can be deduced with equation (2.18). It is important to take into account that in the electric power P_{FC}, calculated from the measured voltages and currents, the peripherals power losses are already included.

It is worth noting that the hydrogen power is temperature independent, while the electric power does vary with it.

In the following figure, the efficiency of the fuel cell is plotted on the right, for the five different temperatures, while the hydrogen power is plotted on the left.

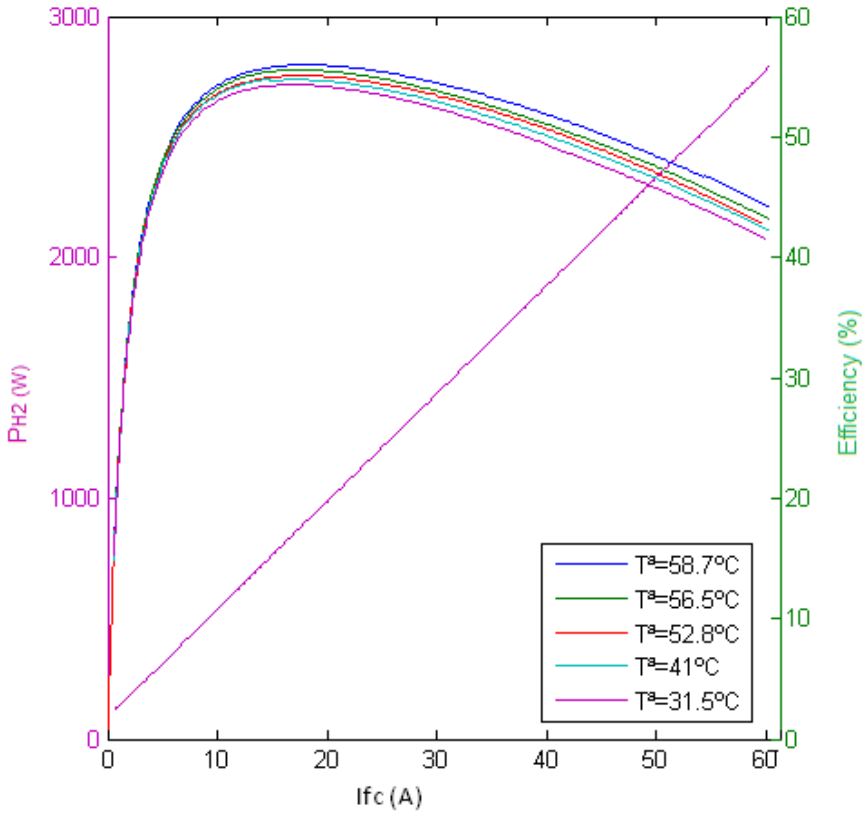

Figure 2.16. *Efficiency and hydrogen power versus fuel cell current, for different temperatures*

- ## Losses in the peripherals

In the electric model explained in Section 2.2, the losses in the peripherals were modeled as a current source parallel to the fuel cell output.

To calculate the power losses in the peripherals, it is necessary to obtain the current flowing though them using equation (2.17).

The first step consists on choosing the I_{FC} current values that are going to be evaluated and calculating their corresponding current density, knowing that the conductor area is $145cm^2$.

Introducing the current densities in the following graph, their associated operation temperatures can be obtained.

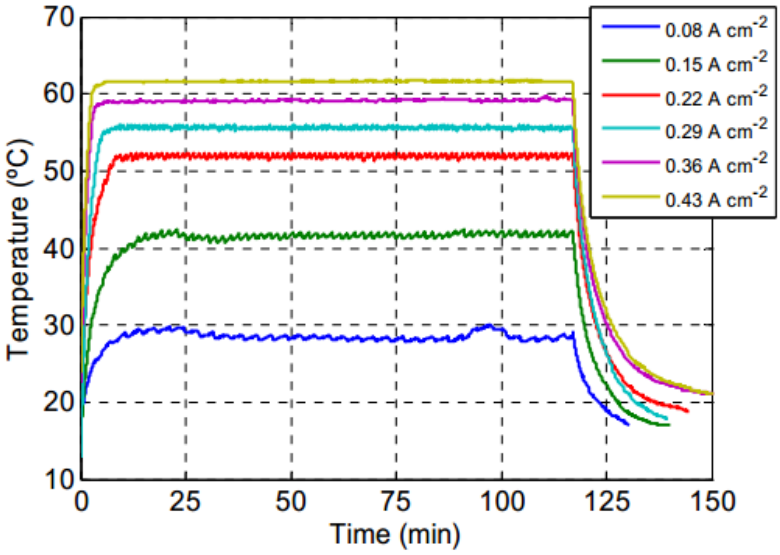

***Figure 2.17**. Operation temperature for different current densities [5]*

Once the temperature is known, the fuel cell current values are introduced in the polarization curve (Figure 2.15) and the fuel cell voltages are obtained.

I_{FC} (A)	I_{FC} density (A/cm^2)	Temperature (° C)	V_{FC} (V)
0	0	-	32
5	0.034	22	29.5
10	0.07	40	27
15	0.1	32	27.5
20	0.138	40	27
30	0.207	49	25.5
40	0.276	54	23.9
50	0.34	57	22.5
60	0.41	60	21

Table 2.4. *Parameters of current and voltage to obtain the peripherals power losses*

After this, the last step to obtain the peripherals power losses, P_{per}, consists on obtaining the peripherals current, I_{per}, and substituting it in the following equation:

$$P_{per} = V_{fc} \cdot I_{per} \tag{2.20}$$

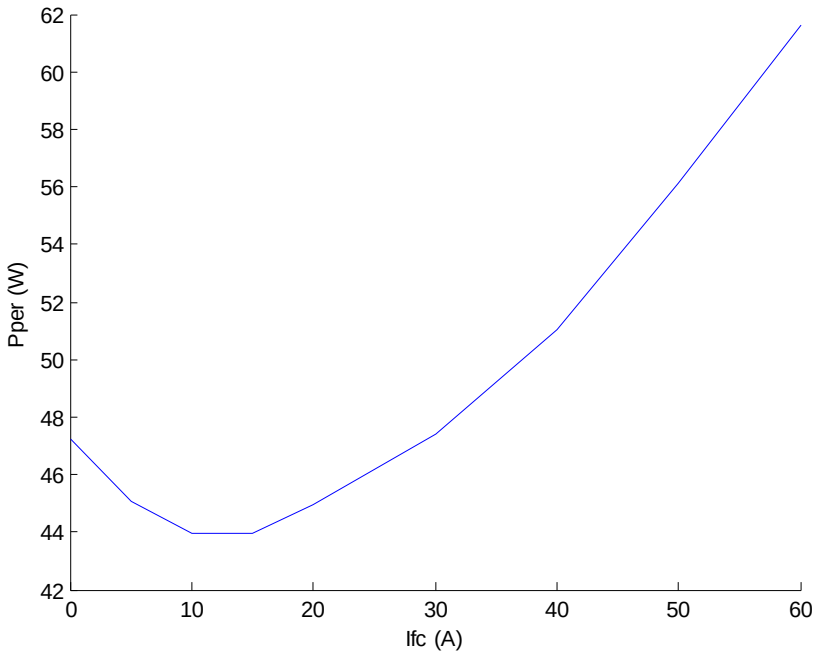

Figure 2.18. *Power losses in the peripherals vs. the delivered current*

- Power balance

First of all, the hydrogen power available is supplied to the system. However, the useful electrical power achieved is smaller, since in the fuel cell has inner power losses and the peripherals must be fed. As it has been previously studied, the power is loss inside the fuel cell due to the activation, ohmic and concentration phenomena.

To better understand the whole system, it is interesting to carry out a power balance as follows:

$$P_{losses} = P_{H2} - P_{per} - P_{FC} \tag{2.21}$$

In Figure 2.19, a diagram of the power flow of the system is shown:

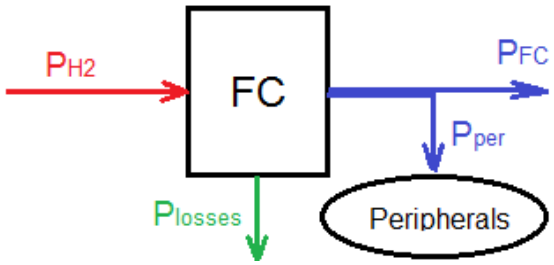

Figure 2.19. *Power balance of the system*

Applying the previous balance to a real fuel cell the following Figure 2.20 is obtained. In this figure all the powers of the cell are included, as well as the internal losses. It can be noted how the hydrogen consumption and the peripherals power is constant, while the delivered power and the internal losses are dependant to temperature. In particular, for low values of temperature the power delivered is smaller and the losses bigger.

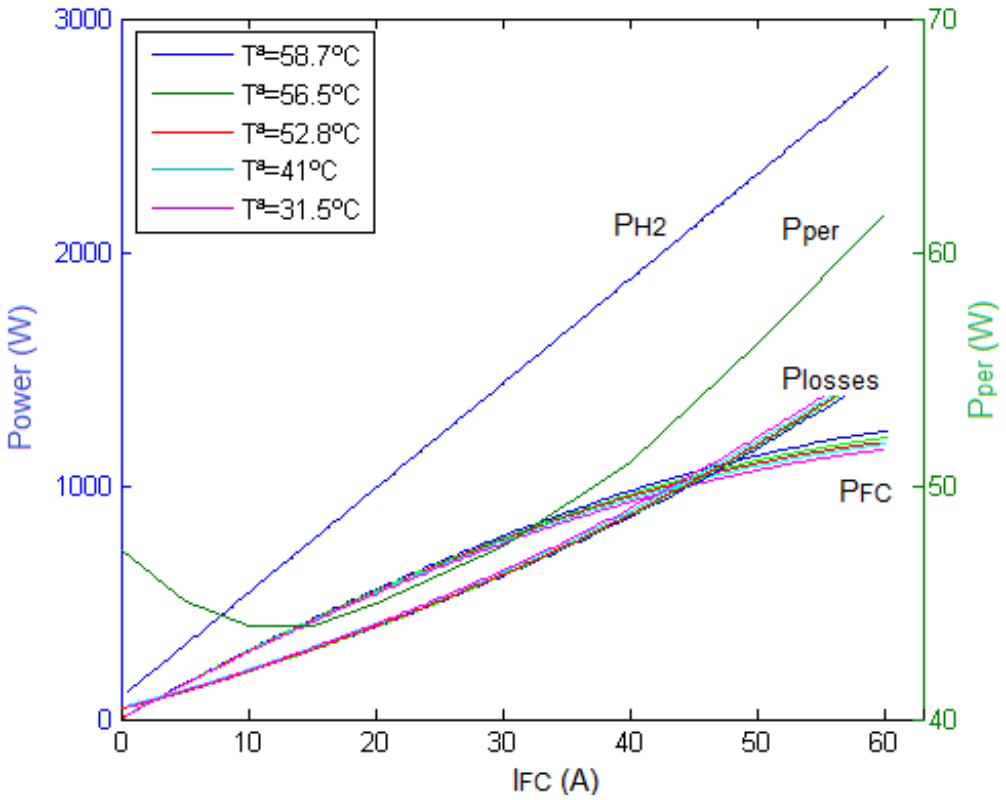

Figure 2.20. *Electric, hydrogen, peripherals and losses powers*

- Parameters as a function of the power generated

The fuel cells are controlled by the power delivered. Thus, the following step consists on drawing different parameters as a function of the power generated.

Particularly, the parameters plotted are the fuel power and the efficiency, in Figure 2.21.

It can be observed that as the generated power increases, proportionally more hydrogen must be supplied. This is caused especially for the concentration phenomena.

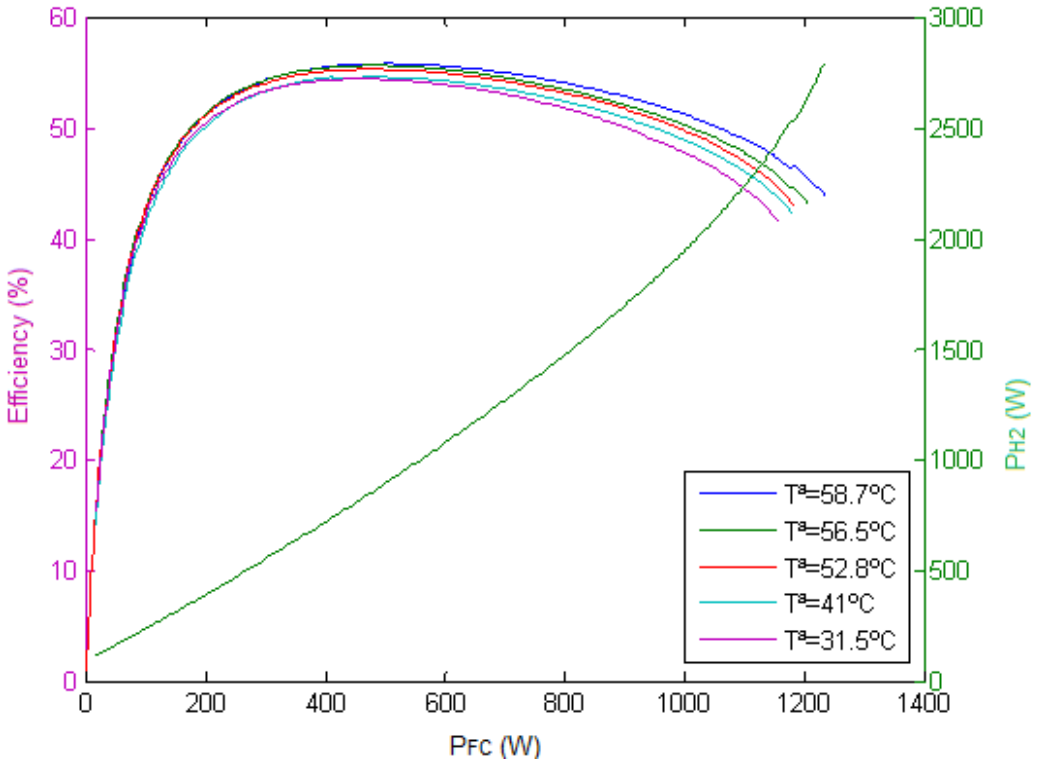

Figure 2.21. *Hydrogen power and efficiency versus fuel cell power*

2.5.3. OTHER FACTORS AFFECTING THE EFFICIENCY

As it has been seen in the previous sections, the efficiency of a fuel cell is mostly dependant to the current delivered and the operation temperature. Nevertheless, it can be also influenced by other factors:

- The pressure effect

The polarization curve of a fuel cell usually rises slightly with the increase of the operating pressure, as it can be seen in Figure 2.22. Furthermore, the consumption of fuel will be smaller (Figure 2.23). Consequently, the efficiency of a PEM fuel cell is better for higher pressures.

However, there exists a limit at 22 PSI beyond which an increase of the pressure is detrimental since the fuel cell is not prepared to deal with it.

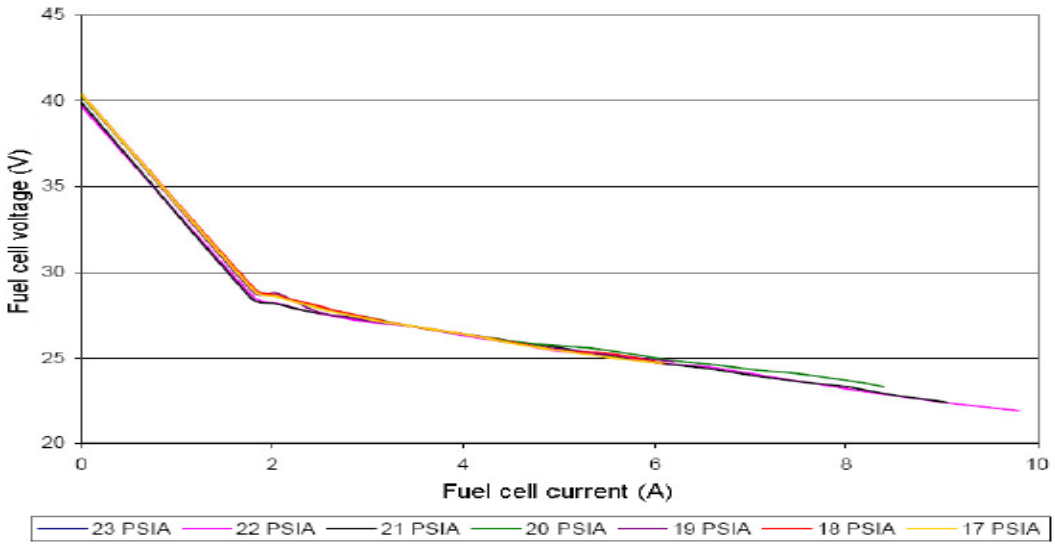

Figure 2.22. *Behavior of the fuel cell depending on the pressure of the input hydrogen [7]*

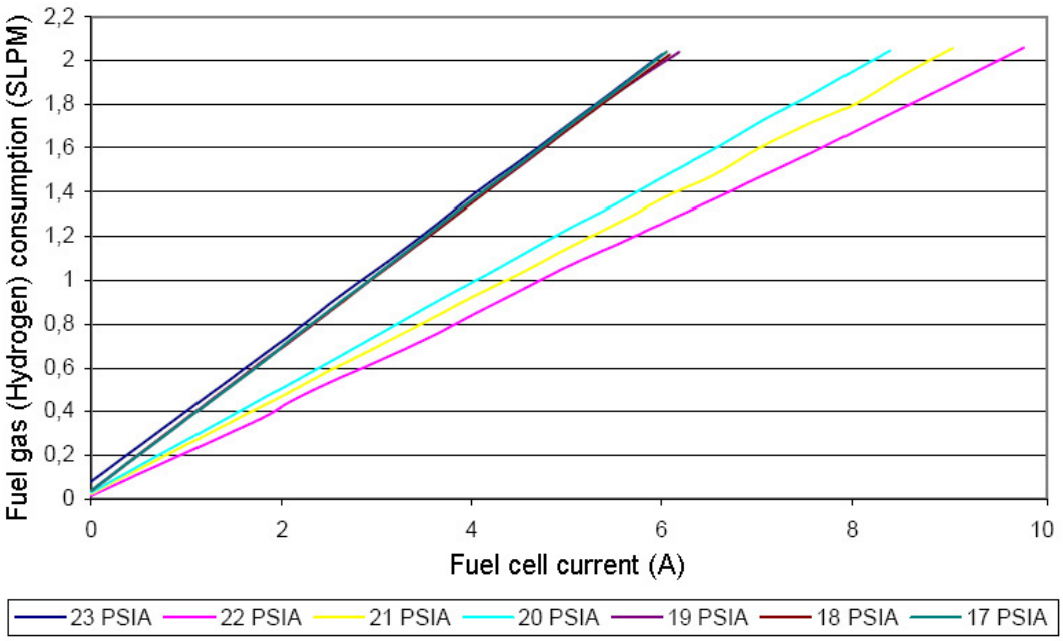

Figure 2.23. *Consumption of hydrogen depending on its pressure [7]*

- The oxygen effect

Fuel cells can include a control system that regulates the pressure between the anode and cathode. This implies that the current in the cell and the oxygen flow determines the hydrogen needed [8].

The ratio of the oxygen flow supplied by the air pump to the oxygen reacted is denominated oxygen excess ratio,

$$\lambda_{O_2} = \frac{W_{O2,in}}{W_{O2,reac}} \tag{2.22}$$

This ratio must take values bigger than one, since on the other hand, the fuell cell will suffer oxygen starvation. Nevertheless, if it takes very high values, the air pump may saturate.

In the following figure it is shown the net electric power, Pfc, versus the excess ratio of oxygen, for different current IFC values.

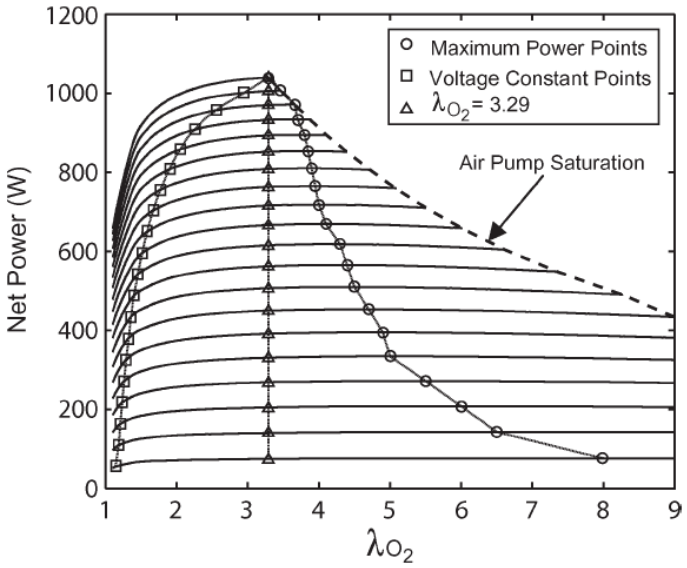

***Figure 2.24**. Excess ratio of oxygen for different fuel cell currents*

It can be seen that for a certain power, the optimal excess ratio is found, corresponding to the minimum current IFC. This means that when the optimal oxygen ratio is achieved, the power is obtained with the minimum fuel consumption.

For instance, given a power of 610 W, the maximum power point corresponds to a current of 17.5 A and an oxygen ratio of $\lambda_{O_2} = 4.35$. Nevertheless, this value of power can also be obtained for other operation points, as the correspondent to 19 A and $\lambda_{O_2} = 1.8$. Thus, it has been checked that regulating the oxygen ratio, a certain power can be achieved with the minimum current possible, and less hydrogen would be consumed.

- The Humidity Effect

The operation of a PEM fuel cell requires sufficient moistening of the gas flow [7]. The cell membrane is humidified by water molecules carried by the hydrogen ions during the exchange ion reaction. Insufficient moistening of water results in dehydration of the membrane, which can lead to its cracking and perforation. That can result in the chemical shortage, mixing of gases, local heating and the possible fire occurrence.

On the other hand, too much water can clog the channels within the flow-field plates. That might cause a phenomenon known as the reverse cell, when the cell affected would produce neutral or negative voltage and it would behave as an electrolyser. The fuel cell could be destroyed by the large amount of heat produced in that situation.

Finally, it can be noted that in order to have a good behavior and efficiency of the fuel cell, the level of humidity must be high, but not excessive.

CHAPTER 3

FUEL CELLS CONNECTIONS

Depending on the application, fuel cells need to deliver different currents and voltages. Furthermore, fuel cells connected to the electric grid need a conversion stage to transform the given DC power to AC.

Particularly, the system available in the university will be connected to the grid, and a conversion stage will be needed, as well as a way to increase the delivered voltage of the fuel cells.

For this purpose, the most used connection configurations are going to be analyzed [9]:

I. SERIES CONFIGURATION

All the fuel cell modules are series-connected, so the current through each of them must be the same and the total voltage output of the system is the sum of the voltages of all the fuel cell. However, there exist an important disadvantage; if any of the modules suffer a fault, it affects the whole system.

Moreover, all the modules are connected to a single power converter, so if it is not working properly, the whole system is invalidated.

This configuration is shown in Figure 3.1.

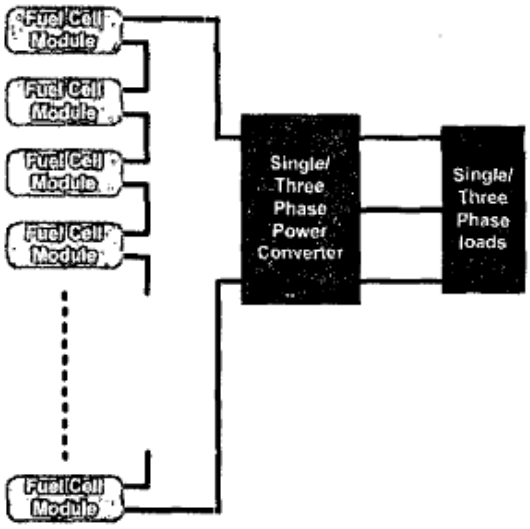

Figure 3.1. *Block diagram of the series configuration [9]*

II. DC DISTRIBUTION CONFIGURATION

In this configuration, each fuel cell module is connected to a DC/DC converter. That way, if one power converter or module has a fault, it does not affect the rest of the system.

All the converters are connected to a DC Bus where the net power is concentrated. However, the voltage value in the Bus is normally lower than the achieved in the Series configuration.

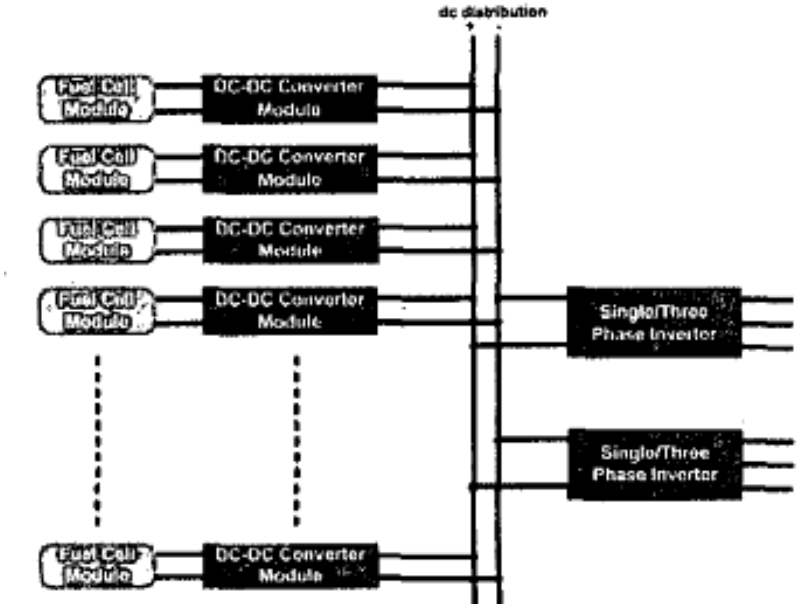

Figure 3.2. *Block diagram of the DC distribution configuration [9]*

III. HFAC DISTRIBUTION CONFIGURATION

This configuration is similar to the previous one. Nevertheless, instead of having DC/DC converters, inverters are used to deliver the power of the fuel cells to a high frequency AC Bus.

The advantages of introducing a HF Transformer in the configuration are that the voltage can be increased to higher values and that the system is electrically isolated.

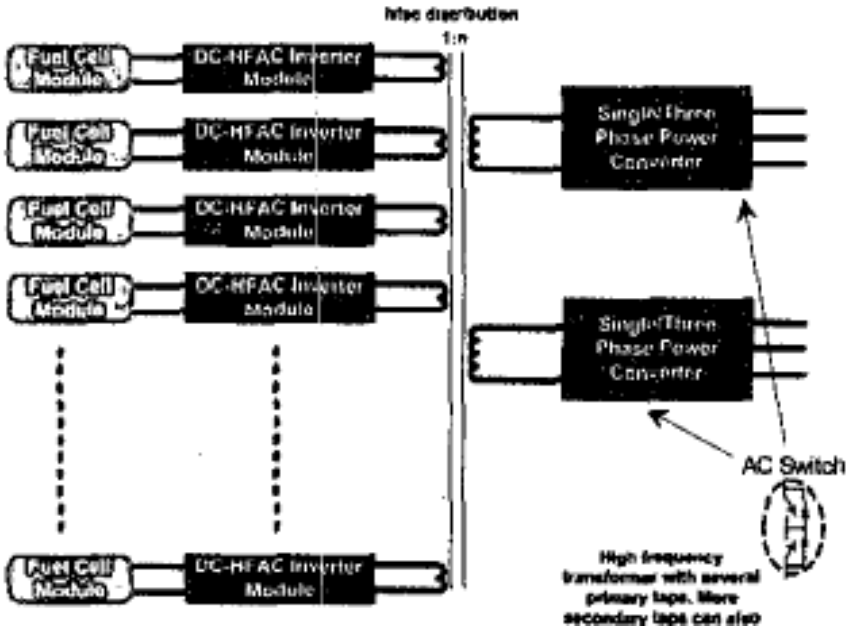

Figure 3.3. *Block diagram of the HFAC distribution configuration [9]*

IV. CASCADED MULTILEVEL CONFIGURATION

This configuration is a variation of the DC distribution configuration. Instead of connecting the power converters to a DC Bus, being all in parallel, the power converters here are series connected and the output voltage can reach higher values.

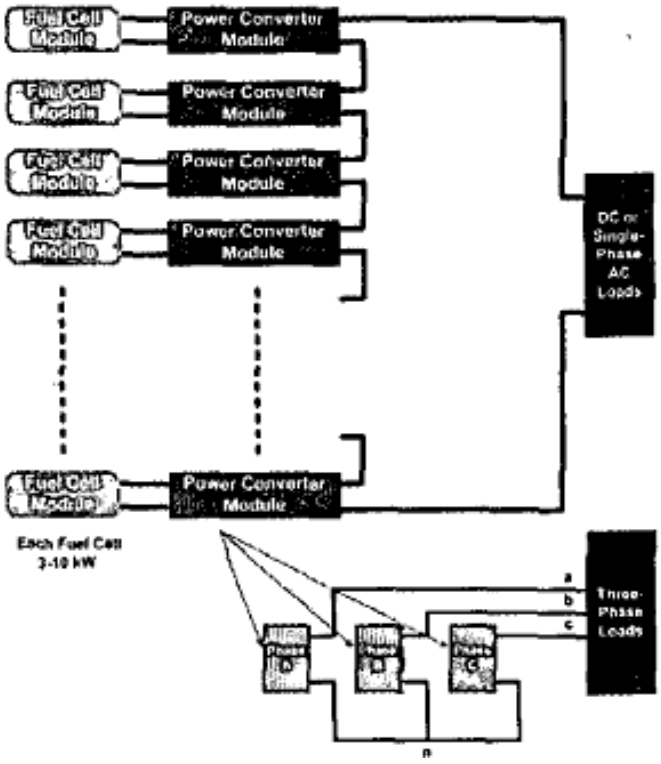

Figure 3.4. *Block diagram of the Cascaded multilevel configuration [9]*

3.1. TYPES OF SERIES CONFIGURATIONS

The actual system at the UPNA comprises four fuel cells. The power generated by them is wanted to be injected to the electricity grid, and therefore the voltage given by each module, of approximately 20 V, must be increased. Consequently, the series configuration is the most adequate.

Among the group of series configurations, there are different options that can be implemented [10]. The most common ones are shown in Figure 3.5.

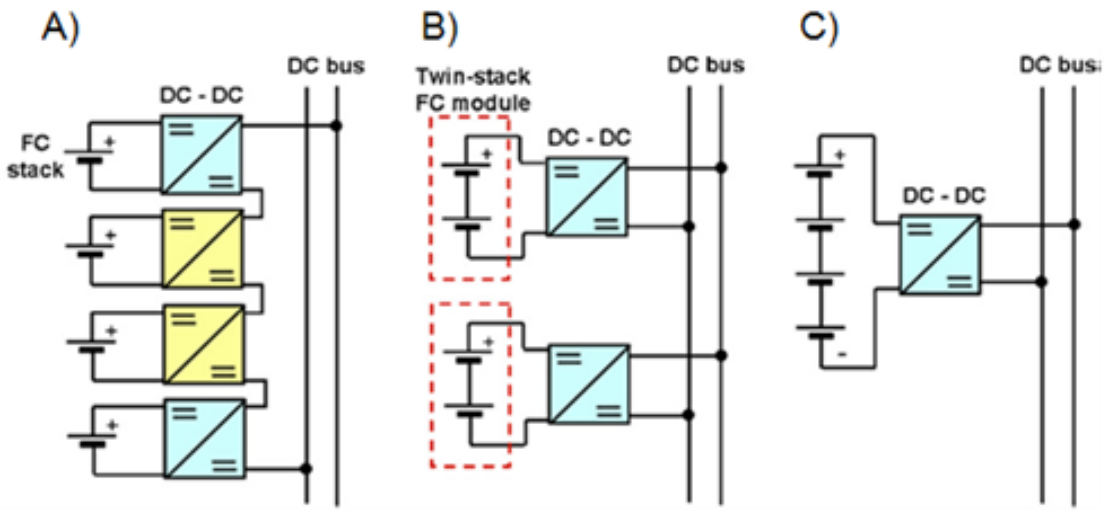

Figure 3.5. *Types of series configurations [10]*

The first option A) consists on having one DC/DC converter for each fuel cell. The converters allow voltage level control of each generator and electrical isolation of a stack when a failure occurs. This technique is recommended for stationary applications like buildings and hospitals. Nevertheless, its price is very high.

The second option proposed B) consists on having one DC/DC converter for two fuel cells series-connected. That way less number of converters are needed (cheaper system), but the output voltage may be smaller than before because the converters are parallel-connected to the DC Bus.

The last configuration C) uses one DC/DC converter for all the fuel cells, providing a more affordable price. With the converter, the output voltage can be increased, but the whole system fails if one of the fuel cells suffers a fault. Thus, it is necessary to use an extra protection system.

3.2. REAL SYSTEM CONNECTION

After studying the different connection options, it has been decided that configuration C) from the previous section is the most adequate for the system available at UPNA. This

decision is taken based on the fact that this is the cheapest configuration, and that the output voltage can reach the desirable values.

The main advantages of this system are its modularity and its simplicity.

However, the problem of this configuration is that the same current must be generated by the four stacks. So if one of the FC fails, the whole system fails. The failed unit has to be replaced or by-passed externally.

The importance of achieving a fault-tolerant FC lies in:

- Protecting the internal components of the FC, which are very sensitive to degraded operation modes, since they can provoke membrane failures
- Ensuring the continuity of power delivery (especially in transportation and for critical loads)

One of the most common faults in a fuel cell stack is the decrease of its voltage under a permitted limit, below which the rest of the system can be poisoned. This is normally produced when a fuel cell does not have enough oxygen for the reaction, and it is called oxygen starvation. When the inner reaction cannot be correctly performed, the fuel cell can start to consume power instead of generating it. In that case, the fuel cell is behaving as an electrolyser. The power consumed is taken from the closest fuel cells, and these starts operating wrong.

There are different techniques to protect fuel cells from reverse voltage, presented in the following lines:

3.2.1. EXTERNAL ANTI-PARALLEL DIODE

When one of the FC modules fails, it is switched off while the others continue operating. To ensure the current flow, an anti-parallel diode is connected.

With PEM fuel cells, if one of the cells suffers from starvation, the flow of current through the membrane converts water into hydrogen and oxygen. The oxygen emerges at the anode side and the hydrogen at the cathode side. Via the piping, this oxygen is taken to the previous cell anode, where it recombines with the hydrogen supplied. Consequently, the current generation is also reduced in neighboring cells, and finally terminates.

There exist different options which include an AP Diode as a solution. These options vary in difficulty and price, and the applications for which they can be used differ.

The first analyzed option consists on introducing a diode in parallel to each fuel cell, in a way that the current generated by the FCs cannot cause any short circuit [11]. Thus, the reduction of current produced when one fuel cell is failing can be avoided. When the FC suffers a fault, the diodes form low ohmic resistance and it is possible to automatically by-pass the defective cells in a simple and economical manner. To maximize the results, each individual cell has a diode connected in parallel. During a defect-free operation, the FC behaves as a current source, and there is no current flow through the diode. The included diodes are shown in the following figure:

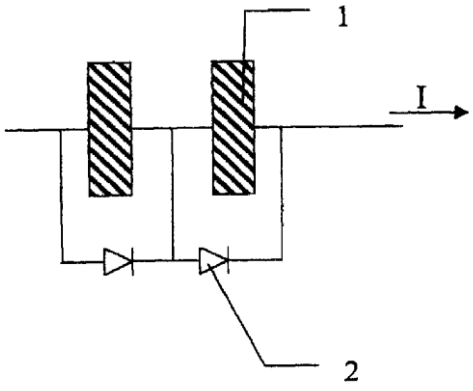

Figure 3.6. *Anti-Parallel diodes [11]*

A second option, a bit more advanced, consists on monitoring the voltage of the fuel cell, and when the voltage of one cell becomes negative, the FC is switched off and the AP diode starts to conduce [12-14]. However, the switching of the diode is not instantaneous, since it depends on the internal impedance of the FC stack and the load current amplitude. Consequently, it is necessary to add diodes in series with the FC in order to increase the voltage threshold which leads to the conduction of the AP diode. This solution is shown in Figure 3.7.

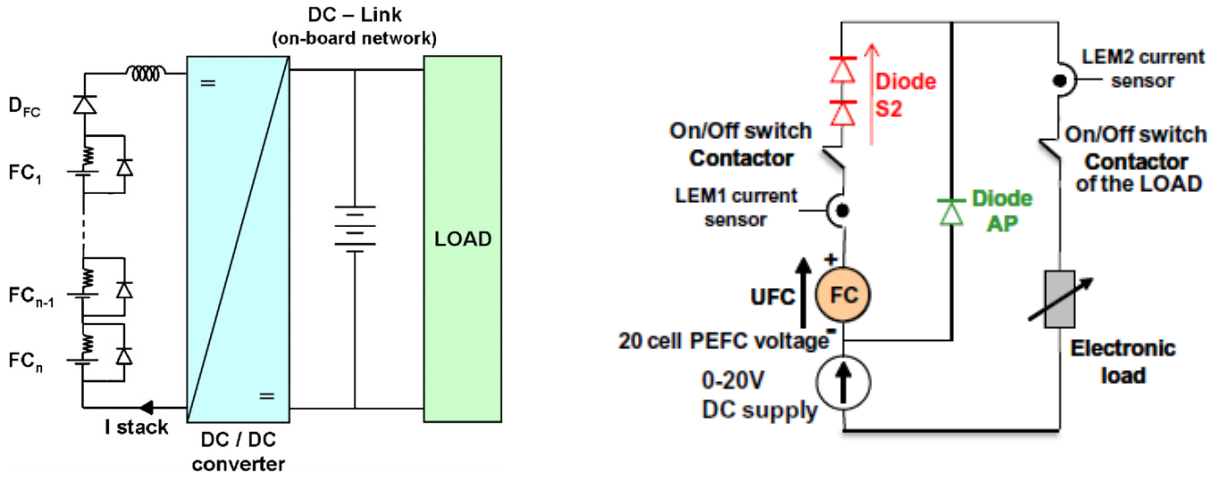

Figure 3.7. *Electric circuit topology showing the PEMFC, the diode AP and the switches*

A third option comprises a switching system composed by a controller, a monitor and a switching circuit for each stack [15]. This system implements a control method that monitors the voltage of the FC, and so it is capable of turning off a faulty stack and re-connecting it again when the fault has passed. If the fault is repeated a certain amount of times, a reduced capacity mode starts to operate. Furthermore, the control can decide the number of stacks connected when there is a change in the current value in order to achieve a correct operating point for the fuel cells.

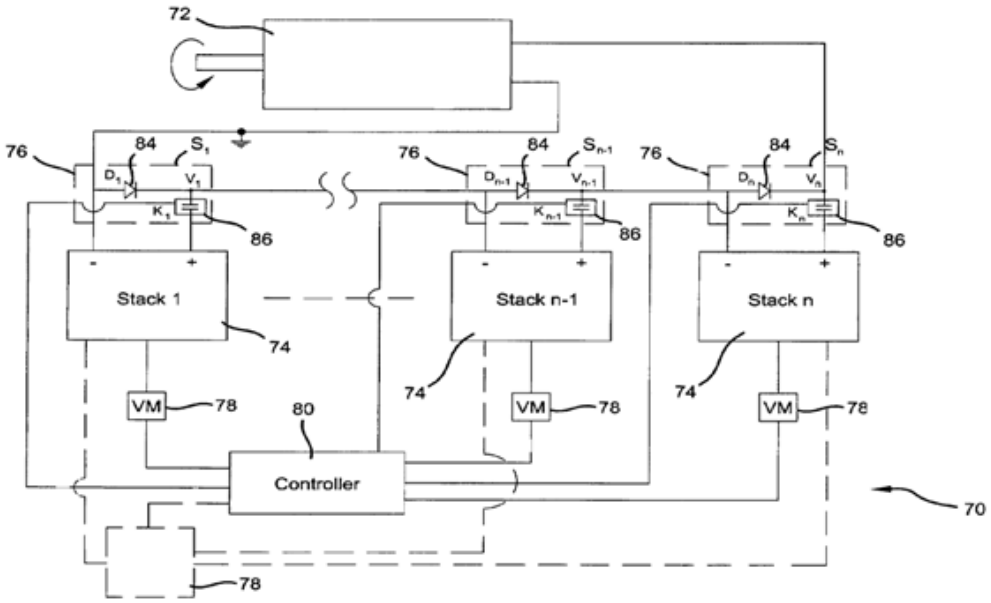

Figure 3.8. *Switching System for FCs [15]*

The last option is adequate for certain applications where the needed voltage output can vary [16]. This structure can connect the fuel cells either in series or in parallel, as shown in Figure 3.9. This structure includes a controlled switch that connects the AP diode when there is a reverse voltage.

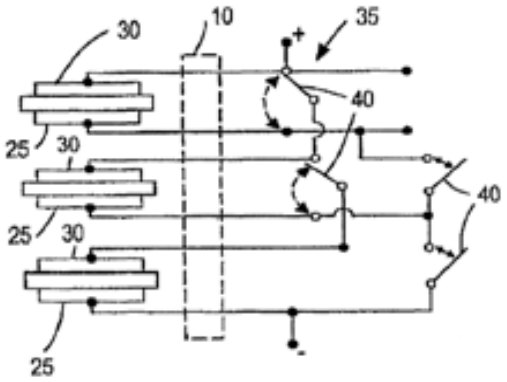

10: insulating housing
25: anode
30: cathode
35: by-pass circuit
40: control element
55: diode
50: converter

Figure 3.9. *Series and Parallel conection structure [16]*

3.2.2. INTEGRATED DIODE

Instead of connecting AP diodes externally to the cells, another option is integrating them in their structure [17].The advantage of having integrated diodes is that a direct electrical connection is formed and there is no need of bus bars or connecting wires. That way the volume, weight and cost of the system is reduced.

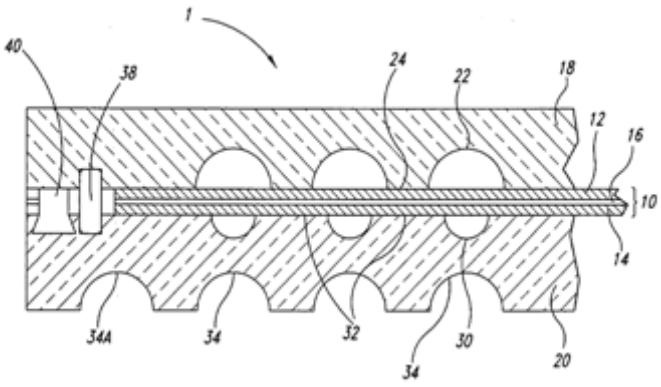

1: Fuel cell assembly
10: Cell
12: Cathode
14: Anode
16: Electrolyte
18: Oxidant plate
20: Fuel plate
22: Oxidant channel
24 & 32: Land area
30: Fuel channel
34: Refrigeration channels
38: Perimeter seal
40: Diode

Figure 3.10. *Integrated protection diodes in a FC stack [17]*

3.3. FC CONNECTION STRATEGY

In Chapter 2 the behavior of a single fuel cell was analyzed. The real system comprises four identical fuel cells, so it may be interesting to choose the number of modules connected at any moment depending on the demanded power, with the purpose of making the system work at the highest efficiency. The power delivered by the system, taking into account the nominal values of the fuel cell stacks, will vary from 0 to 4800W.

A further study of the efficiencies as a function of the power delivered, as the number of FCs connected increase, has been developed. This is based on the fact that a certain power can be delivered using a different number of fuel cells. Moreover, depending on the number of operating fuel cells, the operation point of these cells varies, and the efficiency of the system differs. Thus, it can be noted that regulating the number of turned-on fuel cells for every delivered power, the efficiency of the system can be maximized and less hydrogen can be consumed.

It is important to remember that the fuel consumption is invariant with temperature, while the efficiency of the system changes with it.

The efficiency of the system, when the four FCs are available, can change a lot depending on the considerations applied; two different options have been considered:

A. NO FUEL CONSUMPTION WHILE TURNED-OFF

This first option considers that when one fuel cell is not working, it is totally turned off and its fuel consumption is inexistent. This implies that the total hydrogen consumption corresponds to the operating fuel cells.

This option can be implemented when a prediction of the load is available, since if the fuel cell is turned-off, it takes some time to be operative again and it would not be able to respond when load variation occurs.

The total electric power delivered by the system will be the addition of the power of all the FCs connected. Moreover, the hydrogen consumption of the system will be the sum of all the FCs consumption.

Thus, it follows that the system efficiency is not going to suffer any change due to the connection of more FCs, since the electric power and fuel power will increase or decrease simultaneously.

$$\eta_{\text{total}} = \frac{N_s \cdot P_{FC}}{N_s \cdot P_{H2}} = \frac{P_{FC}}{P_{H2}} = \eta_{FC}\,, \tag{3.1}$$

where N_s is the number of fuel cells series-connected.

The following graph shows the fuel power as a function of the electric power delivered, for 1 to 4 fuel cells connected in series:

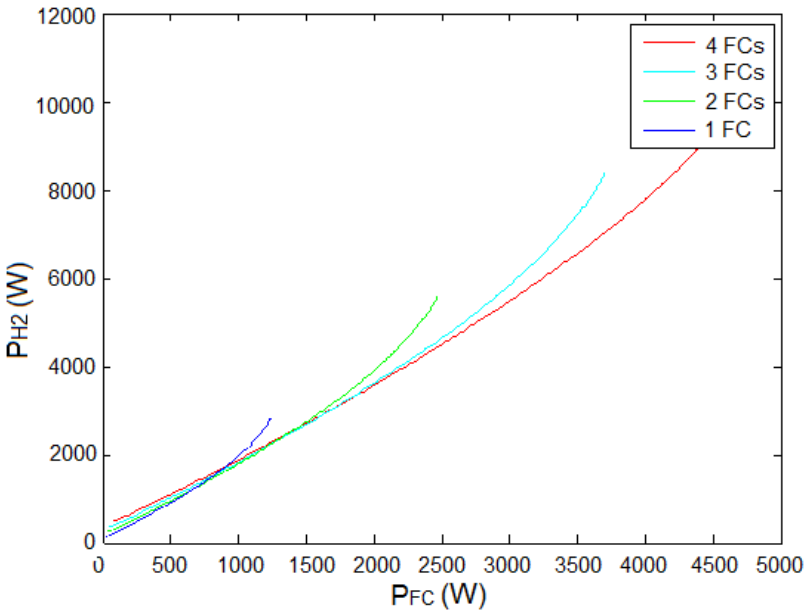

Figure 3.11. *Hydrogen power vs. electric power, for 1 to 4 FCs series-connected, Option A*

It can be seen that the fuel power is invariant with temperature and that the ratio of hydrogen consumption to delivered power must be increased for high powers.

On the other hand, the efficiency does vary with temperature, and so for each number of FCs, there are 5 possible efficiency curves:

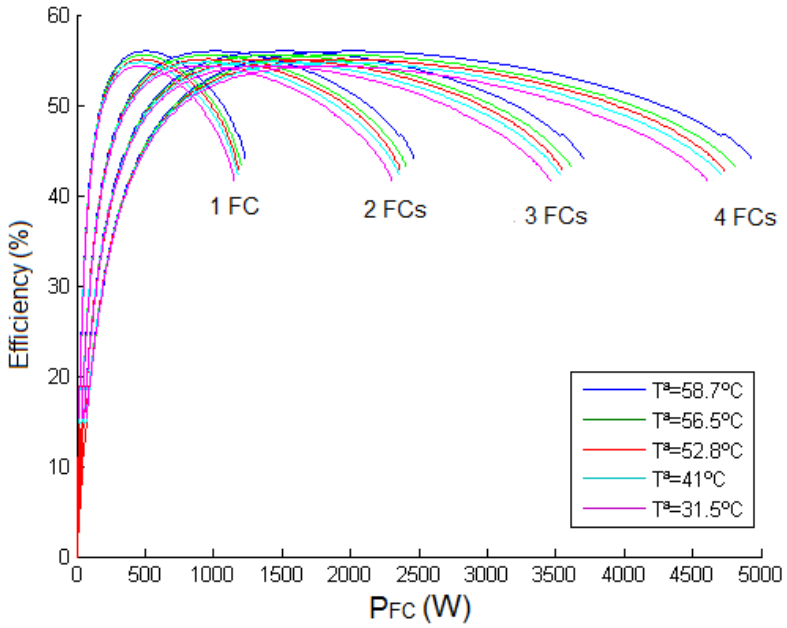

Figure 3.12. *Efficiency vs. electric power, for 1 to 4 FCs series-connected: Option A*

As it can be seen the efficiency of the system, for a certain number of operating fuel cells, varies a lot with temperature. For instance, for a given temperature of 31.5 ℃, the efficiency will be lower than for 58.7 ℃. Moreover, the cutting point of the efficiency curves also differs. For example, the transition between one fuel cell and two will be done at a bigger power for high temperatures than for low ones.

To observe more closely the efficiency curves dependence to the temperature, the following Figure 3.13 has been included:

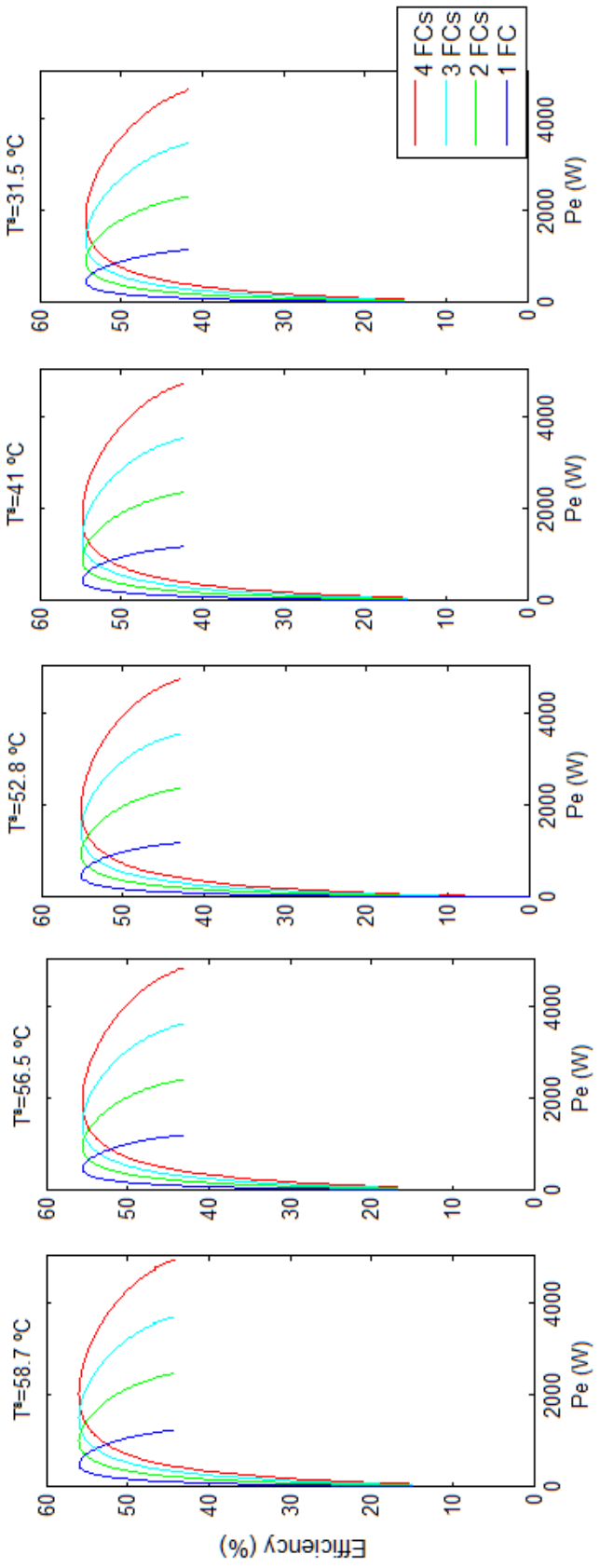

Figure 3.13. *Efficiency vs. electric power, for different temperatures: Option A*

The previous curves have also been plotted in three dimensions, where the maximum efficiency working points (a) and the influence of temperature (b) are better shown:

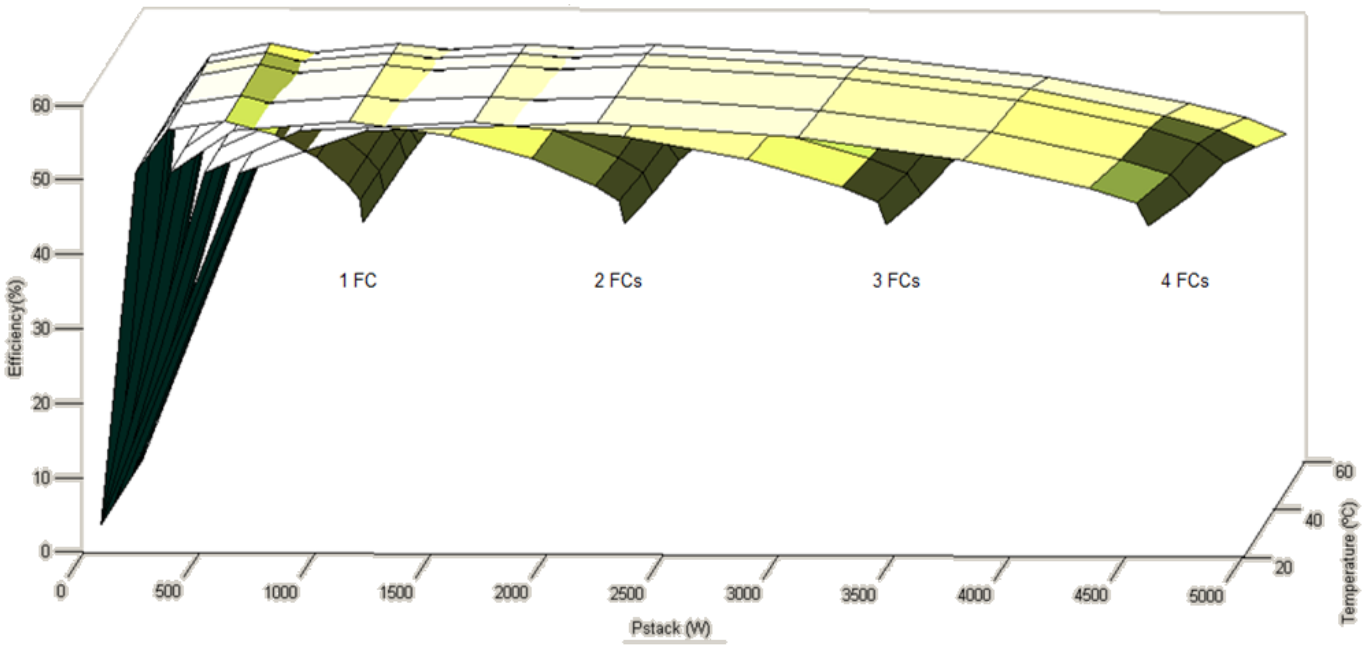

(a) Maximum efficiency working point

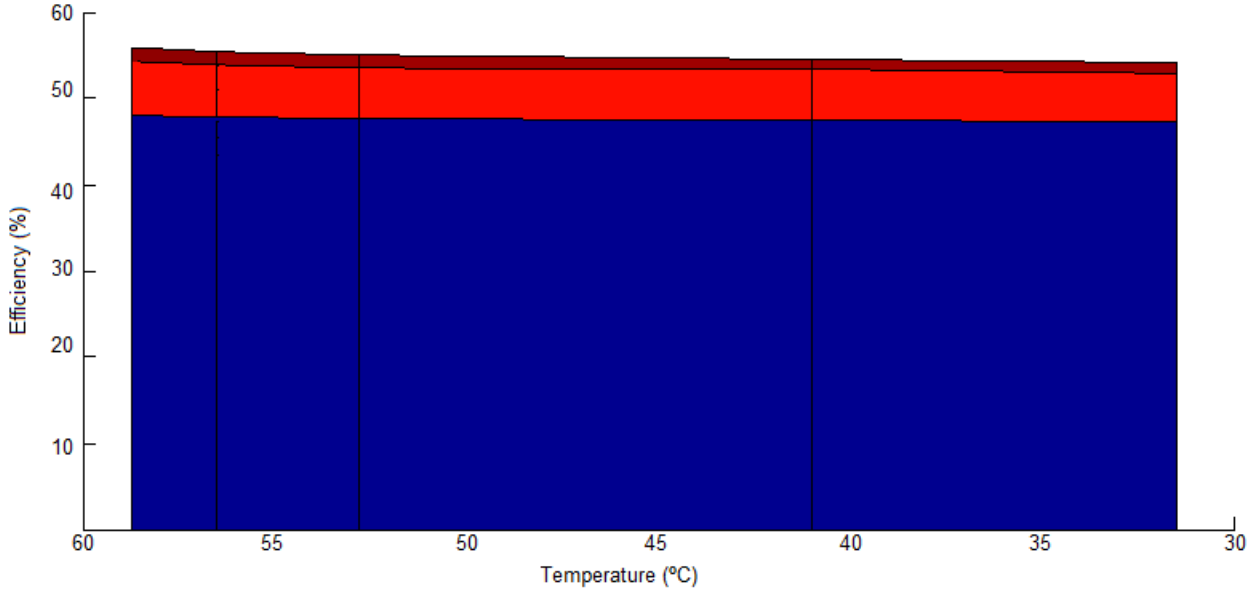

(b) Temperature influence over efficiency

Figure 3.14. *3D-Plot of Efficiency vs. Electric Power vs. Temperature*

In order to understand the previous study, we are going to explain the following example:

The power demanded at a certain moment is 1100 W. as it can be seen in Figure 3.11, to achieve this power, the fuel supplied to the fuel cells vary depending on the number of operating devices. For instance, if the connected number of fuel cells is one, the hydrogen supply will be bigger than for a higher number. Consequently, observing Figure 3.12, the efficiency of the system for one fuel cell is lower than for higher number of fuel cells.

It can be noted that for this particular case, the optimal number of fuel cells connected, based on having the highest efficiency possible, is two. Therefore, it will be interesting to connect or disconnect the fuel cells to have the maximum efficiency all the time. This will be more deeply explained in Chapter 5.

B. MINIMUM PERIPHERAL CONSUMPTION WHILE TURNED-OFF

As with the previous option, the efficiency and hydrogen power as more FCs are connected to the system are going to be analyzed. The main difference lies in the fact that, in the present study, the turned-off FCs have a minimum consumption, since the peripherals must be fed.

Consequently, a turned-off FC will consume the power associated to the peripherals correspondent to 0 A, which is 47.2 W, as seen in Figure 2.18.

In this case, the efficiency is going to be lower than before when any of the FCs are not operating.

$$\eta_{\text{total}} = \frac{N_s \cdot P_{FC} - N_{off} \cdot P_{per}}{P_{H2}} \quad , \tag{3.2}$$

where N_{off} is the number of FCs turned-off.

Given that, for a certain value of fuel, the output power P_{FC} obtained will be smaller than in the previous option.

The following Figure 3.15consists of a graph where the fuel power has been plotted against the electric power delivered, for any temperature.

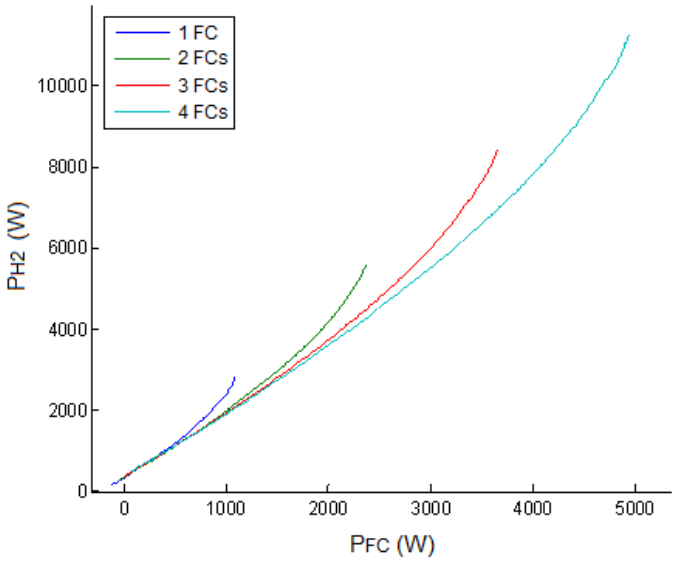

Figure 3.15. *Hydrogen power vs. electric power, for 1 to 4 FCs series-connected, Option B*

It can be noted that at very low operation, there can be negative output power, and this is caused because the generated power is smaller than the needed to feed the peripherals of the turned-off FCs.

As for the previous case, the efficiency of the system for different number of fuel cells connected has been plotted versus the generated power, in Figures 3.16 and 3.17.

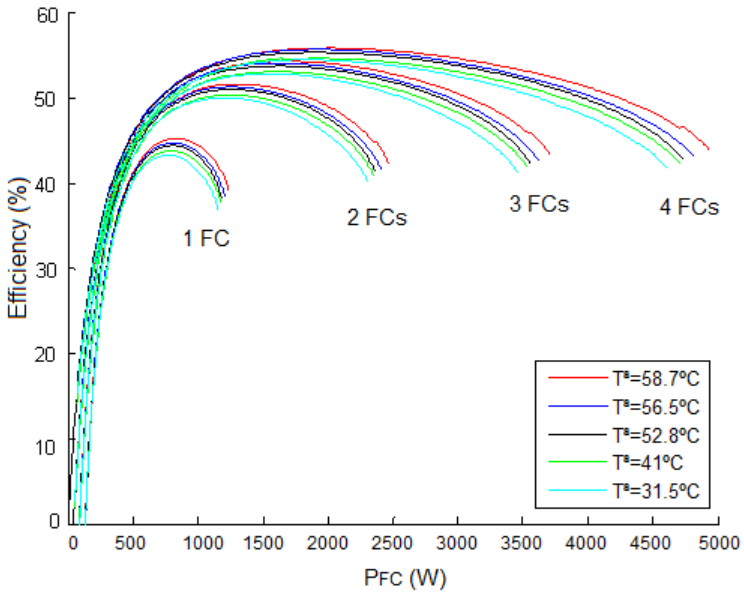

Figure 3.16. *Efficiency vs. electric power, for 1 to 4 FCs series-connected: Option B*

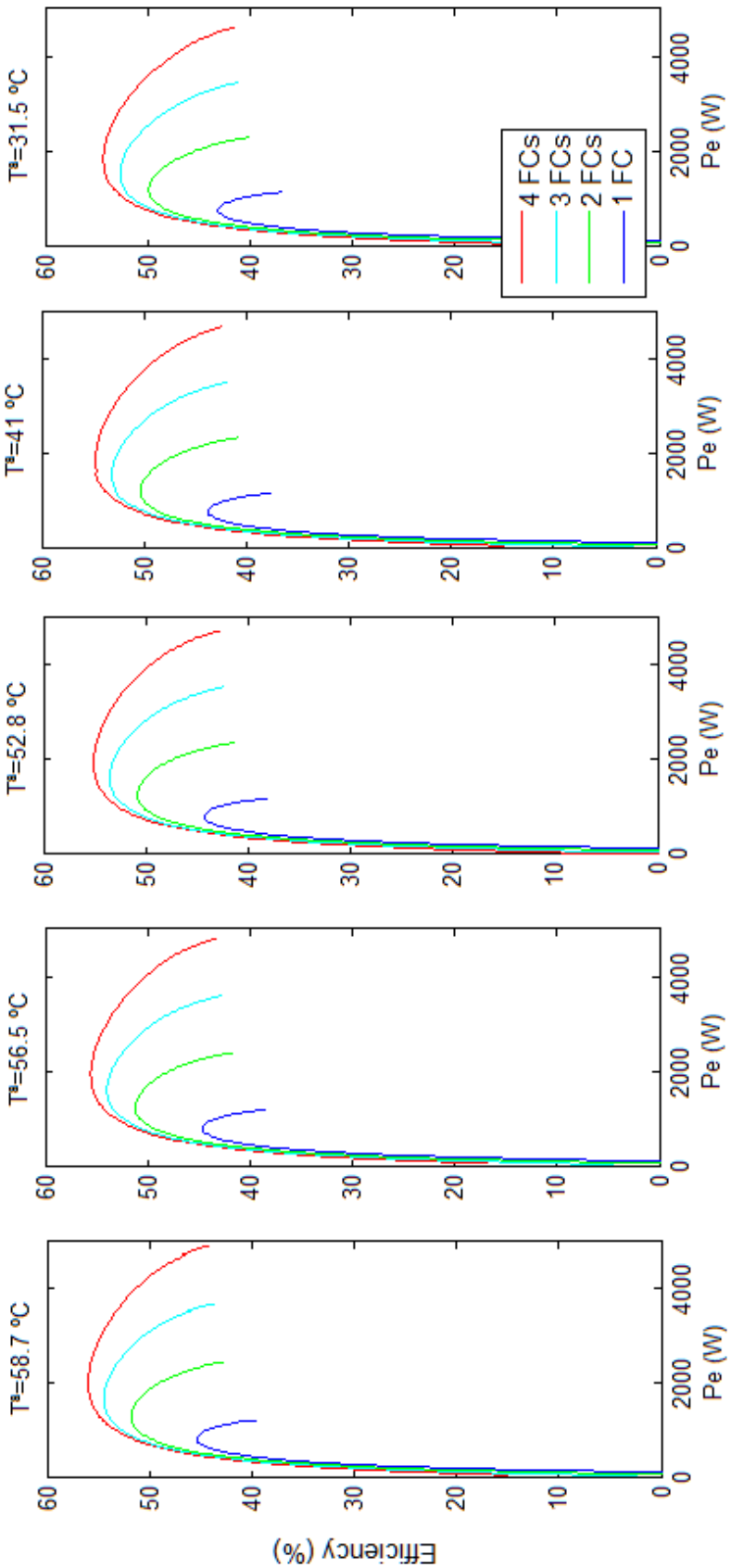

Figure 3.17. *Efficiency vs. electric power, for different temperatures: Option B*

It can be observed that for this case, the most efficient connection for any electric power consists on connecting the four fuel cells in series. Therefore, it makes no sense having any module turned-off.

As a conclusion of this chapter, it is important to note that there has been found a most efficient strategy of connection for fuel cells, which consists on regulating the number of cells turned-on, instead of having all operating the whole time.

Analyzing the efficiency when different numbers of fuel cells are operating, different power ranges can be delimited for which a certain number of operating cells is most efficient.

These power ranges will be used in Chapter 5 to implement a power control capable of regulating the number of fuel cells connected, in order to achieve a maximum efficiency point tracking (MEPT).

CHAPTER 4

RESONANT POWER CONVERTER WITH HF TRANSFORMER

4.1. POWER CONVERTERS USED FOR FUEL CELLS

There exist different conversion topologies that can be connected to fuel cells [18]. In this paper, we are going to talk about the DC/DC resonant structures which present a high frequency transformer. The basic scheme of a DC/DC resonant converter is shown in the following figure:

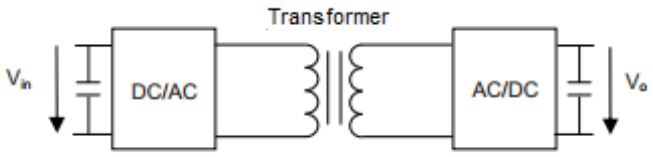

Figure 4.1. *Basic structure of a DC/DC Resonant converter with HF transformer*

As it can be seen, this structure is composed by different conversion stages. Firstly, a constant voltage Vin is introduced in the system. It reaches the inverter, where it is converted into an AC voltage which will feed the resonant tank. Afterwards, the resultant resonant wave will reach the high frequency transformer and after that, it will be introduced into a second conversion stage which will provide a rectified voltage Vbus.

The advantage of using a resonant structure is that the inverter's IGBTs can be soft-switched. This means that by choosing the right values of the resonant elements, a certain resonant frequency, higher than the commutation frequency, can be achieved, and the

commutation can be done in periods when the current is zero (ZCS) or when the voltage is zero (ZVC). That way the commutation losses are minimized.

This kind of structures, thanks to their commutation characteristics, can work at very high frequencies. Because of this, a high frequency transformer can be used. These transformers are smaller than the conventional ones, which implies a reduction on the price and an increase in the power density. Furthermore, the electromagnetic interferences (EMI) are reduced.

On the other hand, this kind of configuration presents the disadvantage of needing an inversion stage, which implies a higher number of transistors and the control required to generate the AC wave that will feed the resonant stage.

Depending on the resonant elements, there are three different configurations:

4.1.1. SERIES RESONANT CONVERTER (SRC)

The resonant tank of this configuration consists of an inductor Lr and a capacitor Cr, connected in series to a resistor Rc, as shown in the following figure:

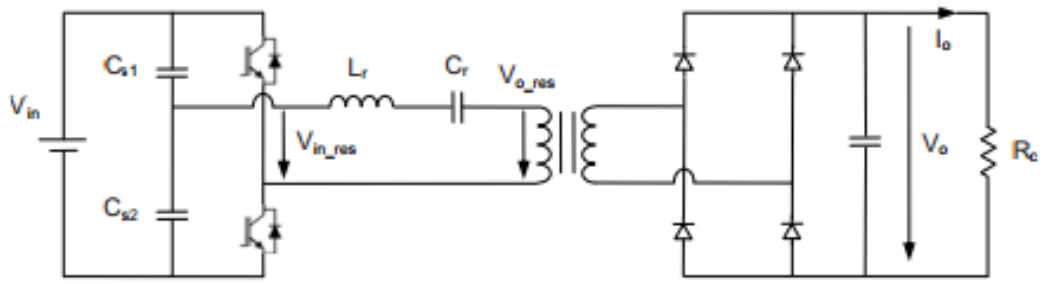

Figure 4.2. *Series resonant converter*

Provided that the resonant elements provoke a positive voltage drop, this is a Buck system.This configuration is especially convenient for high voltages and low currents, since the capacitive filter at the output generates a ripple that can be increased by high currents.

4.1.2. PARALLEL RESONANT CONVERTER (PRS)

The resonant tank of this second configuration comprises a resonant capacitor Cr connected in parallel to a resistor Rc:

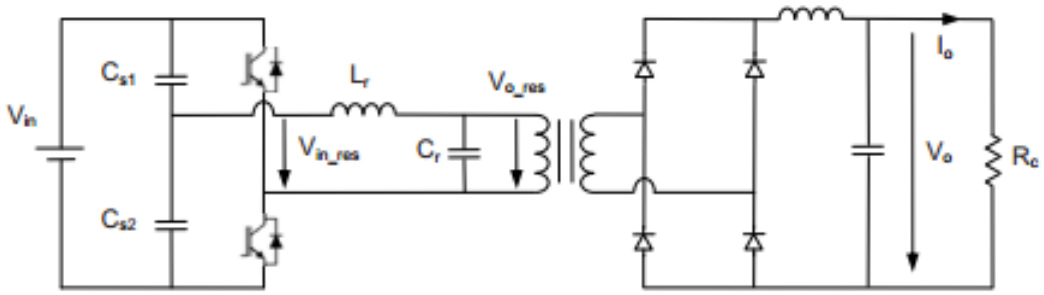

Figure 4.3. *Parallel resonant converter*

In this case, the input and output voltages ratio can be bigger and lower than one, what implies that this converter can be used as a Boost and as a Buck. This topology is recommended for low voltages and high currents provided that the inductive filter is capable of reducing the current ripple.

4.1.3. SERIES-PARALLEL RESONANT CONVERTER (SPRC)

The last configuration proposed consists of a combination of the previous ones. The resonant tank comprises two resonant capacitors, Cr1 and Cr2, one connected in series to the resistor Rc, and the other connected in parallel.

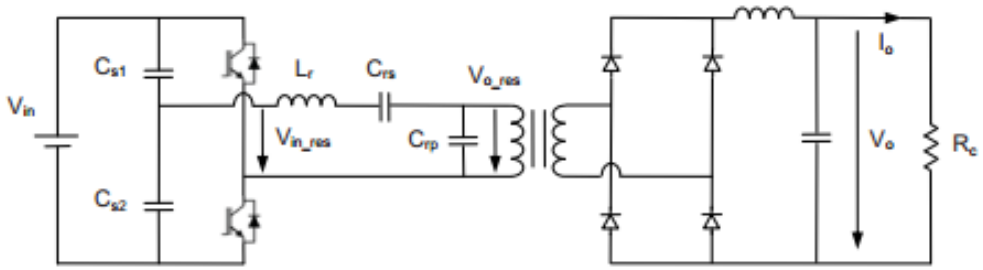

Figure 4.4. *Series-Parallel resonant converter*

Depending on the resonant elements, this configuration can be a Boost or a Buck. Furthermore, these mentioned elements will make the operation of the system more similar to the series or to the parallel configuration. This last topology has been chosen for the connection of the fuel cells studied in the previous chapters, and it will be analyzed and simulated later in this chapter.

As mentioned before, the values of the resonant parameters and the commutation frequency of the inverter determines the output voltage Vbus regulation.

A new parameter Q is defined, as a measure of the quality of the system:

$$Q = \frac{w_{res} \cdot L_r}{R_c} \tag{4.1}$$

being

$$w_{\text{res}} = \frac{1}{\sqrt{L_r \cdot R_c}} \tag{4.2}$$

where

w_{res} , is the resonant frequency, in rad/s

L_r , is the inductor of the resonant tank

R_c , is the resistor of the resonant tank

For any of the structures introduced before, this parameter Q and the input and output voltages ratio will determine if the system is operating in continuous or discontinuous mode. In order to achieve a soft-switching, it is necessary to achieve the discontinuous mode.

4.2. POWER CONVERSION STAGE DESCRIPTION

The resonant converter is going to be connected to the fuel cells evaluated in Chapter 2. In order to adequate the output voltage of the cells to the input voltage of the converter, and intermediate conversion stage must be included; a Boost converter is going to elevate the output voltage of the fuel cells to the voltage level necessary for the resonant converter.

Moreover, the generated power is aimed to be delivered to the electricity grid, and for that the output voltage of the resonant converter, Vbus, must fulfill the grid characteristics. For that, an H-Bridge Inverter has been added between the resonant converter and the grid.

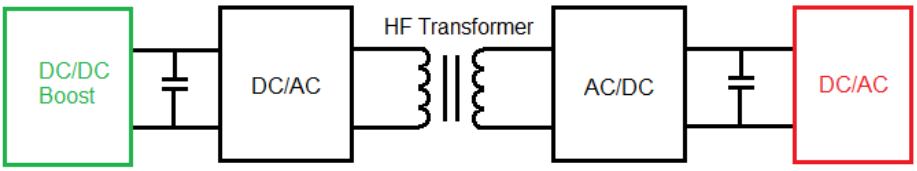

Figure 4.5. *Scheme of the power conversion stage*

The operation point of the fuel cells will be regulated by the Boost, with a control loop for the delivered current. Once the current is determined, the voltage value is fixed following the polarization curve shown in Figure 4.6. Consequently, the power delivered by the fuel cells will be fixed too, as it can be seen in Figure 4.6.

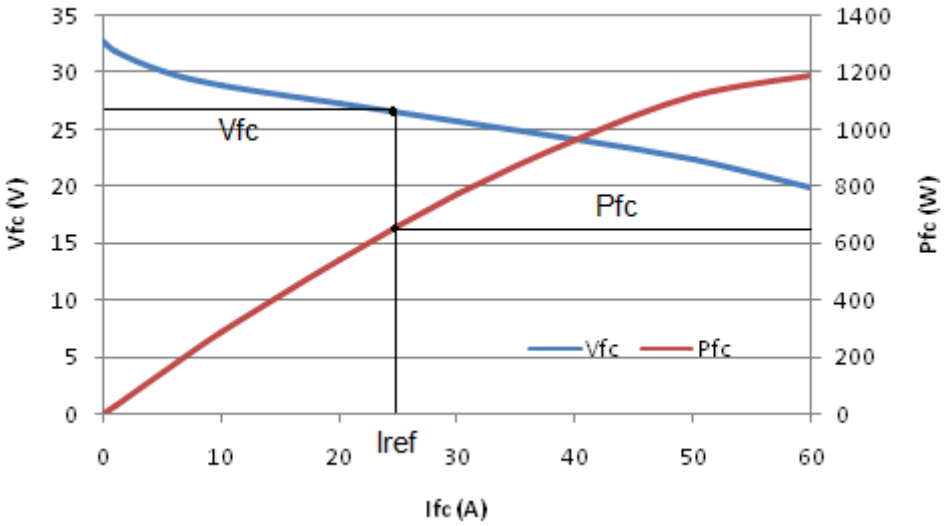

Figure 4.6. *Definition of the fuel cell voltage and power from a reference current*

Afterwards, the Boost delivers the generated power to the DC/DC Resonant Converter. This intermediate stage in not controlled, but determining the value of its output, Vbus, all the voltage levels inside it get fixed. This output voltage will be regulated by the H-Bridge inverter. For that, an external voltage loop is implemented, followed by a faster internal current loop. The voltage is regulated in order to have a voltage level big enough to permit the injection to

the grid. The voltage loop generates the reference current for the current loop, with which the power delivered is controlled. In the steady state, the power injected to the grid will be equal to the generated by the fuel cells.

4.2.1. RESONANT POWER CONVERTER WITH HF TRANSFORMER: ANALYSIS AND SIMULATION

As mentioned in the introduction, the DC/DC resonant converter will be an intermediate stage introduced between a Boost converter and an H-Bridge inverter. Nevertheless this section is based on the analysis of the behavior of this resonant stage alone, and so the Boost will be substituted by a DC voltage source, while the output will consist of a resistance that burns the power generated by the input source.

The resonant converter that is going to be simulated is compound by the following parts shown in Figure 4.7:

- DC/AC Stage: a half-bridge inverter.
- Resonant Tank: series-parallel configuration.
- HF Transformer
- AC/DC Stage: a diode bridge rectifier.

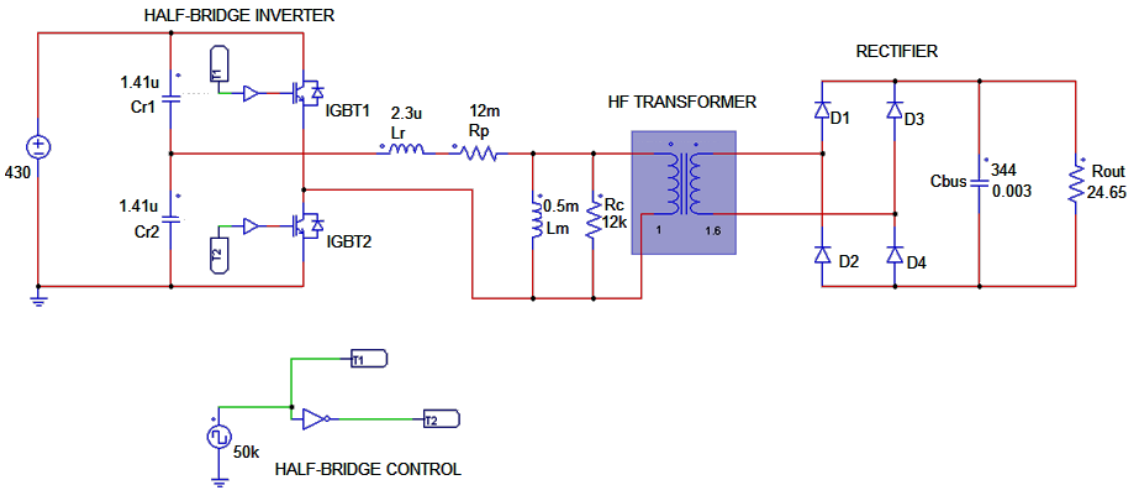

Figure 4.7. *DC/DC Resonant converter with HF transformer modeled in PSIM*

4.2.1.1. Half-Bridge Inverter Commutation

In order to control the switching on and off of the Half-Bridge Inverter's IGBTs, shown in Figure 4.6, a square wave which half the cycle is 1, and the other half is 0, must be created.

That way, this signal will go to the IGBT through a driver, and when its value is 1, the IGBT will be ON, while when it's 0, the IGBT will be OFF.

As there are two switches that commutates complementary, a negation logic gate is used to control the second IGBT.

The control waves generated, as well as the conduction state of the IGBTs, are shown in Figure 4.8. As we can observe, the signals are completely complemented, and for both IGBTs the duty cycle will be:

$$D = \frac{Ton}{Tcom} = 0.5 \tag{4.3}$$

Furthermore, the electric scheme of the converter for the two possible conduction states is also shown.

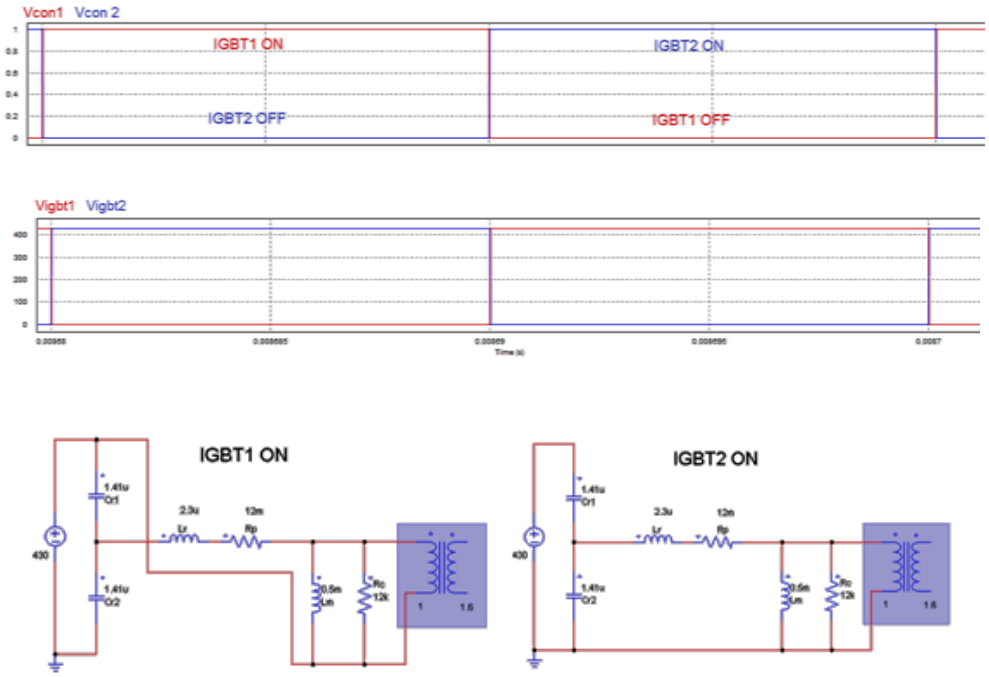

Figure 4.8. *Control waves for the IGBTs and its conduction state*

4.2.1.2. Calculation of the system parameters

The values of the resonant tank elements and the commutation frequency determine the behavior of the system. The simulation performed in this chapter is based on a real resonant converter, provided by the enterprise Ingeteam, and therefore some parameters of the system are already predefined (stored in Table 4.1.).

Nevertheless, others must be calculated, and will be included in Table 4.2.

KNOWN PARAMETERS OF THE SYSTEM	
Half-Bridge Inverter:	$Fcom = 50\ kHz$
Resonant tank:	$Rc = 12\ k\Omega$
	$Lr = 2.3\ \mu H$
Transformer:	$\frac{N_2}{N_1} = \frac{V_2}{V_1} = k = 1.6$
	$Lm = 0.5\ mH$
	$Rp = 12\ m\Omega$
Output:	$Cout = 3\ \mu F$

Table 4.1. *Known parameters of the system*

1. Calculation of the voltage source and the resistance at the output:

First of all, as the aim of the complete system is to be connected to the grid, the output voltage of the resonant converter must be adjusted to the grid peak voltage value:

$$V_{grid\ ,peak} = \sqrt{2} \cdot 230 = 325\ V \tag{4.4}$$

However, as the output of the resonant converter is a DC wave, an Inverter must be introduced before being connected to the grid. As the inverter is a buck converter, the Vbus at the output of the resonant converter must be bigger than the grid's peak voltage, and therefore the chosen value is:

$$Vbus = 344\ V \tag{4.5}$$

The HF transformer has a transformation ratio of 1.6, so the value of Vbus seen in the primary side (considering an ideal transformer) will be:

$$Vprim = \frac{Vbus}{k} = \frac{344}{1.6} = 215\ V \tag{4.6}$$

Provided that the input voltage in divided in two in the Half-Bridge Inverter, the input voltage source will have a value of:

$$Vin\ =\ 2 \cdot Vprim\ =\ 430\ V \tag{4.7}$$

Since the maximum power of the system is almost 5 kW, the value of the resistance needed to burn all the power will be:

$$R_{out}\ = \frac{Vbus^2}{P_{out}} = \frac{(344\ V)^2}{5000\ W} = 23.7\ \Omega \tag{4.8}$$

2. Calculation of the resonant elements:

As explained before, this DC/DC resonant converter works at high frequency in order to use a smaller and cheaper transformer. In this case, the commutation frequency chosen for the Half-Bridge is 50 kHz. The commutation period will be:

$$T_{com}\ = \frac{1}{F_{com}} = \frac{1}{50000Hz} = 20\mu s \qquad \rightarrow \qquad \frac{T_{com}}{2} = 10\mu s \tag{4.9}$$

On the other hand, another singularity of this topology is that the inductances and capacitances have been chosen to have a certain resonance that enables a zero-current switching. Having a security coefficient of 0.8, it can be deduced that the resonance frequency of the system is:

$$\frac{T_{res}}{2} = \frac{T_{com}}{2} \cdot 0.8 = 8\ \mu s \tag{4.10}$$

$$F_{res}\ = \frac{1}{T_{res}} = \frac{1}{16\mu s} = 62500\ Hz \tag{4.11}$$

In the following picture the currents are shown, and the soft-switching period is indicated:

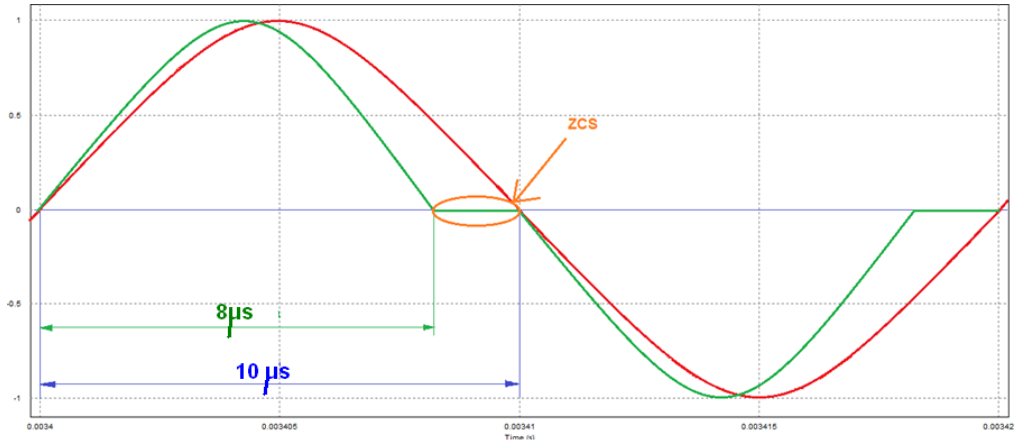

Figure 4.9. *Resonance of the converter and security coefficient*

After knowing the resonance frequency, and using the Lr given, the value of Cr can be obtained easily applying the following equations:

$$Fres = \frac{1}{2\pi\sqrt{2 \cdot C_r \cdot L_r}} \tag{4.12}$$

$$C_r = \frac{1}{(2\pi \cdot F_{res})^2 \cdot 2 \cdot L_r} = \frac{1}{(2\pi \cdot 62500)^2 \cdot 2 \cdot 2.3\text{H}} = 1.41\text{F} \tag{4.13}$$

3. Calculation of the maximum resonant current

Once the parameters of the resonant block are known, it may be useful to calculate the maximum value that the resonant current Ires can achieve. That way, we can know if this value is appropriate for the elements of the circuit, and deduce whether they are going to be damaged during standard conditions.

$$Z_r = \sqrt{\frac{2 \cdot C_r}{L_r}} = \sqrt{\frac{2 \cdot 1.41\mu\text{F}}{2.3\mu}} = 1.07\ \Omega \tag{4.14}$$

$$I_{res,max} = \frac{P_{out}}{4 \cdot C_r \cdot V_{in} \cdot F_{con}} \cdot Z_r = \frac{5000\ W}{4 \cdot 1.41\,\mu F \cdot 430V \cdot 50000Hz} \cdot 1.07\ \Omega = 44.2\ A \qquad (4.15)$$

To sum up, the parameters calculated above are stored in the following table:

NEW PARAMETERS CALCULATED	
Input Voltage Source:	Vin = 430V
Resonant Tank:	Fres = 62.5 kHz
	Cr1 = Cr2 = 1.41 µF (precharged to 215V)
Output:	Rout = 23.7 Ω

Table 4.2. *Calculated parameters of the system*

4.2.1.3. Simulation Results

First of all, we are going to evaluate the input and output voltages, Vin and Vbus, as well as the commutation orders, V_{con1} and V_{con2}, and the voltages in the input capacitors, V_{CR1} and V_{CR2}:

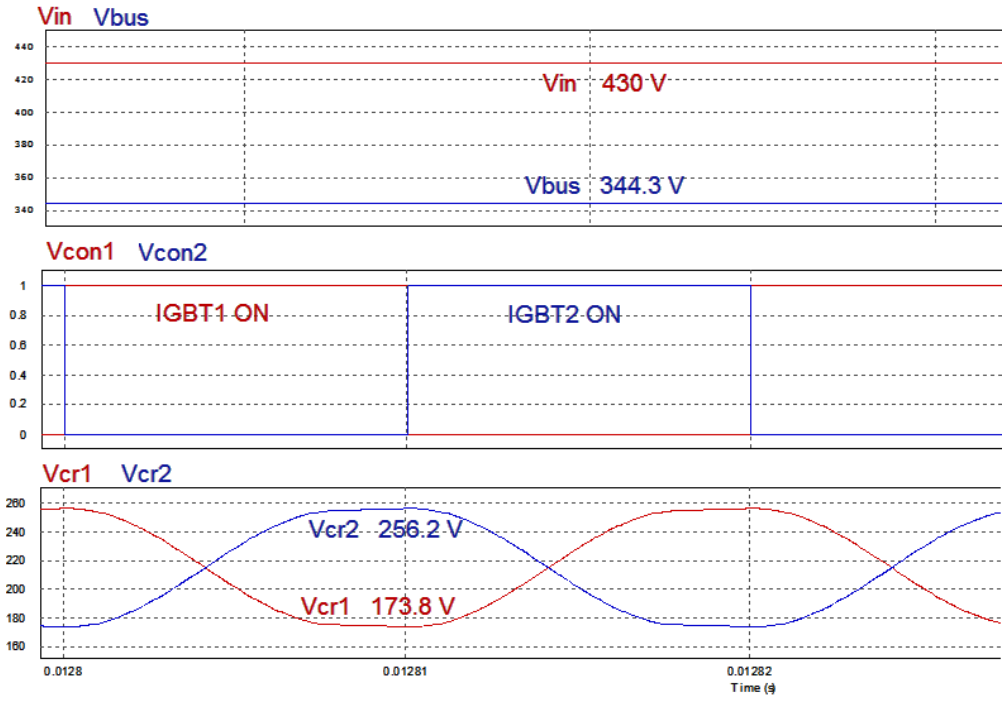

Figure 4.10. *Simulation of Vin, Vbus, Vcon1, Vcon2, Vcr1 and Vcr2*

As it can be seen in the previous Figure 4.10, the values of V_{CR1} and V_{CR2} vary above and below their mean value, 215 V (Vin/2).

The relation between commutation of the IGBTs and the voltages V_{CR1} and V_{CR2} can be deduced:

- When IGBT1 ON and IGBT2 OFF → VCR1 decreases while VCR2 increases.
- When IGBT1 OFF and IGBT2 ON → VCR1 increases while VCR2 decreases.

The next step consists on analyzing the resonant currents in the converter, shown in Figure 4.11. The maximum value of Ires is 45.16 A, almost the same that the value obtained theoretically with equation (4.15).

Because of the resonance, there is a time every period when the current is almost zero. The remaining value observed is the correspondent to the current flowing through the magnetization inductor Lm and its parallel branch where Rc is. However the current in Rc is too small to be taken into account.

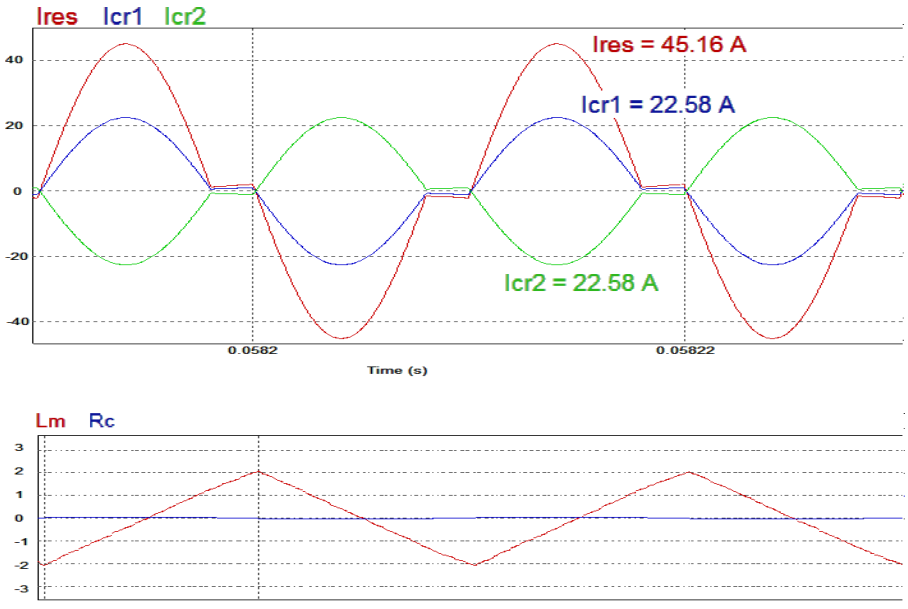

Figure 4.11. *Resonant currents with their peak values and currents trought Lm and Rc*

In the following Figure 4.12 the voltages in both sides of the transformer, when considered ideal, are shown. It can be seen that the secondary side have higher voltages, and that there is voltage drop at the end of every semi-period, when the resonant current becomes almost zero. This voltage drop is the correspondent to the voltage in the inductor Lr, since when the current circulating through it will be minimal and its voltage will become close to zero.

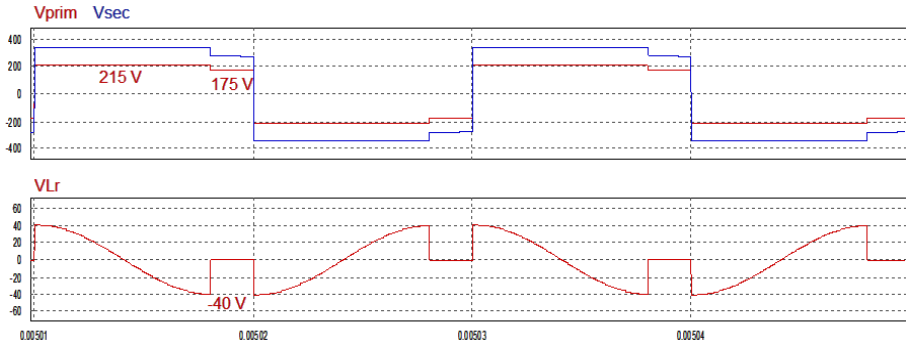

Figure 4.12. *Ideal transformer voltages seen in the primary and secondary side and voltage in Lr.*

- *Analysis of the magnetization current, I_{Lm}*

The next study consists on analyzing both the resonant and the magnetization currents for different magnetization inductances.

Firstly, the system has been simulated for a magnetization inductor with a value of 0.5mH.

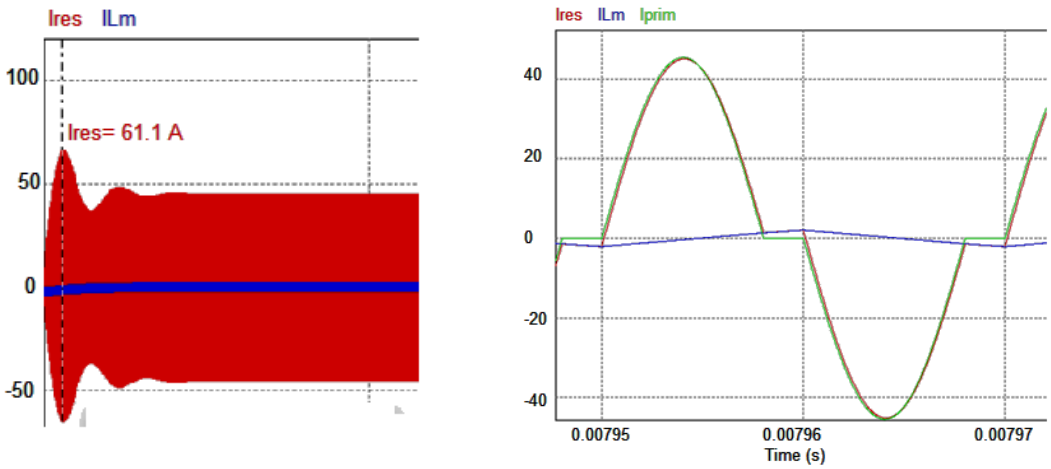

Figure 4.13. Resonant current and current though Lm when Lm=0.5 mH

In the left part of Figure 4.13, Ires achieves a peak of current of 61 A at the beginning, during the transient state. On the other hand, when it achieves the permanent state, the maximum current is 42.5 A.

In addition, in the right picture of Figure 4.13, it is very easy to observe that at the end of every semi-period the value of Ires that remains is equal to I_{Lm}. Therefore, at that moment the current in the primary side of the transformer, Iprim, will be zero.

After this simulation, the value of the magnetization inductor equal to 0.5 mH has been proved good experimentally, since it is not too small nor too big; if this value were lower, the variation of the current I_{Lm} in Ton would be much bigger, and the resonant current seen would not reach a zero value (the soft switching wouldn't be achieved).

Afterwards, other values of Lm have been simulated in order to prove that the chosen value is correct.

I. TRYING LOWER VALUES OF Lm

Firstly, the value of Lm tested was 0.1mH. In Figure 4.14, it can be observed that the peak in the transient state is much bigger than in the previous case, approaching values such us 150 A.

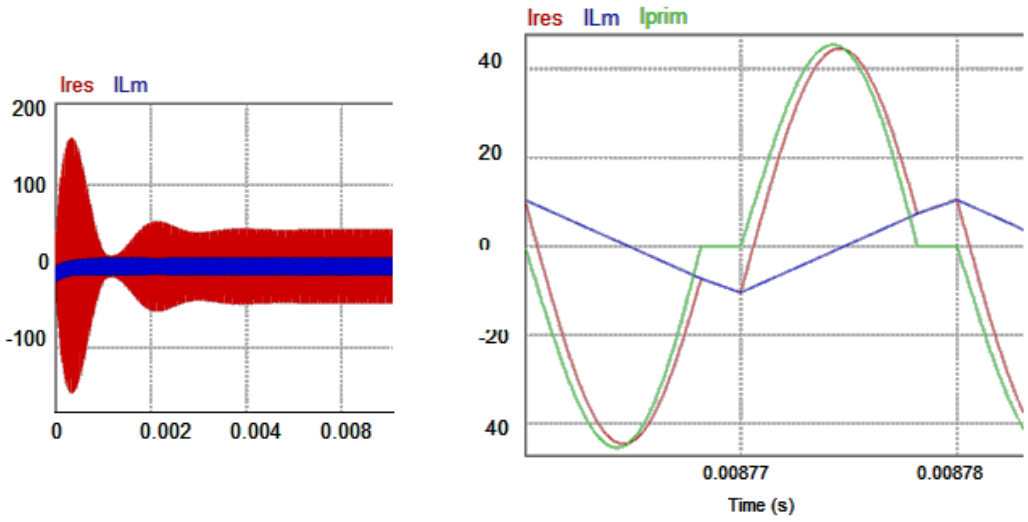

Figure 4.14. *Resonant current and current though Lm when Lm=0.1 mH*

On the other hand it can also be seen that the current ILm is bigger than before (here the ILm takes values of 10 A, while in the previous example the peak value was smaller than 3.5 A.

The next value simulated has been 10 µH. In this case, the peak at the beginning reaches 630 A, as seen in Figure 4.15.

During the permanent state, it can be seen that the value of the peak of ILm is even bigger than the sinusoidal peak of Ires. Since the main objective of having a resonance is to be able to commutate the switches at almost zero values, it can be confirmed that such a low value of Lm is negative for the purposes of the converter.

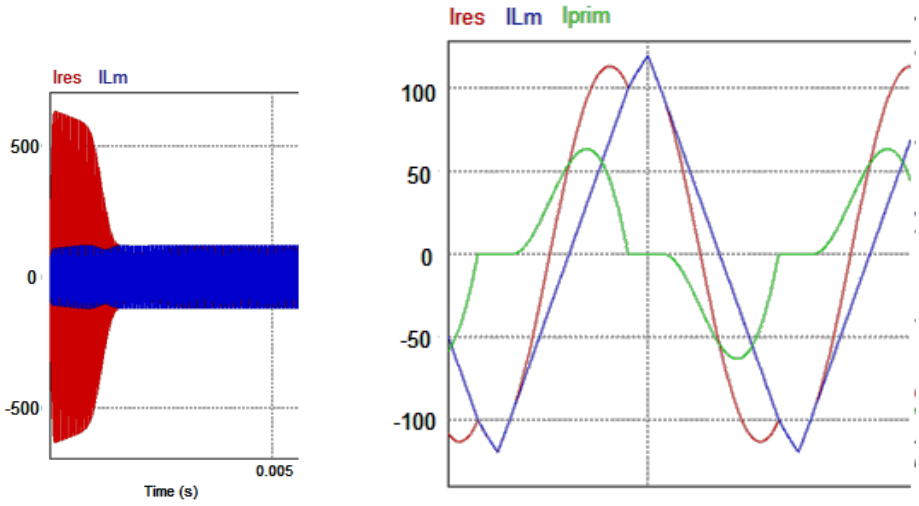

Figure 4.15. *Resonant current and current though Lm when Lm=10 µH*

II. TRYING HIGHER VALUES OF Lm

The following simulation has been done for a value of Lm equal to 5mH, whose results are stored in Figure 4.16.

In this case, the initial peak is 60 A. furthermore, the current in the primary side of the transformer is equal to the resonance current, since the current thought the magnetization inductor is almost zero, and a bit lower than the value had in Figure 4.13.

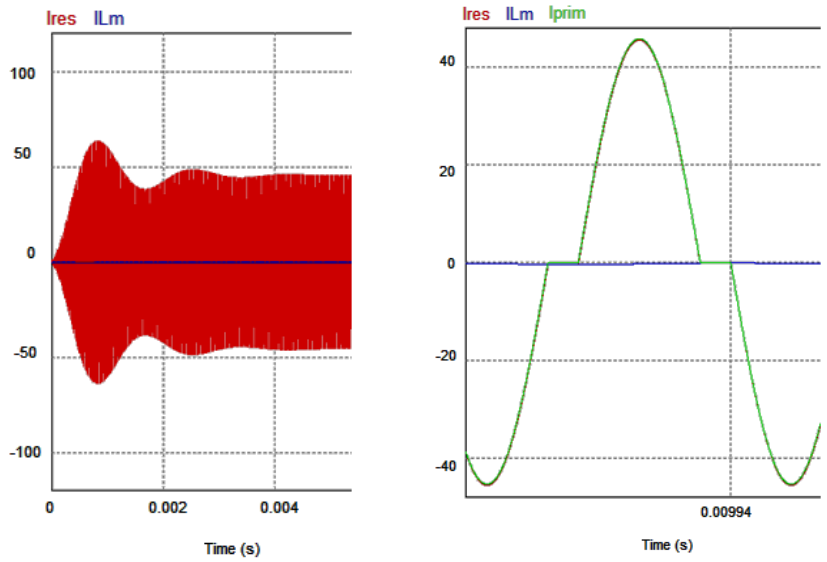

Figure 4.16. *Resonant Current and Current though Lm when Lm=5mH*

To sum up, the values analyzed in this study are stored in the following table:

Lm (mH)	Ires,peak (A)	Ires, steady (A)	Iprim (A)	ILm (A)
50	60	45	45	0.02
5	60	45	45	0.4
0.5	**61**	**45**	**45**	**3.5**
0.1	150	47	49	10
0.01	630	116	65	120

Table 4.3. *Influence of the value of Lm on the currents of the system*

The chosen value of the magnetization inductor, 0.5 mH, has been proved as correct since the current trough it is neither too high not too low. For high currents, as happens for lower values of Lm, the soft-switching cannot be performed, while for very low currents, as happens for higher values, the commutation of the IGBTs cannot be done.

This intermediate stage is not controlled and its currents and voltages values depend on the controls implemented in the Boost and H-Bridge inverter.

4.2.2. ON GRID CONNECTION: ANALYSIS AND SIMULATION

The next step consists on connecting the output of the resonant converter to the grid. Since this output, Vbus, is a DC wave, it will be inverted in a DC/AC H-Bridge converter to achieve a 50 Hz sinusoidal wave.

In the following Figure 4.17, the circuit implemented in PSIM is shown. It also includes the control of the H-Bridge.

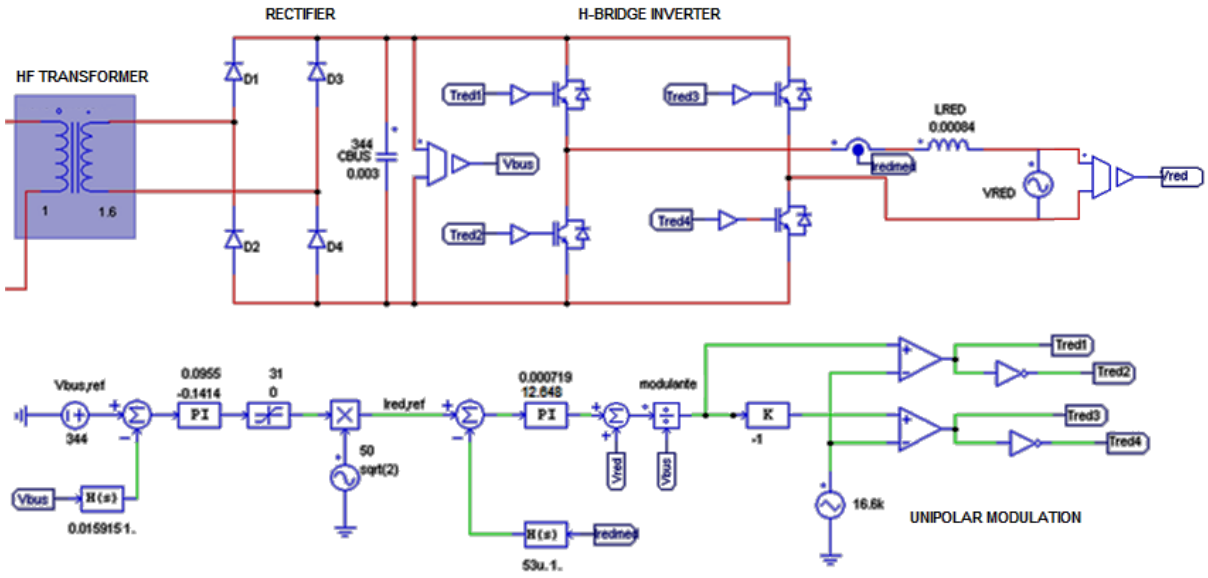

Figure 4.17. *On grid connection of the system using an H-bridge inverter*

As the H-Bridge is a buck converter, the value of Vbus must be bigger than the peak value of the grid voltage.

$$Vbus \geq 230 \cdot \sqrt{2} = \ 325.26\ V \tag{4.16}$$

As defined in Section 4.2.1, the desired value is close to 344 V.

4.2.2.1. H-Bridge Control

In order to implement the control needed to make the H-Bridge operate correctly, an external voltage loop and an internal current loop must be defined. The voltage loop will be the responsible for regulating the resonant converter's output voltage, Vbus. Furthermore, it will generate a current reference introduced in the current loop. This last loop will regulate the current delivered to the electricity grid, Igrid.

On the other hand, to ensure the correct operation of the control loops, the internal loop must be at least one decade faster than the voltage loop, since the generated Iref must be seen as constant.

Finally, the PI controller of the current loop will generate a control wave Ucom that will be used for doing a Pulse Width Modulation. This modulation consists on comparing the control wave with a triangular wave, Vtri, generated at the commutation frequency required for the IGBTs, 16.6 kHz. Depending on the values of Ucom and Vtri, different pulses will be created, and those will be the switching signals of the Inverter IGBTs.

The H-Bridge converter will comprise 4 IGBT switches, as shown in Figure 4.26. In order to control them, it's possible to use two different PWM methods:

I. Bipolar modulation

This kind of modulation is the easiest one, since the switches are separated into two pairs, composed by the diagonal transistors, and so only one modulation signal must be generated.

As an advantage, it can be mentioned that this method doesn't generate variations in the common mode voltage, Vcm, provided that the harmonic components have a 180° offset, and as a consequence common mode currents won't be generated.

However, the principal disadvantage of this method is that the current harmonics are bigger (in fact, they will be twice the value obtained in the next method). Furthermore, the value of the inverter's inductor must be four times bigger than the proposed in the following modulation.

II. Unipolar modulation

This commutation method is the one used our simulation. It has been chosen principally in order to have smaller harmonics. This modulation works at twice the commutation frequency.

In this case, the switches don't commutate in anti-parallel, but each pair separately, and so two different commutation signals must be created.

Furthermore, common mode currents are generated.

- *CURRENT LOOP*

In order to obtain a sinusoidal wave at the output of the inverter, a current control loop has to be implemented. This control loop works with a reference current adjusted to the grid current's properties.

The duty cycle of this kind of modulation, taking into account that it works at a frequency F=2·Fcom, can be expressed as follows:

$$\frac{Ton}{Tcom/2} = \frac{Ton}{T} = \frac{Ucom}{Vtri} = D = \frac{M}{Vtri} sen\left(2\pi \cdot f_{grid} \cdot t\right) \tag{4.17}$$

To achieve the model of the H-Bridge converter, shown in Figure 4.18, the voltages relation at its output is used:

$$v_{Linv} = v_{grid} - v_{AB} \tag{4.18}$$

By definition, the voltage in an inductor can be expressed as:

$$v_L = L_{inv} \cdot \frac{di_{Linv}}{dt} = L_{inv} \cdot \frac{di_{grid}}{dt} \tag{4.19}$$

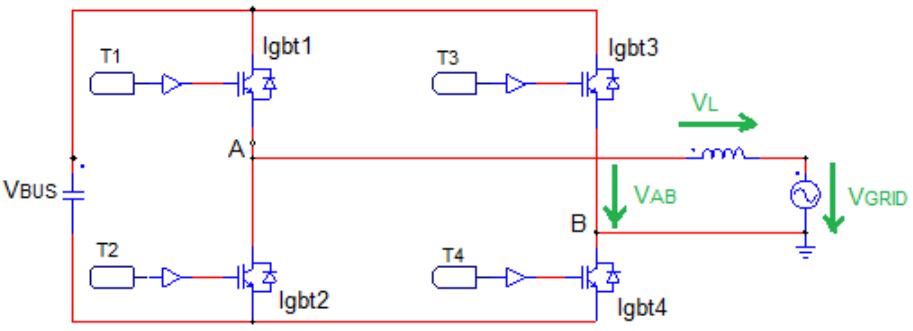

Figure 4.18. *H-Bridge Inverter and its output voltages*

Furthermore, the mean value of V_{AB} for a commutation period can be expressed in function of the duty cycle D and the input voltage V_{bus}:

$$\langle v_{AB} \rangle_T = v_{grid} = V_{bus} \cdot D \tag{4.20}$$

Combining the previous equations (4.18), (4.19) and (4.20) the Inverter can be modeled in the s-domain as:

$$I_{grid} = \frac{1}{Linv \cdot s} \cdot \left(V_{grid} - V_{bus} \cdot D \right) \tag{4.21}$$

From this expression we can obtain the model of the inverter, which will therefore be dependent on the duty cycle D.

- **Calculation of the Inverter Inductor Value**

The ideal behavior of the H-Bridge converter consists on giving to the grid all the power generated by the system. Therefore the following equation must be satisfied:

$$Pin = Pout \cong 5\ kW \tag{4.22}$$

The current ripple on the inductor delivered to the grid must not exceed a certain value, which has been imposed to 10%.

$$\int_0^{ton} di_{Linv} = \Delta i_L = \frac{1}{L_{inv}} \int_0^{ton} (V_{bus} - v_{grid}) \, dt \tag{4.23}$$

As it can be seen, the DC bus voltage, Vbus, has been considered constant because for the time evaluated it hardly changes.

Furthermore, the current ripple is dependant to the duty cycle, and it will be maximized when D=0.5:

$$\Delta i_{Linv} = \frac{(V_{DC} - v_{grid}) \, t_{on}}{L_{inv}} = \frac{(V_{DC} - v_{grid}) \, D \cdot T}{L_{inv}} = \frac{V_{DC} \cdot (1 - D)D}{2 \cdot L_{inv} \cdot F_{com}} = 0.1 \cdot I_{Linv} \tag{4.24}$$

The maximum current that can flow through the inductor is:

$$I_{Linv,max} = I_{L,ef} \cdot \sqrt{2} = \frac{P_{out}}{V_{grid}} \cdot \sqrt{2} = \frac{5000 \, W}{230 \, V} \cdot \sqrt{2} = 30.74 \, A \tag{4.25}$$

Therefore, the maximum current ripple permitted is:

$$\Delta i_{L,max} = \frac{V_{DC} \cdot (1 - 0.5)0.5}{2 \cdot L_{inv,min} \cdot F_{com}} = I_{Linv,max} \cdot 0.1 = 3.07A \tag{4.26}$$

From the previous equation we can deduce the value of the inductor as follows:

$$L_{inv,min} = \frac{V_{DC}}{8 \cdot \Delta i_{L,max} \cdot fcon} = \frac{344 \, V}{8 \cdot 3.07 \, A \cdot 16600 \, Hz} = 8.43 \cdot 10^{-4} \, H \tag{4.27}$$

Another advantage of using a unipolar modulation instead of a bipolar one is, as said before, that the value of the inductor is four times smaller.

- **Transfer function of the system**

The transfer function used to model the PI controller of the current loop is:

$$PI(s) = K_p \cdot \frac{T_n \cdot s + 1}{T_n \cdot s} \tag{4.28}$$

Where:

Kp is the proportional constant

Tn is the ratio of Kp/Ki, being Ki the integral constant

The transfer function of the sensor is:

$$S(s) = \frac{K_{sc}}{\tau_{sc} \cdot s + 1} \tag{4.29}$$

Where:

Ksc is the current sensing constant

τ_{sc} is the current sensing time constant

The transfer function of the inverter with its modulation is:

$$I(s) = \frac{V_{bus}}{V_{tri}} \cdot \frac{1}{L_{inv} \cdot s} \tag{4.30}$$

Therefore, the transfer function of the whole system, in open loop is:

$$L(s) = K_p \frac{T_n \cdot s + 1}{T_n \cdot s} \cdot \frac{V_{bus}}{V_{tri}} \frac{1}{L_{inv} \cdot s} \cdot \frac{K_{si}}{\tau_{si} \cdot s + 1} \tag{4.31}$$

- **Calculation of the PI parameters:**

The next step consists on calculating the unknown transfer function L(s) parameters. The sensor constants will be given, and the inverter parameters have already been calculated. Therefore, the unknown parameters left are the correspondent to the PI controller, namely Kp and Tn.

For that, the phase margin and the cut-off frequency of the loop must be known:

- $PM = 50°$
- $Fcg = 2000Hz \quad \rightarrow \quad \omega_{gc} = 4000\pi rad/s$

The parameters needed to obtain Kp and Tn are:

- $K_{si} = 1$
- $F_{si} = 3000\ Hz \ \rightarrow \ \omega_{sc} = 2\pi \cdot F_{si} = 6000\pi \frac{rad}{s} \ \rightarrow \ \tau_{sc} = \frac{1}{\omega_{si}} = 5.3 \cdot 10^{-5}$ s
- $V_{tri} = 1\ V$
- $V_{bus} = 344\ V$
- $F_{com} = 16600\ Hz$
- $L_{inv} = 8.43 \cdot 10^{-4}\ H$

The control loop can be done including or not a compensation for the grid voltage, as we well see in the following lines.

A) Without V_{grid} compensation

The block diagram of this control is shown in the following figure:

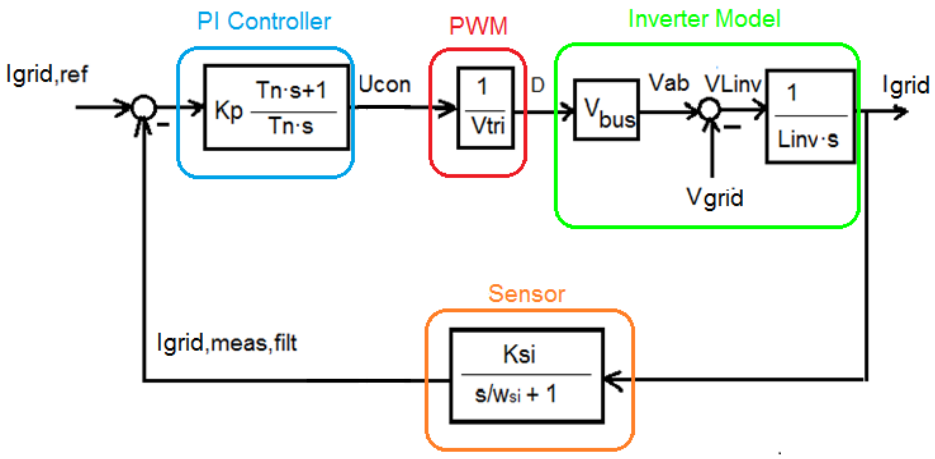

Figure 4.19. *Block diagram of the current loop without Vgrid compensation*

This block diagram can be expressed as a transfer function, as done in equation (4.31).

The time constant Tn can be obtained as follows:

$$PM = 50° = arctg(T_n \cdot \omega_{gc}) - arctg(\tau_{sc} \cdot \omega_{gc}) \ \rightarrow \ Tn = 0.72\ ms \qquad (4.32)$$

Knowing that the absolute value of the open loop for the cut-off frequency is equal to 1, the proportional constant can be obtained:

$$\left|L(j\omega_{gc})\right| = 1 = \frac{K_p \cdot V_{bus} \cdot K_{sc}}{T_n \cdot V_{tri} \cdot L_{inv} \cdot \omega_{gc}{}^2} \sqrt{\frac{(T_n \cdot \omega_{gc})^2 + 1}{(\tau_{sc} \cdot \omega_{gc})^2 + 1}} \rightarrow K_p = 0.0368 \qquad (4.33)$$

The aim of the current loop is achieving a grid current, Igrid, equal to the reference current at every moment. Both this currents have been simulated in order to see how accurate is the control loop implemented. The results are shown in the next figure:

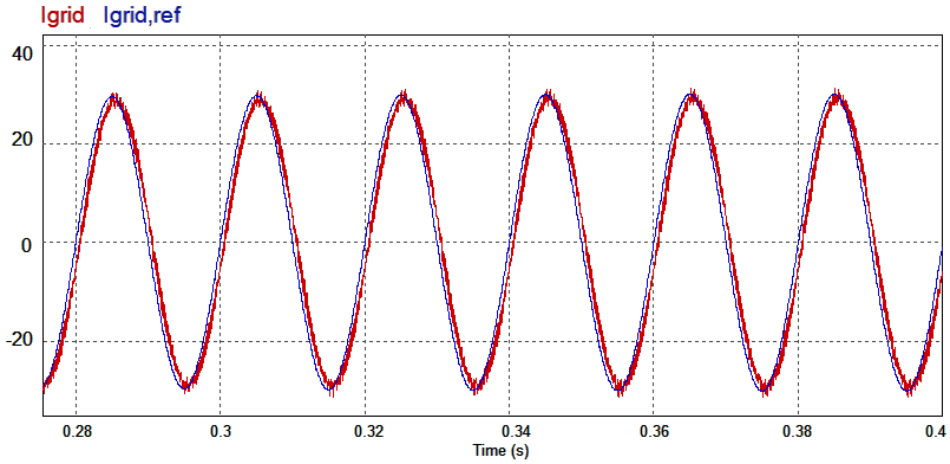

Figure 4.20. *Simulation of the current loop input and output without Vgrid compensation*

It can be noted that the grid current is delayed from the reference current, and this is caused by the perturbation of the grid voltage, which is not constant. In order to achieve a better current tracking, the following loop is implemented.

B) With V_{grid} compensation

The block diagram of this control is shown in Figure 4.21.

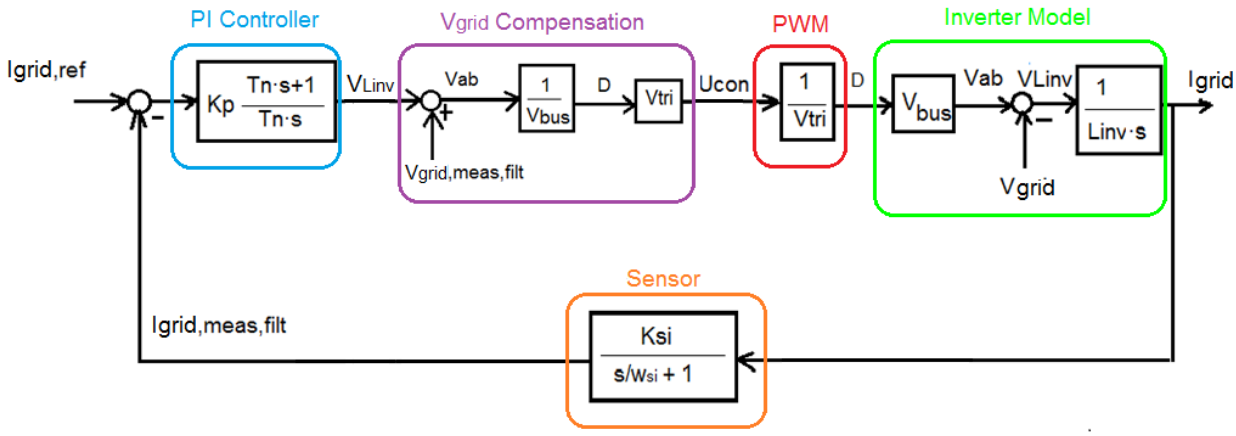

Figure 4.21. *Block diagram of the current loop with Vgrid compensation*

After adding the compensation, the transfer function for the system in open loop is:

$$L(s) = K_p \frac{T_n \cdot s + 1}{T_n \cdot s} \cdot \frac{1}{L_{inv} \cdot s} \cdot \frac{K_{si}}{\tau_{si} \cdot s + 1} \tag{4.34}$$

Like in the previous sub-paragraph A), the Tn and Kp parameters are obtained:

$$PM = 50° = arctg(T_n \cdot \omega_{gc}) - arctg(\tau_{sc} \cdot \omega_{gc}) \;\rightarrow\; T_n = 0.72\, ms \tag{4.35}$$

$$\left|L(j\omega_{gc})\right| = 1 = \frac{K_p \cdot K_{sc}}{T_n \cdot V_{tri} \cdot {\omega_{gc}}^2} \sqrt{\frac{(T_n \cdot \omega_{gc})^2 + 1}{(\tau_{sc} \cdot \omega_{gc})^2 + 1}} \;\rightarrow\; K_p = 12.65 \tag{4.36}$$

The loop input and output currents have been simulated as well, and the current tracking is shown in Figure 4.22.

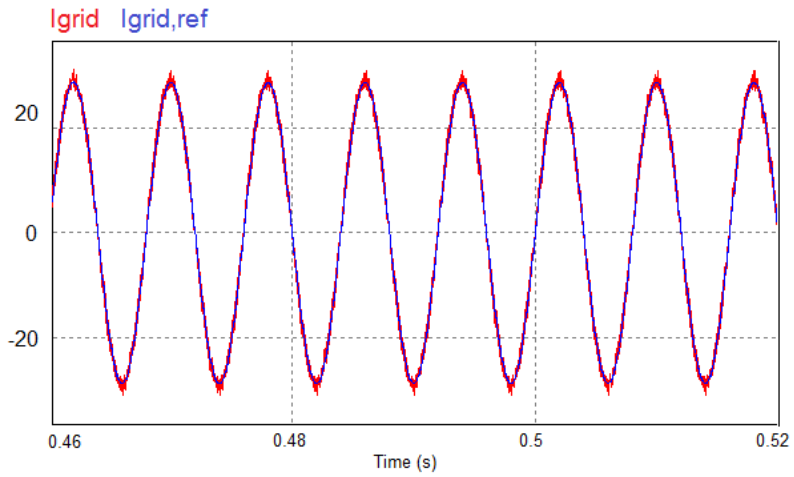

Figure 4.22. *Simulation of the current loop input and output without Vgrid compensation*

It can be noted that in this case the grid current follows the reference current much more closely, so it can be assumed that this control is more accurate that the implemented before.

- *VOLTAGE LOOP*

As told before, the DC Bus Voltage Vbus must be controlled, since it is important that its value remains constant. Furthermore, the reference current for the Current Loop must be generated. Both this actions are achieved implementing a Voltage Loop.

Supposing the power constant through the inverter, a mean power balance is done where the input P_{DC} and output P_{AC} powers are equal. Afterwards, the current flowing though the DC Bus can be calculated:

$$P_{AC} = P_{DC} \quad \rightarrow \quad V_{rms} \cdot I_{rms} = V_{DC} \cdot I_{DC} \quad \rightarrow \quad I_{DC} = \frac{V_{rms} \cdot I_{rms}}{V_{DC}} \tag{4.37}$$

Having into account the relation between the input current of th Inverter, shown in Figure 4.23, the current flowing though the Bus capacitor can be calculated:

$$i_c = i_{ext} - i_{DC} \tag{4.38}$$

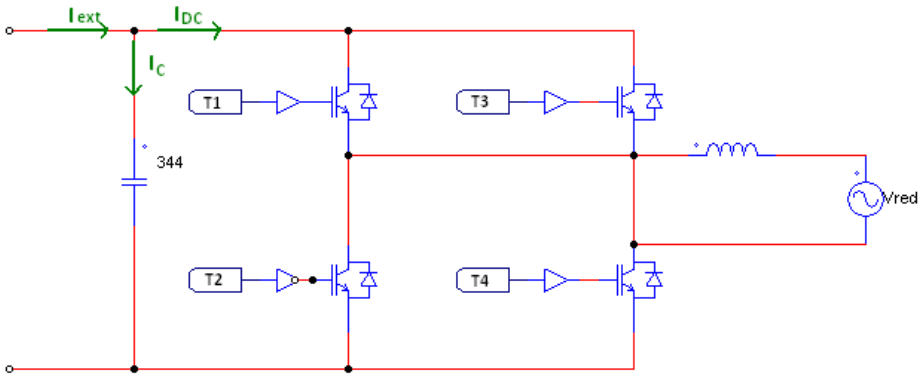

Figure 4.23. *Inverter input currents relation*

Moreover, the current flowing thought the H-Bridge capacitor can be expressed as:

$$i_c = \frac{dv_{DC}}{dt} \tag{4.39}$$

Finally, after combining equation (4.63) and (4.64), the DC Bus voltage can be defined, in the S-Domain, as:

$$V_{bus}\ (s) = \frac{1}{C_{bus}\cdot s}[\ I_{ext}\ (s) - I_{DC}\ (s)\ ] \tag{4.40}$$

The voltage loop analyzed comprises a PI Controller, an internal and faster current loop (evaluated in the previous sub-section), the model of the Inverter and a sensor, as shown in the following figure:

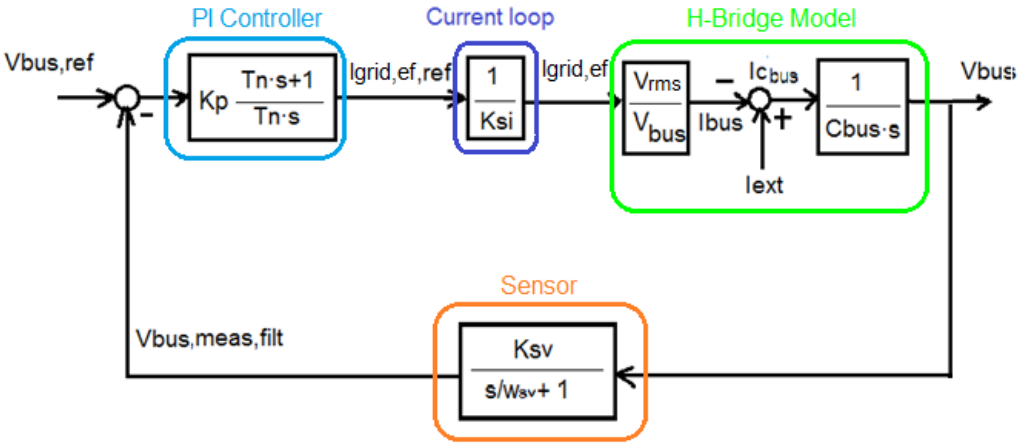

Figure 4.24. *Block diagram of the Voltage Loop of the H-Bridge Inverter*

The internal current loop could be modeled with its closed loop transfer function. However, as this internal loop is much faster than the voltage loop evaluated now, it can be modeled with just a constant block.

Finally, the open loop transfer function for the voltage control of the H-Bridge inverter is:

$$L(s) = K_p \frac{T_n \cdot s + 1}{T_n \cdot s} \cdot \frac{1}{K_{si}} \cdot \frac{V_{ef}}{V_{bus}} \cdot \frac{1}{C_{bus} \cdot s} \cdot \frac{K_{sv}}{\tau_{sv} \cdot s + 1} \tag{4.41}$$

- **PI Controller Parameters**

The sensor and the H-Bridge parameters are already known, so the next step consists on calculating the PI controller parameters, namely Kp and Tn.

The known parameters are:

- $Cbus = 3\ mF$
- $Ksv = 1$
- $Fsv = 10\ Hz \quad \rightarrow \quad \omega_{sv} = 2\pi \cdot Fsv = 20\pi \frac{rad}{s} \quad \rightarrow \quad \tau_{sv} = \frac{1}{\omega_{sv}} = 0.0016\ s$
- $V_{tri} = 1\ V$
- $V_{rms}/V_{bus} = 1/\sqrt{2}$

Furthermore, the values of the phase margin and the cut-off frequency must be given:

- $F_{gc} = 5\ Hz \quad \rightarrow \quad \omega_{gc} = 10\pi rad/s$
- $PM = 45°$

Finally, the phase margin and the proportional constant are obtained:

$$PM = 45° = arctg\left(T_n \cdot \omega_{gc}\right) - arctg\left(\tau_{sv} \cdot \omega_{gc}\right) \quad \rightarrow \quad T_n = 0.0955\ s \tag{4.42}$$

$$\left|L\left(j\omega_{gc}\right)\right| = 1 = \frac{K_p \cdot V_{ef} \cdot K_{sv}}{T_n \cdot K_{si} \cdot V_{bus} \cdot C_{bus} \cdot {\omega_{gc}}^2} \sqrt{\frac{\left(T_n \cdot \omega_{gc}\right)^2 + 1}{\left(\tau_{sv} \cdot \omega_{gc}\right)^2 + 1}} \quad \rightarrow \quad K_p = 0.141 \tag{4.43}$$

4.2.2.2. Simulation results for the H-Bridge converter

To analyze the behavior of the H-Bridge Converter that enables the connection of the system to the grid, the whole power conversion block, which comprises the Boost, the DC-DC Resonant converter and the H-Bridge Inverter, has been simulated in PSIM.

I. Pulse Width Modulation

In the following Figure 4.25, the waves corresponding to the commutation signals are generated. Part a) corresponds to a further taken picture, where the grid frequency can be observed paying attention to the commutation signal frequency. On the other hand, parts b), c) and d) are taken more closely in order to see how the switching signals are generated from the comparison of the commutation signals and the triangular wave.

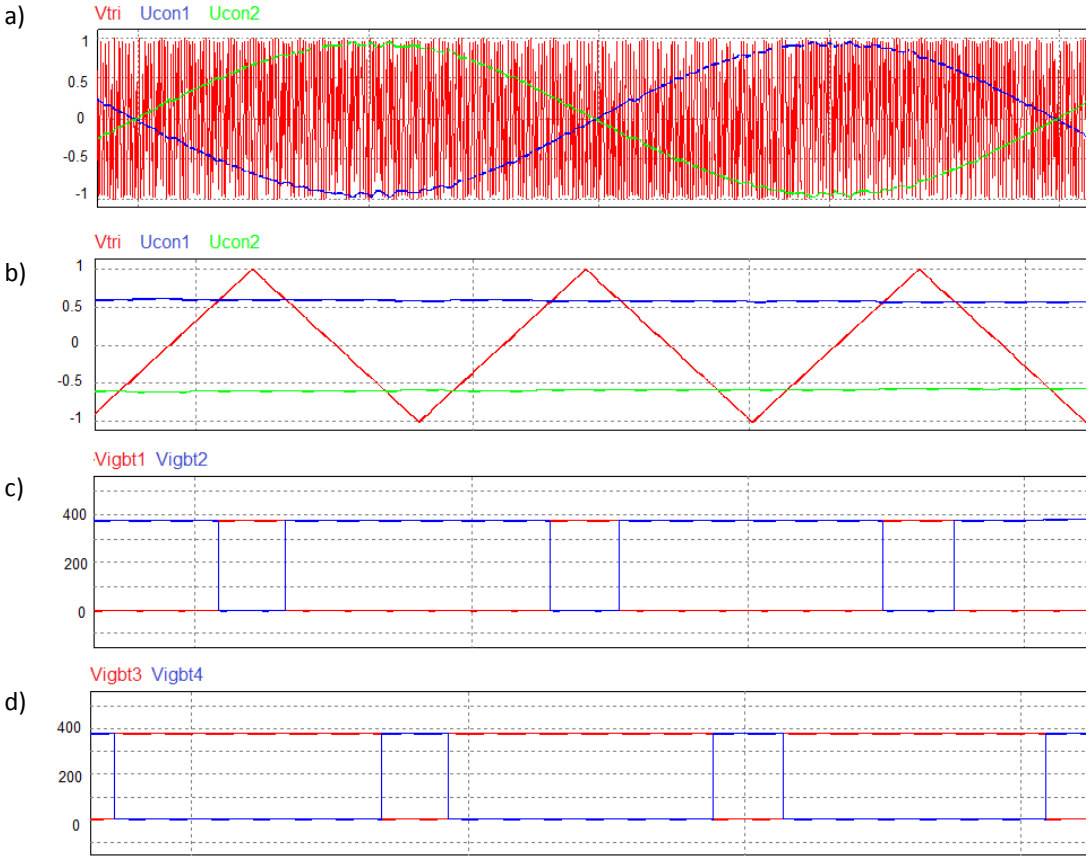

Figure 4.25. *Unipolar modulation and switching signals*

The switching commands obtained with this modulation are:

i. $Ucon1 > Vtri \rightarrow IGBT1\ ON\ \&\ IGBT2\ OFF$

ii. $Ucon1 < Vtri \rightarrow IGBT1\ OFF\ \&\ IGBT2\ ON$

iii. $Ucon2 > Vtri \rightarrow IGBT3\ ON\ \&\ IGBT4\ OFF$

iv. $Ucon2 < Vtri \rightarrow IGBT3\ OFF\ \&\ IGBT4\ ON$

II. Grid Voltage and Current

The current and voltage of the electricity grid has been simulated in Figure 4.26. It can be noted that both of them are sinusoidal and with a frequency of 50Hz (T=20 ms).

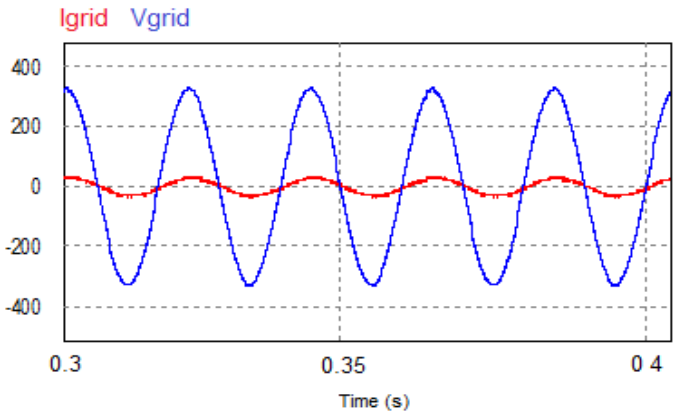

Figure 4.26. *Simulation of the Grid Voltage and Current*

4.2.3. BOOST CONVERTER: ANALYSIS AND SIMULATION

The output of the fuel cells is a low voltage that must be increased before connecting them to the DC/DC resonant converter. Therefore, a Boost converter is used. This Boost comprises an inductance L_{boost} of 0.75 mH at its entry, a diode D0 and an IGBT switch for the commutation, and a capacitor $C_{out,boost}$ of 80 µF at its output. The output of the boost must be 430 V, which is the DC/DC resonant converter's input we decided before.

The implementation in PSIM of this converter, as well as its control, is shown in the following Figure 4.27.

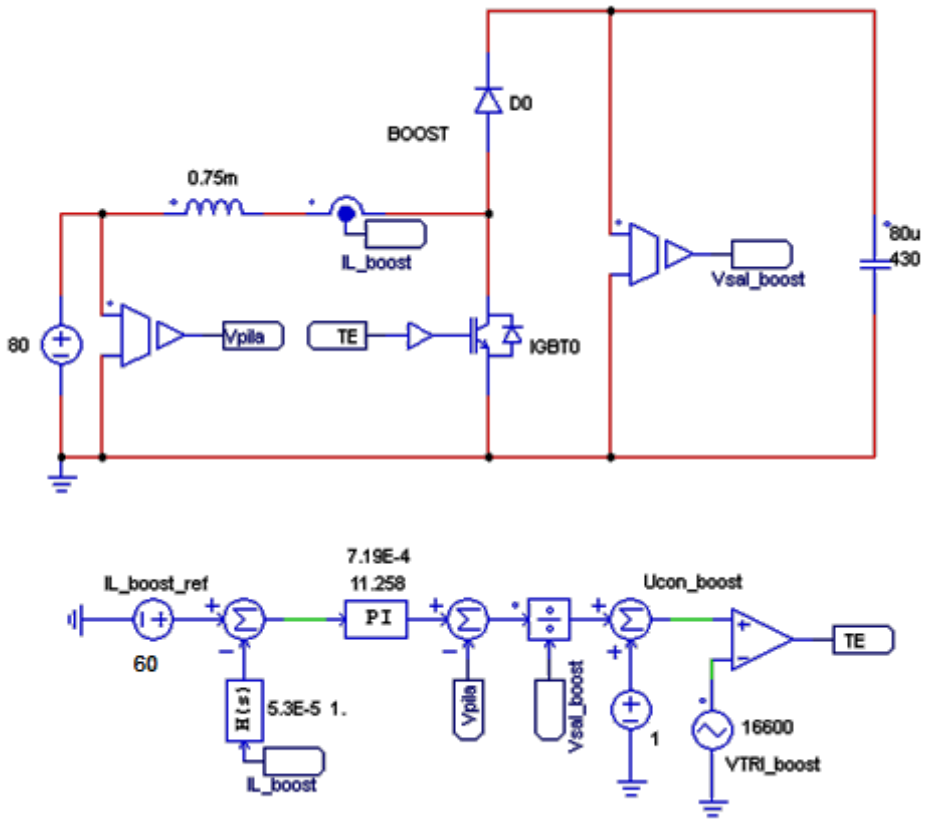

Figure 4.27. *Boost and its control*

In order to obtain the desired output, a current control loop like the one seen above must be implemented. Furthermore, this converter is the responsible of regulating the operating point of the fuel cells.

The system is designed for a nominal power of 4.8 kW, which is the maximum power that can be delivered by the FCs. As the highest current delivered by the fuel cells is 60A (Chapter 2), they are modeled as an input voltage source of 80 A.

4.2.3.1. Boost Control Loop

Given a certain value of input voltage, it is necessary to control the current flowing though the Boost Inductor, Lboost, provided that this current will be the given by the FCs when the whole system is connected. For that, a current loop as the shown in Figure 4.38 has been implemented. The output signal of the control loop is the control voltage Ucom that will be introduced in the PWM to create the switching commands for the IGBT.

The commutation frequency will be 16.6 kHz. The time when the IGBT is turned on will be called Ton, whereas when it is turned off, it will be called Toff. On the other hand, the diode operates complementary, so it will be conducing current during Toff.

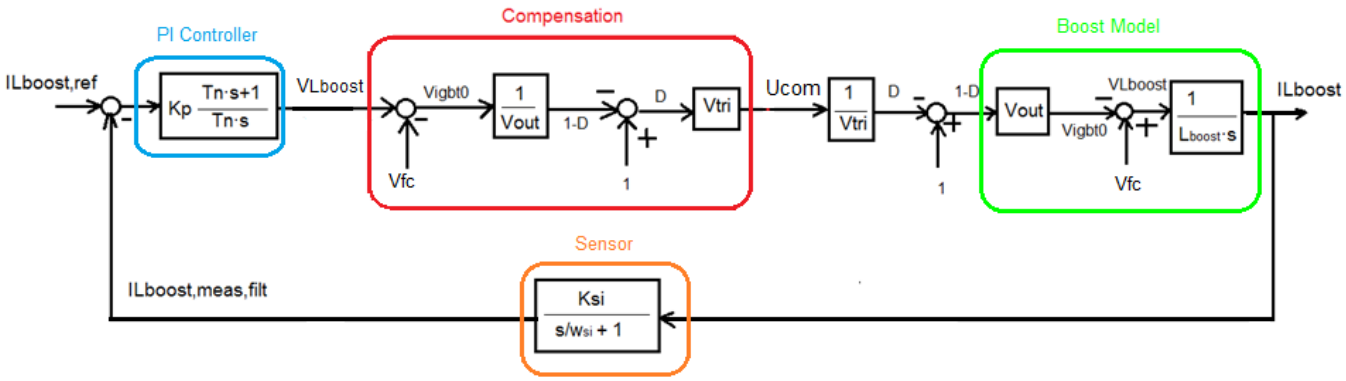

Figure 4.28. *Block diagram of the Boost Control Loop*

It can be noted that the control of the current is done in a closed loop.

The plant of the Boost is modeled as shown in "Boost model" of Figure 4.28. the delivered voltage from the fuel cells, Vfc, is considered a perturbation since it changes not linearly with the delivered current. In order to avoid that this variation affects the system, it must be compensated in the control, as shown in Figure 4.28.

In the PSIM simulation the current flowing though the inductor will be measured, and after being filtered, it will be compared to the reference current of 60 A in order to obtain the control error, which will enter the PI controller to achieve a more accurate tracking.

- **Calculation of the PI Parameters**

The transfer function of the current loop can be easily obtained from the block diagram shown in Figure 4.28. It will be as follows:

$$|L(s)| = K_P \frac{T_n \cdot \mathrm{s} + 1}{T_n \cdot \mathrm{s}} \cdot \frac{1}{L_{boost} \cdot \mathrm{s}} \cdot \frac{K_{si}}{\tau_{si} \cdot \mathrm{s} + 1} \tag{4.44}$$

The operation characteristics of the loop are:

- Phase margin: $PM = 50°$

- Gain cross frequency: $F_{gc} = 2000\ Hz \quad \rightarrow \quad \omega_{gc} = 4000\pi\ rad/s$

All the parameters that must be known are shown in the transfer function (4.16). The ones corresponding to the sensor are given, as well as the ones for the Boost:

- $Lboost = 0.75\ mH$
- $Ksi = 1$
- $Fsi = 3000\ Hz \ \rightarrow \ \tau_{si} = \frac{1}{2\pi F_{si}} = 5.3 \cdot 10^{-5}$ s
- $Vout, boost = 430\ V$
- $Vtri = 1\ V$

Therefore, the only parameters left to obtain are the PI constants Kp and Tn, for which the following equations can be used:

$$PM = 50° = arctg(Tn \cdot \omega_c) - arctg(\tau_{si}\omega_c) \ \rightarrow \ Tn = 0.72\ ms \tag{4.45}$$

$$|L(j\omega_c)| = 1 = \frac{K_P \cdot K_{si}}{T_n \cdot L_{boost} \cdot {\omega_c}^2}\sqrt{\frac{(T_n \cdot \omega_c)^2 + 1}{(\tau_{si} \cdot \omega_c)^2 + 1}} \ \rightarrow \ Kp = 11.2586 \tag{4.46}$$

4.2.3.2. Simulation results

First of all, it is important to see if the voltage values are the wanted ones. In Figure 4.39 it is shown that the output value obtained for an input of 80 V, considered when the four fuel cells are working at full load, is 430 V, the required one.

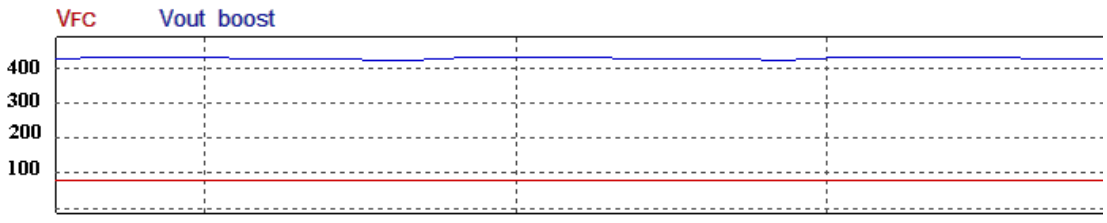

Figure 4.29. *Boost input and output voltage*

Furthermore, it is interesting to see the commutation of the transistor and the duty cycle D obtained. In fact, the duty cycle is quite big in order to increase the voltage level so much:

$$D = \frac{Ucom}{Vtri} = Ucon = 1 - \frac{Vin}{Vout} = 1 - \frac{80}{430} = 0.814 \qquad (4.47)$$

The operation of the PWM is also shown:

- When $Vcom > Vtri \rightarrow IGBT\ ON \rightarrow Vigbt = 0\ V$
- When $Vcom < Vtri \rightarrow IGBT\ OFF \rightarrow Vigbt = Vout, boost = 430\ V$

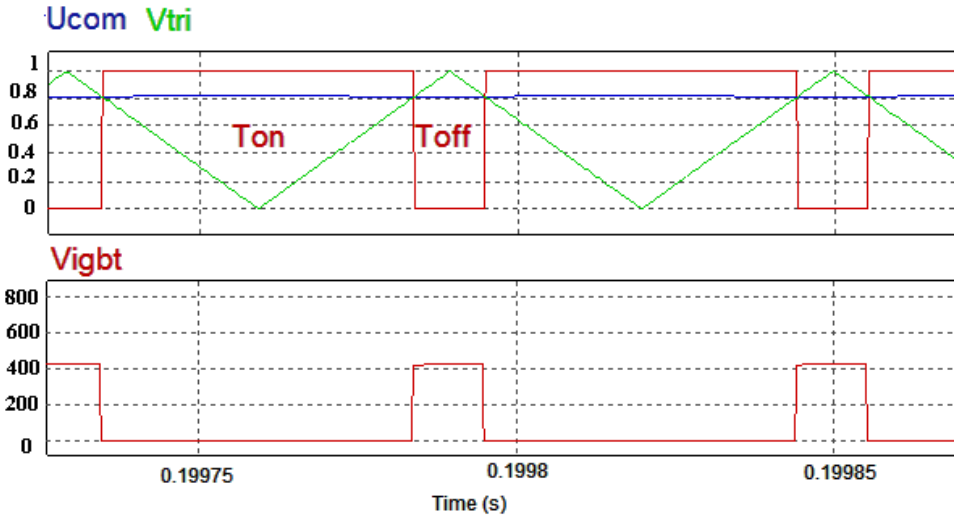

Figure 4.30. *PWM and control signals of the Boost*

Another important aspect to study is the current and voltage in the Boost Inductor, Lboost. In Figure 4.31, the current ripple provoked by the charge and discharge of Lboost can be seen, as well as the voltage VLboost, whose mean value is zero.

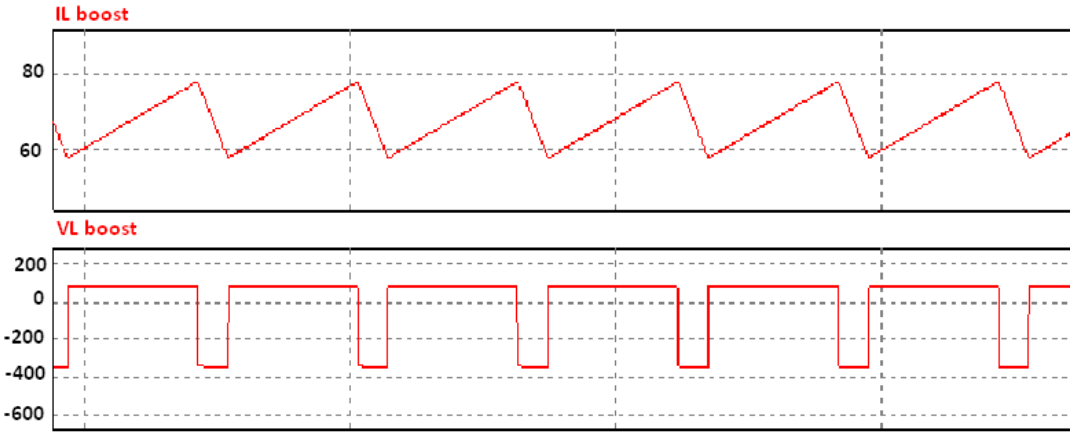

Figure 4.31. *Current and Voltage in the Boost Inductor*

During Ton the inductor is charging, the current flowing though it increases and its voltage is maintained positive. On the other hand, during Toff it is discharging, the current decreases and the voltage is negative.

The current ripple in the boost can be obtained with the following equation:

$$\Delta i_{L,boost} = \frac{V_{out,boost} \cdot (1-D)D}{L_{boost} \cdot F_c} = \frac{430V \cdot (1-0.814)0.814}{0.75mH \cdot 16600Hz} = 5.23\ A \quad (4.48)$$

It is important to consider the fact that when the actual fuel cells are connected to the Boost, the input voltage that here was considered constant, varies. Thus, the duty cycle and the current ripple differs from the calculated before. Therefore, it is important to recalculate the maximum current ripple that can take place in the system. In particular, this maximum ripple will be generated when the duty cycle is minimum, which as deduced from equation 4.47, happens for the maximum voltage delivered by the cells. When there is no load, the voltage given each fuel cell is 33 V, and consequently the maximum voltage delivered by the system, compound by four FCs, is 132V. The minimum duty cycle is:

$$D_{min} = 1 - \frac{V_{in,max}}{V_{out}} = 1 - \frac{132}{430} = 0.693 \quad (4.49)$$

The maximum ripple in the boost inductor can be now calculated:

$$\Delta i_{L,boost,max} = \frac{V_{out,boost} \cdot (1-D_{min})D_{min}}{L_{boost} \cdot F_c} = 7.35\ A \quad (4.50)$$

Furthermore, it must be taken into account that even if in this simulation the entry of the boost is a voltage source, and therefore it is not affected by the current ripple, the whole system will have the FCs at its entry, and this current ripple may cause problems on them. This effect will be deeper analyzed in Chapter 5.

4.2.3.3. Power losses in the Boost

The losses analysis is performed for the highest duty cycle, achieved for the minimum Vfc. That is, for a delivered voltage of 80 V and a duty cycle of 0.814. This is done because this situation presents the maximum losses since the IGBT, which is the elements with more losses, operates during more time.

First of all, the elements that are conducing current at a certain time are going to be analyzed in Figure 4.32:

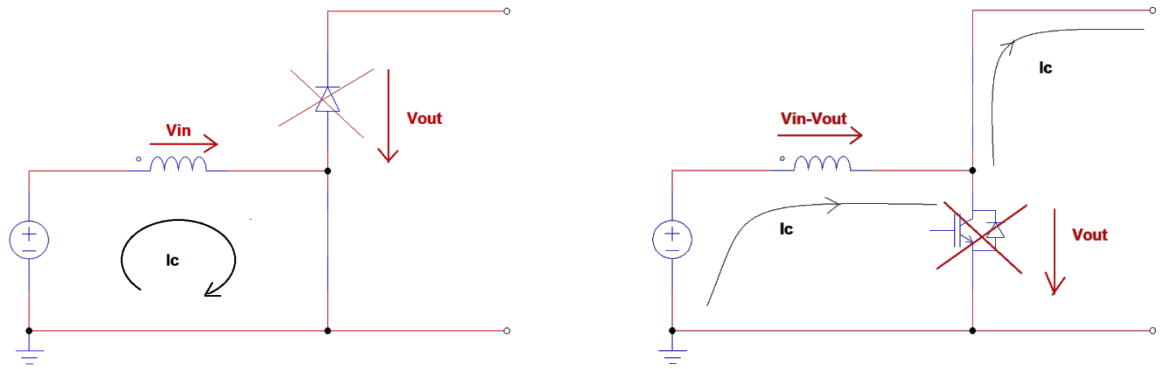

a) For Ton *b) For Toff*

Figure 4.32. *Conducting elements in the Boost*

a) For Ton:

As seen, the transistor is the conducting element during:

$$Ton = D \cdot Tc$$

$$Ton = 0.814 \cdot \frac{1}{16600\ Hz} = 49\,\mu s$$

b) For Toff:

The diode is the element that conducts current during:

$$Toff = Tc - Ton =$$

$$= \frac{1}{16600\ Hz} - 49\,\mu s = 11.24\ \mu s$$

For a certain commutacion period, the elements D0 and IGBT0 will operate as shown in the following figure:

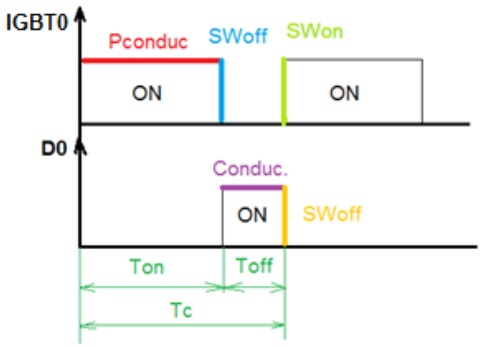

Figure 4.33. *Commutation of the Boost converter elements*

The losses analysis is going to be performed for two different Boost Configurations. The first one is the considered for the simulation, while the second one is the real Boost structure characterized for having two IGBTs.

- *Configuration 1:*

I. Power losses in IGBT0:

In the transistor, there is going to be power losses during the conduction, and both in the switching ON and OFF, as shown in Figure X. Therefore, the total energy lost in a cycle will be:

$$E_{IGBT0} = E_{COND} + E_{SW,OFF} + E_{SW,ON} \tag{4.51}$$

In order to calculate the losses we must take certain values of the IGBT from its data sheet. In the following table the needed parameters are included:

Datasheet	Real circuit
$I_c = 50A$	$I_c = 60A$
$V_{GE} = 15V$	$V_{GE} = 18V$
$V_{CC} = 400V$	$V_{CC} = 430V$
$Tj = 175ºC$	$Tj = 175ºC$

Table 4.4. *IGBT parameters [19]*

It has been considered that the real circuit is the most disadvantageous case, for the maximum current possible to deliver by the cells and the nominal temperature for the IGBT.

a. Conduction losses

First of all, entering in the following graph with the current flowing though the Elevator, $Ic = 60\ A$, and the gate-emitter voltage, $V_{GE} = 18V$, we can obtain a collector-emitter voltage $V_{CE} = 2.2\ V$.

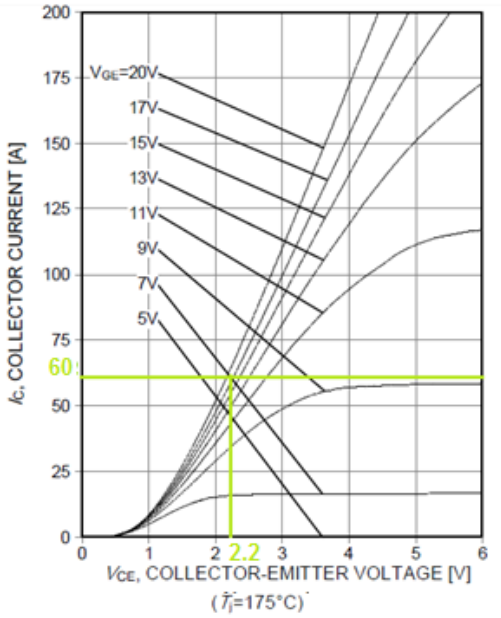

Figure 4.34. *Ic-VCE Characteristic [19]*

The power losses for conduction are therefore:

$$P_{COND} = I_C \cdot V_{CE} = 60\ A \cdot 2.2\ V = 132\ W \tag{4.52}$$

Since these losses occur during Ton, the energy losses for conduction can be deduced as:

$$E_{COND} = P_{COND} \cdot Ton = 132\ W \cdot 49\ \mu s = 6.47 \frac{mJ}{cycle} \tag{4.53}$$

b. Switching losses

The next losses that we are going to analyze are the produced in the switching of the transistor. We are going to take the turn-on and turn-off energy from the IGBT data sheet, stored in the following table:

Switching Characteristic, Inductive Load, at T_{vj} = 175°C

Parameter	Symbol	Conditions	Value			Unit
			min.	typ.	max.	
IGBT Characteristic						
Turn-on delay time	$t_{d(on)}$	T_{vj} = 175°C, V_{CC} = 400V, I_C = 50.0A, V_{GE} = 0.0/15.0V, r_G = 7.0Ω, L_σ = 90nH, C_σ = 60pF L_σ, C_σ from Fig. E Energy losses include "tail" and diode (IKW50N60H3) reverse recovery.	-	23	-	ns
Rise time	t_r		-	31	-	ns
Turn-off delay time	$t_{d(off)}$		-	273	-	ns
Fall time	t_f		-	24	-	ns
Turn-on energy	E_{on}		-	1.42	-	mJ
Turn-off energy	E_{off}		-	1.13	-	mJ
Total switching energy	E_{ts}		-	2.55	-	mJ

Table 4.5. *Switching characteristic of the IGBT [19]*

The current and voltage values for which the turn-on and turn-off energy is taken differs from the real circuit values. Therefore, in order to calculate the switching energy losses for one cycle in our system:

$$E_{SW,ON} = E_{SW,ON,DS} \cdot \frac{\mathrm{Vcc}}{\mathrm{V_{CC,DS}}} \cdot \frac{\mathrm{Ic}}{\mathrm{I_{C,DS}}} = 1.13\ mJ \cdot \frac{430\ V}{400\ V} \cdot \frac{60\ A}{50\ A} = 1.46 \frac{mJ}{cycle} \qquad (4.54)$$

$$E_{SW,OFF} = E_{SW,OFF,DS} \cdot \frac{\mathrm{Vcc}}{\mathrm{V_{CC,DS}}} \cdot \frac{\mathrm{Ic}}{\mathrm{I_{C,DS}}} = 1.42\ mJ \cdot \frac{430\ V}{400\ V} \cdot \frac{60\ A}{50\ A} = 1.83\ \frac{mJ}{cycle} \qquad (4.55)$$

Finally, the total energy losses in the transistor can be obtained substituting the calculated values in equation (4.51):

$$E_{IGBT0} = 6.47\ mJ\ + 1.83\ mJ + 1.46\ mJ = 9.76 \frac{mJ}{cycle}$$

Furthermore, taking into account the Ton and Toff, the total power losses in the transistor can be calculated:

$$P_{IGBT0} = \frac{1}{Tc} \int_0^{Ton} P_{COND} \cdot dt + P_{SW,OFF} + P_{SW,ON} =$$

$$= P_{COND} \cdot D + E_{SW,OFF} \cdot Fc + E_{SW,ON} \cdot Fc =$$

$$= 132W \cdot 0.814 + 1.83mJ \cdot 16.6kHz + 1.46mJ \cdot 16.6kHz = 162.1\ W \qquad (4.56)$$

II. Diode losses

The energy losses in the diode D0, as shown in Figure X, are going to be caused by the conduction and the switching off, since the switching on losses are very small compared to the other two.

$$E_{D0} = E_{COND} + E_{SW,OFF} \tag{4.57}$$

As we did with the transistor, now we have to look to the diode datasheet to obtain the following parameters:

Datasheet	Real circuit
$I_f = 30A$	$I_f = 60A$
$V_{cut} = 400V$	$V_{cut} = 430V$
$T_{cut} = 175℃$	$T_{cut} = 175℃$

Table 4.6. *Diode Parameters [20]*

a. Conduction losses

Introducing the forward current of 60 A in the following graph, for a temperature Tcut=175℃, the forward voltage will be 2.5 V.

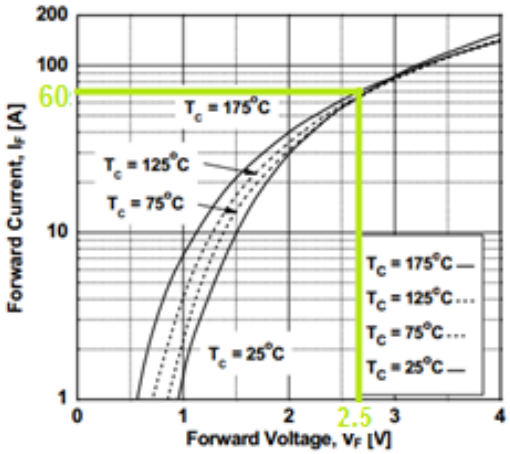

Figure 4.35. *Forward characteristics [20]*

Therefore, the conduction power losses can be obtained as:

$$P_{COND} = If \cdot Vf = 60\ \text{A} \cdot 2.5\ \text{V} = 150\ W \tag{4.58}$$

Since the diode will be conducing during Toff, the conduction energy losses will be:

$$E_{COND} = P_{COND} \cdot Toff = 150\ W \cdot 11\ \mu s = 1.65 \frac{mJ}{cycle} \tag{4.59}$$

b. Switching losses

In the following table, the reverse recovery energy of the diode can be seen, which corresponds to the switch-off energy for a cut-off Voltage of 400 V, a forward current of 30 A and a cut-off temperature of 175 ºC.

Symbol	Parameter	Test Conditions		Min.	Typ.	Max	Units
V_{FM}	Diode Forward Voltage	I_F = 30A	T_C = 25ºC	-	2.1	2.6	V
			T_C = 175ºC	-	1.7	-	
E_{rec}	Reverse Recovery Energy	I_F =30A, dI_F/dt = 200A/µs	T_C = 175ºC	-	127	-	uJ
t_{rr}	Diode Reverse Recovery Time		T_C = 25ºC	-	47	-	ns
			T_C = 175ºC	-	212	-	
I_{rr}	Diode Peak Reverse Recovery Current		T_C = 25ºC	-	3.7	-	A
			T_C = 175ºC	-	8.8	-	
Q_{rr}	Diode Reverse Recovery Charge		T_C = 25ºC	-	87	-	nC
			T_C = 175ºC	-	933	-	

Table 4.7. *Electrical characteristics of the diode [20]*

Nevertheless, the voltage and current in the real system diode are different to the datasheet values, and so we will adapt the energy losses using the following equation:

$$E_{SW,OFF} = E_{REC} = E_{REC,DS} \cdot \frac{\text{V}_\text{f}}{\text{V}_\text{f,DS}} \cdot \frac{\text{I}_\text{f}}{\text{I}_\text{f,DS}} = 0.127\ mJ \cdot \frac{430\ V}{400\ V} \cdot \frac{60\ A}{30\ A} = 0.27 \frac{mJ}{cycle} \tag{4.60}$$

Therefore, the total energy losses in the diode can be obtained substituting the calculated values in equation (4.57), as following:

$$E_{D0} = 1.65\ mJ\ \ 0.27\ mJ = 1.92 \frac{mJ}{cycle}$$

Taking into account the conducting time of the diode, Toff, the total power losses in D0 are:

$$P_{D0} = \frac{1}{Tc} \int_0^{Toff} P_{COND} \cdot dt + P_{SW,OFF} =$$

$$= P_{COND} \cdot (1 - D) + E_{SW,OFF} \cdot Fc =$$

$$= 150\ W \cdot (1 - 0.814) + 0.27\ mJ \cdot 16.6\ kHz = 32.4\ W \qquad (4.61)$$

Furthermore, the total energy and power losses in the boost will be the sum of the transistor and the diode losses:

$$\boldsymbol{E_{LOSS,BOOST} = E_{IGBT0} + E_{D0} = 11.68\ mJ/cycle}$$

$$\boldsymbol{P_{LOSS,BOOST} = P_{IGBT0} + P_{D0} = 194.5\ W}$$

The Boost efficiency can also be calculated using the equation below:

$$\eta = 1 - \frac{P_{LOSS,BOOST}}{P_{BOOST}} = 1 - \frac{194.5W}{4800W} = 0.9595 \quad \rightarrow \quad 95.95\% \ , \qquad (4.62)$$

where P_{BOOST} is the total power that goes through the Boost converter.

- *Configuration 2:*

The real boost provided by Ingeteam has a slightly different configuration. Instead of having one IGBT, it comprises two parallel IGBTs:

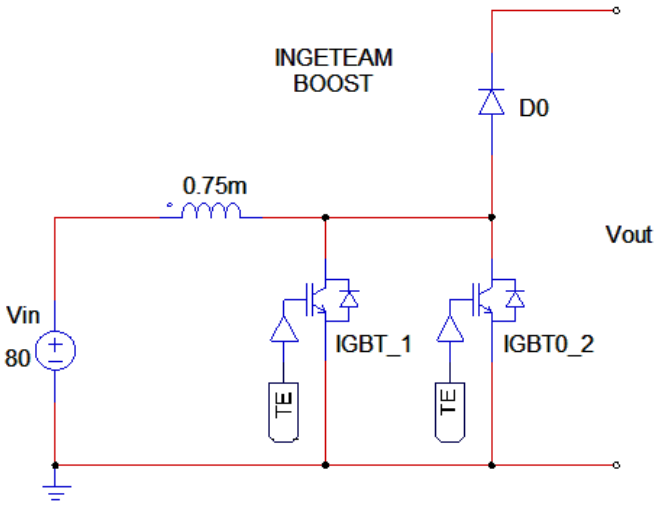

Figure 4.36. *Ingeteam real Boost*

The main difference with respect the previous structure is that during Ton, both IGBTs will be conducing, and the current through them will be $\frac{Ic}{2} = 30\ A$.

As it will be deduced thought the following lines, since the flowing current will be smaller, the converter will have fewer conduction losses. On the other hand, the switching losses will be twice, so we will analyze which structure is more convenient.

I. Transistor losses

First of all, as for the previous structure, the main values of the circuit are stored in the following Table:

Datasheet	Real circuit
$I_c = 50A$	$I_c = 30A$
$V_{GE} = 15V$	$V_{GE} = 18V$
$V_{CC} = 400V$	$V_{CC} = 430V$
$Tj = 175℃$	$Tj = 175℃$

Table 4.8. *Real Boost operation values*

a. Conduction Losses

First, the conduction losses for one IGBT will be calculated, taking into account that the current though it will be smaller than before and its conduction time Ton will be maintained. The losses in the two transistors will be twice than the calculated for one.

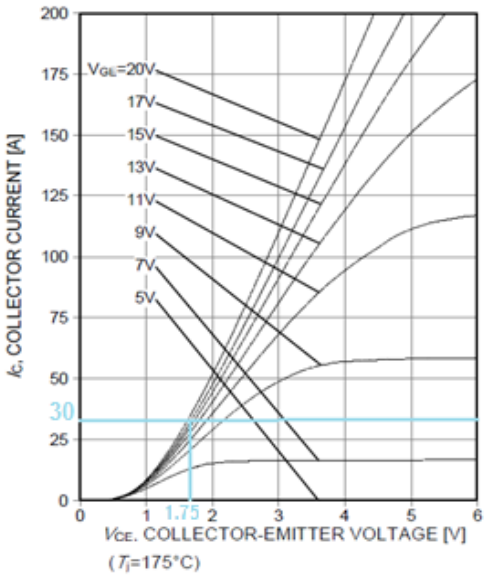

Figure 4.37. *Ic-VGE characteristic of the IGBT [19]*

Using the flowing current though the transistor, Ic, and the gate-emitter voltage, VGE, the collector-emitter voltage VCE can be obtained from Figure 4.37.

To obtain the conduction losses in the transistor, both in energy and in power terms, the next equations can be used:

$$P_{COND} = 2 \cdot Ic \cdot V_{CE} = 2 \cdot 30\ A \cdot 1.75V = 105\ W \tag{4.63}$$

$$E_{COND} = P_{COND} \cdot Ton = 105\ W \cdot 49\ \mu s = 5.1 \frac{mJ}{cycle} \tag{4.64}$$

b. Switching Losses

As done for the previous structure, the turn-on and turn-off energy will be taken from the IGBT data sheet. That energy values correspond to the datasheet voltage and current

(stored in Table 4.5) which differs from the real circuit voltage and current. Therefore, the energy losses will have to be scaled:

$$E_{SW,ON} = 2 \cdot \left(E_{SW,ON,DS} \cdot \frac{\mathrm{Vcc}}{\mathrm{V_{CC,DS}}} \cdot \frac{\mathrm{Ic}}{\mathrm{I_{C,DS}}} \right) = 2 \cdot \left(1.13\, mJ \cdot \frac{430\, V}{400\, V} \cdot \frac{30\, A}{50\, A} \right) = 1.46 \frac{mJ}{cycle} \quad (4.65)$$

$$E_{SW,OFF} = 2 \cdot \left(E_{SW,OFF,DS} \cdot \frac{\mathrm{Vcc}}{\mathrm{V_{CC,DS}}} \cdot \frac{\mathrm{Ic}}{\mathrm{I_{C,DS}}} \right) = 2 \cdot \left(1.42\, mJ \cdot \frac{430\, V}{400\, V} \cdot \frac{30\, A}{50\, A} \right) = 1.83 \frac{mJ}{cycle} \quad (4.66)$$

Consequently, the total energy losses can be calculated substituting the obtained energy values in equation (4.51):

$$E_{2-IGBT0} = 5.1\, mJ\ + 1.83\, mJ + 1.46\, mJ = 8.4 \frac{mJ}{cycle}$$

The power losses can be calculated using Ton, as in equation (4.56):

$$P_{2-IGBT0} = \frac{1}{Tc} \int_0^{Ton} P_{COND} \cdot dt + P_{SW,OFF} + P_{SW,ON} =$$

$$= P_{COND} \cdot D + E_{SW,OFF} \cdot Fc + E_{SW,ON} \cdot Fc =$$

$$= 105 \cdot 0.814 + 1.83mJ \cdot 16.6kHz + 1.46mJ \cdot 16.6kHz = 140.1\, W$$

II. Diode losses

The energy and power losses in the diode are the same than the previous configuration losses since the only modified elements are the transistors.

$$E_{D0} = 1.92 \frac{mJ}{cycle}$$

$$P_{D0} = 32.4\, W$$

The total energy and power losses of the Boost will be:

$$\boldsymbol{E_{LOSS,BOOST} = E_{2-IGBTT0} + E_{D0} = 10.32\ mJ/cycle}$$

$$\boldsymbol{P_{LOSS,BOOST} = P_{2-IGBT0} + P_{D0} = 172.5\ W}$$

The Boost efficiency can be calculated as:

$$\eta = 1 - \frac{P_{LOSS,BOOST}}{P_{BOOST}} = 1 - \frac{172.5W}{4800W} = 0.9641 \quad \rightarrow \quad 96.41\% \qquad (4.67)$$

- ***Structures comparison***

In the Table 4.9, it has been included the losses and efficiency values for each structure, namely the 1-IGBT and the 2-IGBTs structures.

It can be noted that having two IGBTs instead of one improves slightly the efficiency of the Boost power converter.

Anyway, both structures have very small losses and would be an appropriate choice.

BOOST	
1-IGBT Structure	**2-IGBTs Structure**
$P_{IGBT\ 0} = 162.1\ W$	$P_{2-IGBT0} = 140.1\ W$
$P_{D0} = 32.4\ W$	$P_{D0} = 32.4\ W$
$P_{LOSS,BOOST} = 194.5\ W$	$P_{LOSS,BOOST} = 172.5\ W$
$\eta = 95.95\%$	$\eta = 96.41\%$

Table 4.9. *Comparison of the two analyzed structures*

CHAPTER 5

FINAL STRUCTURE: POWER CONVERTER AND FUEL CELLS

5.1. INTRODUCTION

In order to achieve the final structure, capable of delivering to the electricity grid the power generated by the fuel cells, the following elements must be connected:

- 4 FCs series-connected
- Boost converter
- Resonant HF converter
- Inverter

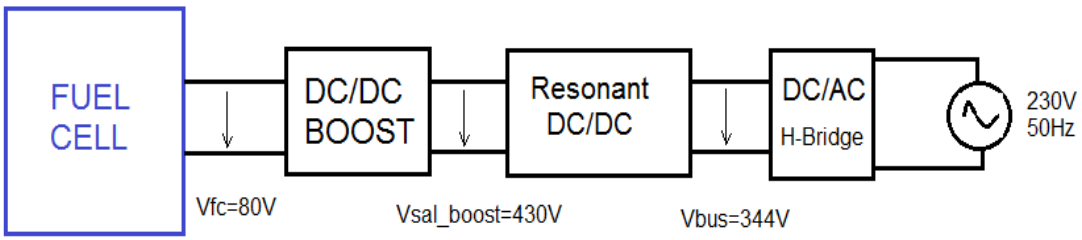

Figure 5.1. *Final structure including the voltage level at each stage*

Given this final structure, where all the elements developed in previous sections are connected, it is important to evaluate if this connection is optimal for all of them. Furthermore, a study of the voltage levels among them has been done.

Moreover, it must be noted that the operation of the fuel cells may be affected by the ripple and resonance generated in the power converter.

To obtain the maximum power, for which the whole system has been designed, the fuel cells will deliver 62 A and 80 V, at an optimal operation temperature of 55 ℃. The power generated will be delivered to the electricity grid, and some typologies of power control have been developed along this section in order to regulate the operating point of the fuel cells.

5.2. EFFECT OF THE CONVERTER'S CURRENT AND VOLTAGE RIPPLE ON THE FC

5.2.1. RESONANT TANK: 100 KHZ RIPPLE

First of all, it has been evaluated if the resonant currents of the DC/DC Resonant Converter affect the fuel cell stacks.

The resonance is a very high frequency effect and it could be prejudicial to the fuel cells operation. Therefore the currents between the FC stack and de DC/DC Converter, namely the Resonant tank input current, the Boost input and output currents and the FC stacks output current, have been simulated.

The results of the simulation are shown in Figure 5.2, where it can be seen that the resonance doesn't reach the Boost, since it is all absorbed by the 80 µF capacitor placed between the Boost and the Half-Bridge Inverter.

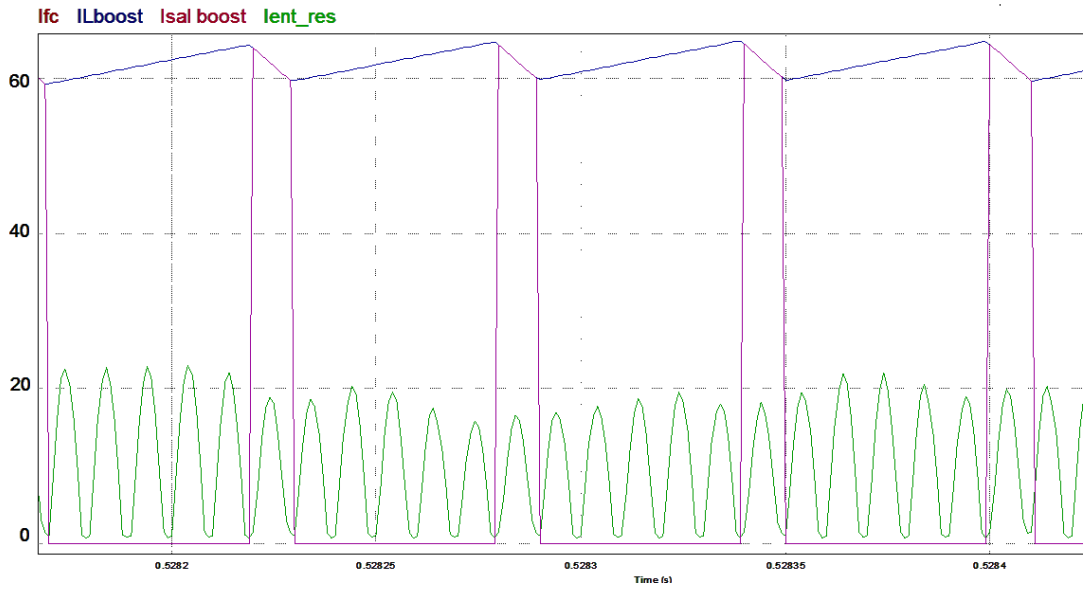

Figure 5.2. *Simulation of the currents that could be affected by the resonance*

5.2.2. BOOST: 16.6 KHZ CURRENT RIPPLE

The main difference between operating with the whole system instead of letting the fuel cell work alone is that the 16.6 kHz current ripple generated in the Boost reaches the FC, as shown in Figure 5.3. That ripple affects the fuel cell voltages too, as shown in Figure 5.4, since voltages and currents are related by the polarization curve.

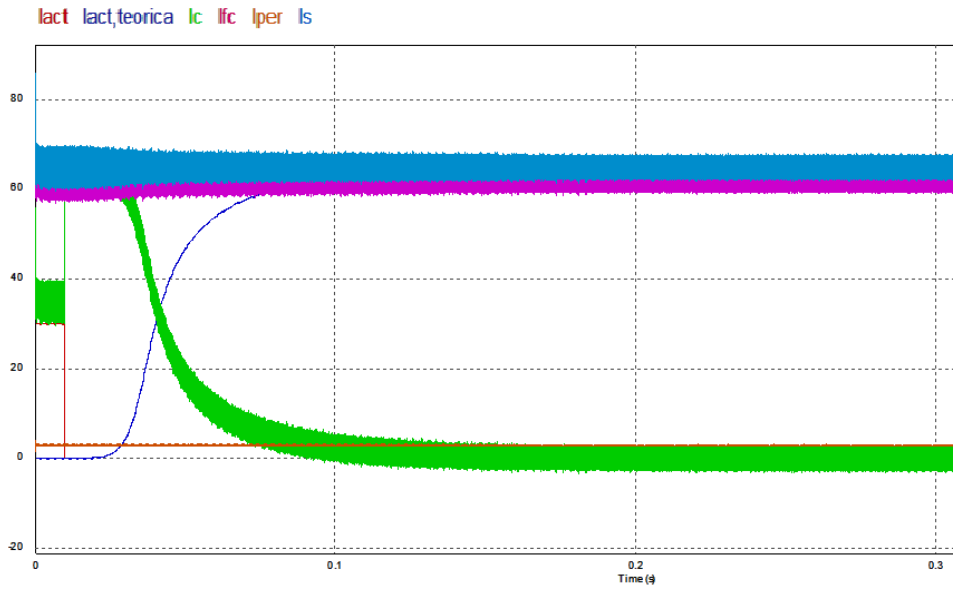

Figure 5.3. *Currents delivered by the FC when they are connected to the rest of the system, at T=55* °C

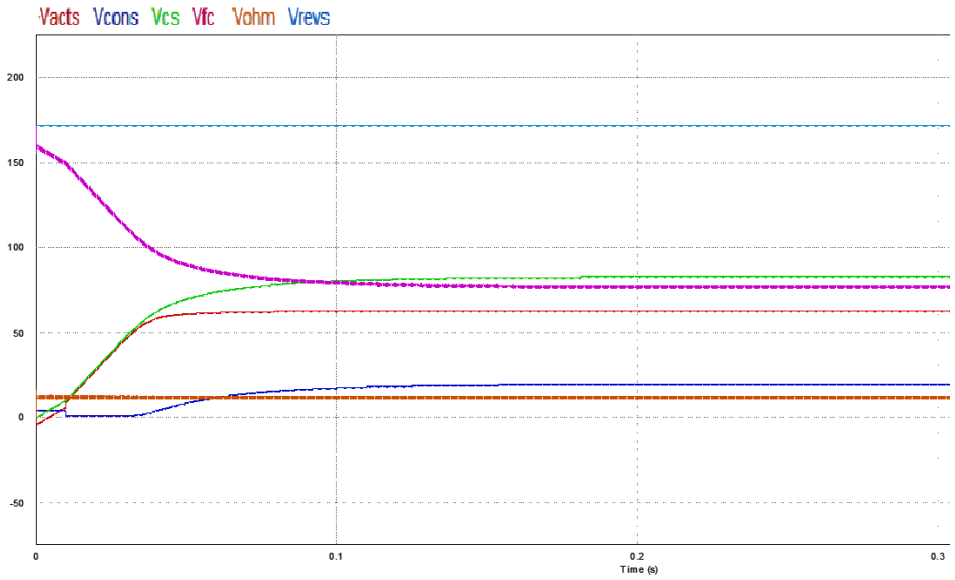

Figure 5.4. *Voltages in the FC stacks when they are connected to the rest of the system, at T=55 ℃*

Nevertheless, the mean values of the currents and voltages remain the same, as proved below:

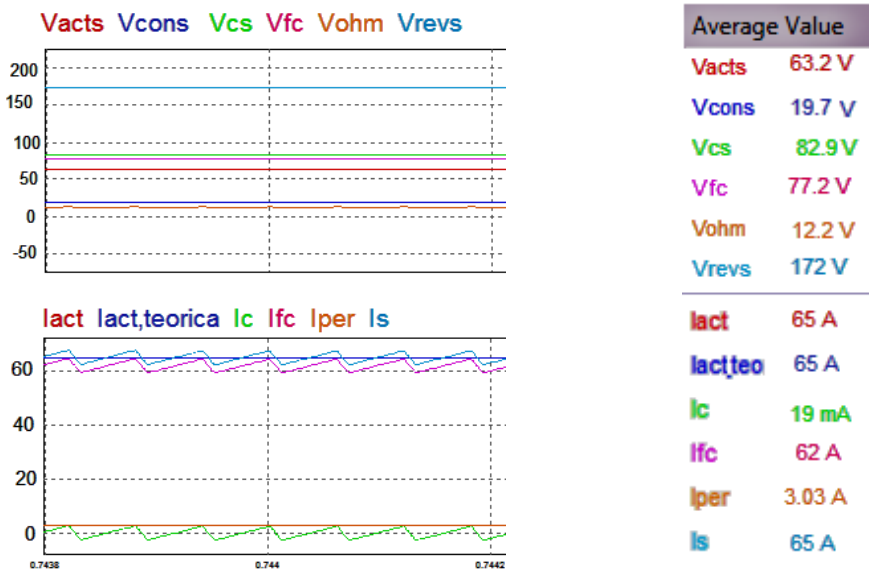

Figure 5.5. *Average value of the Currents and Voltages in the FC*

Since there is a ripple in the current and voltage, the power delivered by the stacks will have a ripple too, as seen in Figure 5.6.

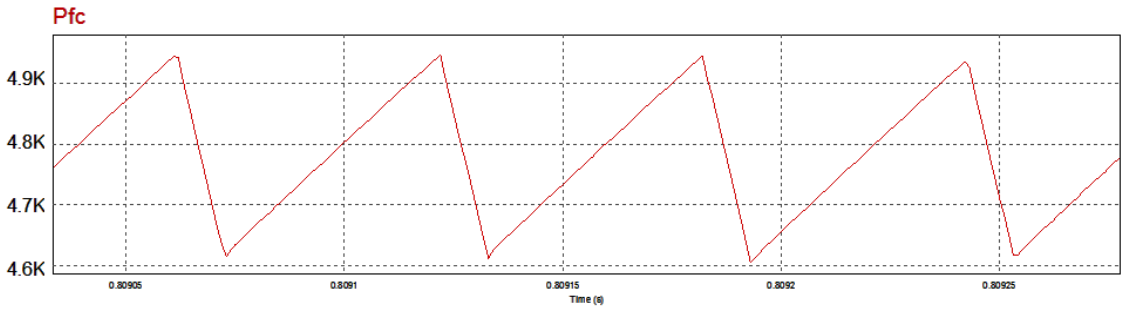

Figure 5.6. *Power ripple delivered by the fuel cell, at T=55ºC*

The value of the power oscillates between 4.6 kW and 4.95 kW, and the mean value is:

$$Pfc, mean = Vfc, mean \cdot Ifc, mean = \ 77.16\ V \cdot 62\ A = 4.78\ kW \qquad (5.1)$$

In order to analyze the effect of the current ripple, the fuel cell has been studied alone. To introduce the current ripple in the simulation model a switch has been used, as shown in Figure 5.7. This switch enables a sinusoidal source in parallel to the DC current.

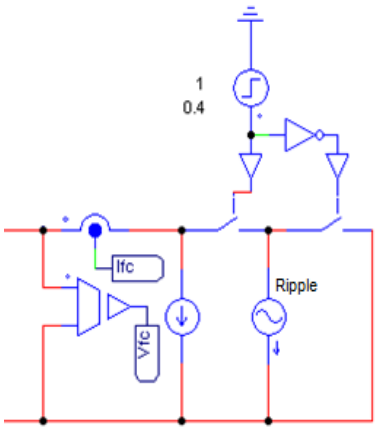

Figure 5.7. *Additional current ripple*

The system has been simulated for 55 ºC and a DC current of 60 A. However, when the stack reaches the stationary state, a 100 Hz sinusoidal ripple has been added, with a value of 6 A from peak to peak. The results from the simulation are shown in the following figure:

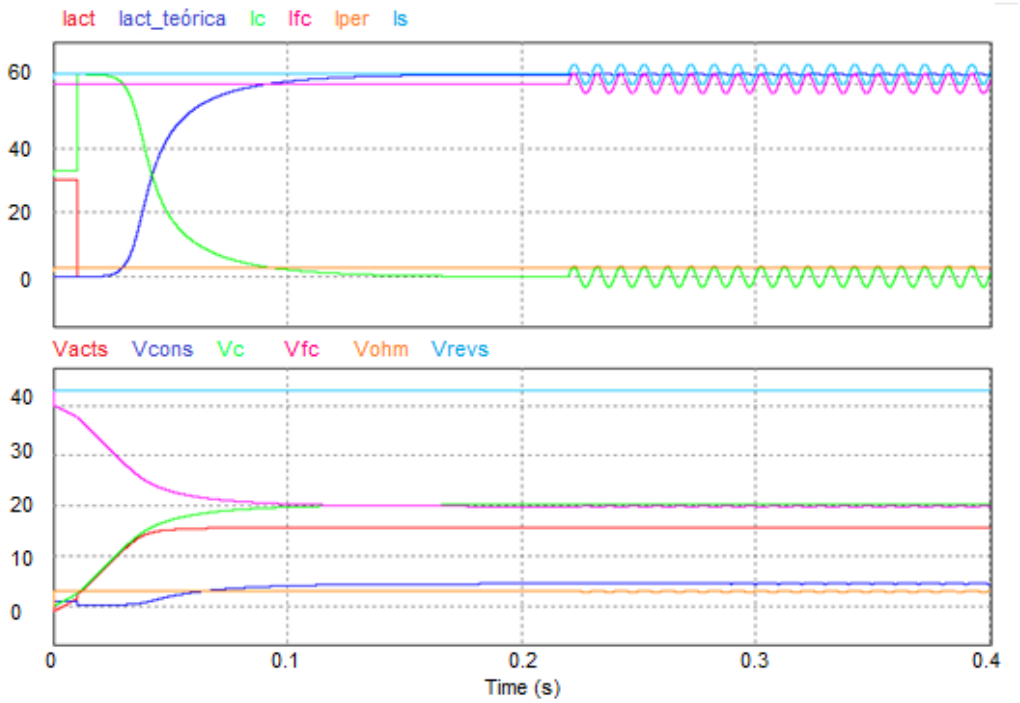

Figure 5.8. *Voltages and Currents for T=55ºC, IFC=60 A and a sinusoidal current ripple added at t=0.22s, whose characteristics are 100 Hz of frequency and 6 A of amplitude.*

As it can be seen, a ripple in the output current affects the rest of the fuel cell currents, as well as the voltages. So the next step consists on analyzing if this ripple might affect the power delivered by the stack.

Maintaining the previous characteristics, the power given by the stack for different frequency ripples is stored below:

RIPPLE	POWER
DC Current	Pfc= 1193 W
F=0.1Hz	Pfc=1190 W
F=1Hz	Pfc=1190.4 W
F=10Hz	Pfc=1192.2 W
F=100Hz	Pfc=1192.7 W

Table 5.1. *Power delivered by the stack for various current ripples*

The power delivered by the fuel cells is not really affected by the current ripple, even if this effect is slightly bigger for low frequencies. On the other hand, for high ones, the capacitor cannot see the ripple and the fuel cell stack behaves like when a DC current is flowing.

5.2.3. H-BRIDGE INVERTER: 100 HZ RIPPLE

Since the conversion stage is connected to the electricity grid, a 100 Hz current ripple is added to the system, and it could affect the fuel cell currents and voltages. Since this frequency is not very high, it could perturb the chemical behavior of the fuel cell.

5.3. ANALYSIS AND SIMULATION OF THE WHOLE SYSTEM

The complete system simulation scheme, in PSIM, has been included in Annex 3.

5.3.1. VOLTAGE LEVELS CHECKING

The first study that has been done consists on checking if the voltage levels among the elements of the system are correct. When the maximum power is delivered, that is 4.8 kW, there are some predefined voltage values for which the system is operating correctly.

These adequate voltage values were analyzed in Section 4, and are the following:

- Vfc = 80 V
- Vout,boost = 430 V
- Vbus = 344 V
- Vgrid= $\sqrt{2} \cdot 230$ V (peak-to-peak)

The simulation of the system has been done to check if these values are maintained, and it is shown in Figure 5.9.

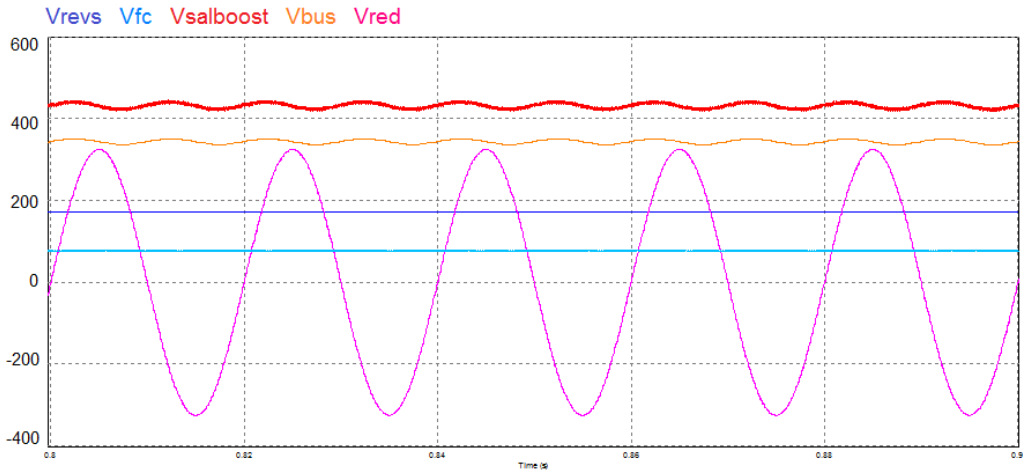

Figure 5.9. *Simulation of the voltage levels at each block of the system*

The DC Bus voltage must be kept constant, and for that it is regulated with a voltage control loop. It has been simulated in the following figure:

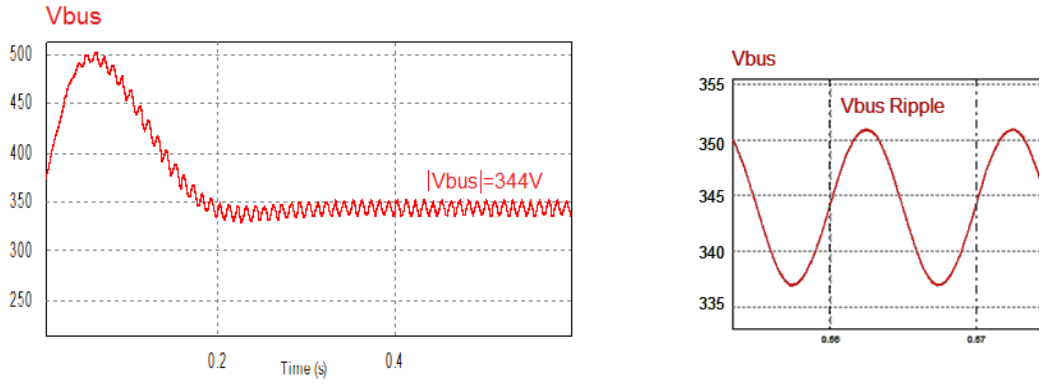

Figure 5.10. *Simulation of Vbus and its ripple*

As it can be observed, even though the mean value of Vbus in the steady state corresponds to its optimal value, 344 V, there is a 100 Hz sinusoidal voltage ripple that makes Vbus oscillate between 336.84 V and 351.15 V. Therefore, the amplitude of this ripple is 14.3V.

$$\Delta v_{bus} = \frac{14.3\ V}{344\ V}.100 = 4.15\ \% \tag{5.2}$$

As this proportion is small, the chosen value of the bus capacitor, Cbus, is considered good enough.

5.3.2. POWER ANALYSIS OF THE SYSTEM

Afterwards, the power of the system has been studied. The input power is the generated by the FC, which will flow though the whole system to be finally injected into the electricity grid. This input and output power is shown in the following Figure 5.11:

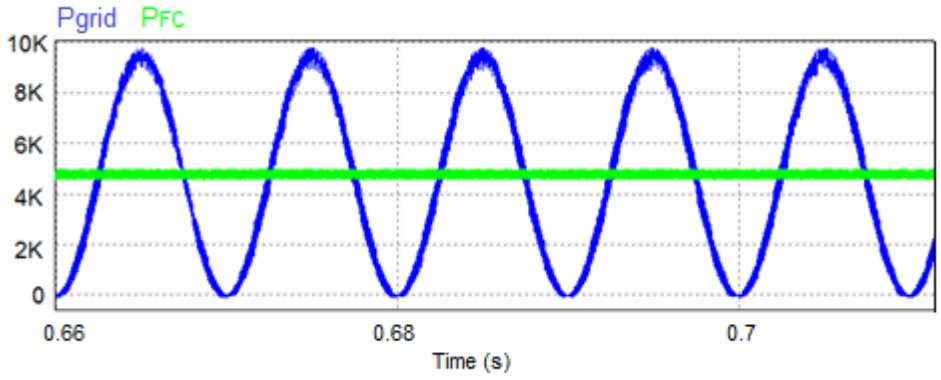

Figure 5.11. *Simulation of the power generated by the FC, and the power fed into the grid*

5.4. POWER CONTROL LOOPS FOR THE FINAL SYSTEM

It is important to implement a power control that enables us to demand the amount of power that we want to extract from the FC. That way, depending on the power asked, a reference current is created and introduced in the Boost Current Loop.

For that, three different options are proposed. The first two options are prepared for the system working with the four fuel cells all the time. The simplest one comprises an open loop achieved with the PSIM element “Look-up Table”, while the second one is a closed loop implemented with a “C-Block”. On the other hand, the third option consists on a closed loop that connects and disconnects fuel cells with the purpose of achieving a maximum efficiency operation.

5.4.1. OPEN-LOOP CONTROL

As mentioned before, this control is implemented using an element called “Look-up Table”, shown if Figure 5.12, which consists on a table where different data can be stored. In or case, we have introduced the values of power and current of four fuel cells, obtained from the simulation of one FC made in Chapter 2.

That way, when a certain reference power Pref is introduced, the “Look-up Table” will give the FC current Iref needed to generate Pref. This value of Iref will be the reference current introduced in the Boost Current Loop.

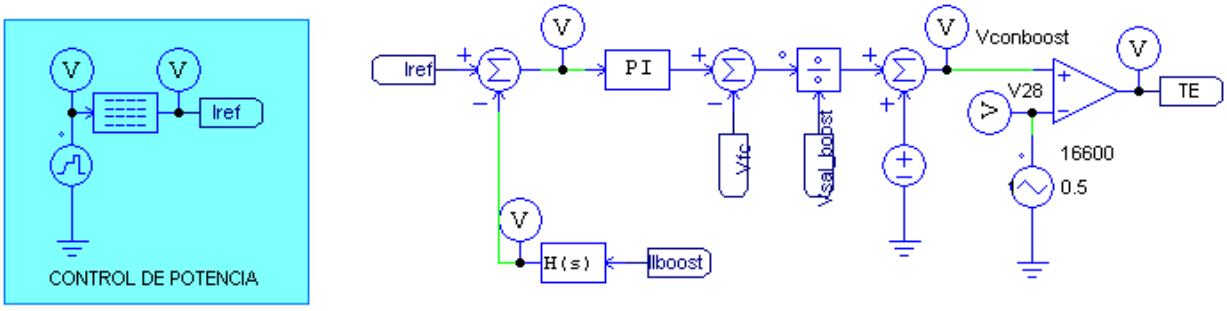

Figure 5.12. *Open Control Loop for Power*

The main disadvantage of this control is that the temperature changes are not implemented, since the values stored in the “Look-up Table” correspond to only one temperature, in our case, 55℃. Therefore, when the fuel cells are working at a different temperature the created Iref is not to be the correspondent for the power demanded, and there is an error between the power generated by the stack and Pref.

To check the behavior of this loop for different temperatures, we have done a simulation, shown in Figure 5.13, in which the reference power changes from 3000W to 2000W.

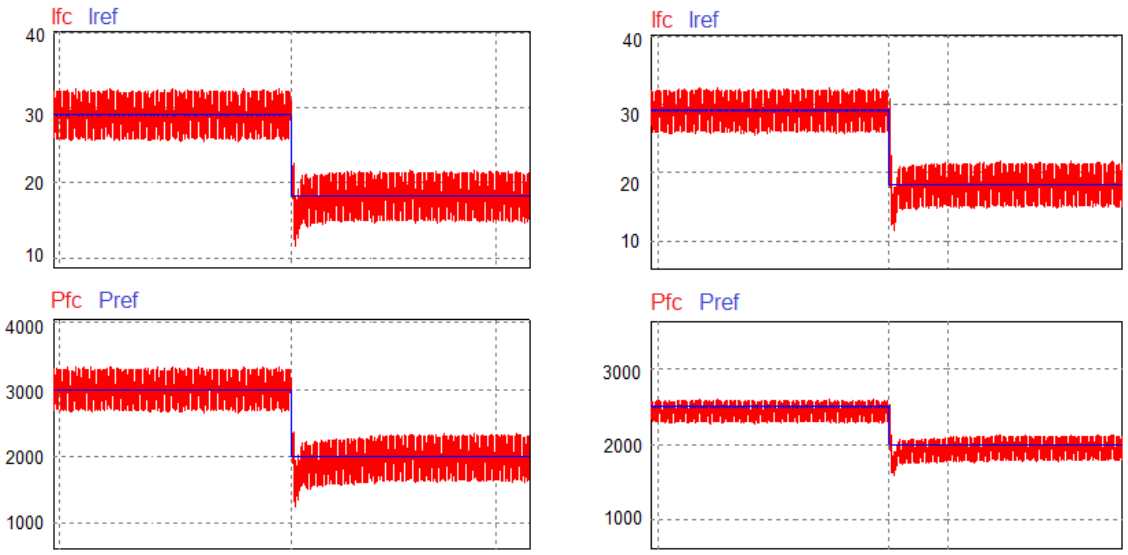

Average Value	
Ifc	18.24 A
Iref	18.24 A
Pfc	2007 W
Pref	2000 W

A) $T = 55$ ℃

Average Value	
Ifc	18.24 A
Iref	18.24 A
Pfc	1905 W
Pref	2000 W

B) $T = 25$ ℃

Figure 5.13. *Simulation of the reference power and current for different temperatures*

5.4.2. CLOSED-LOOP CONTROL

In order to implement the power closed loop it is necessary to write a code in a "C-block". The simulation scheme is shown in the following figure:

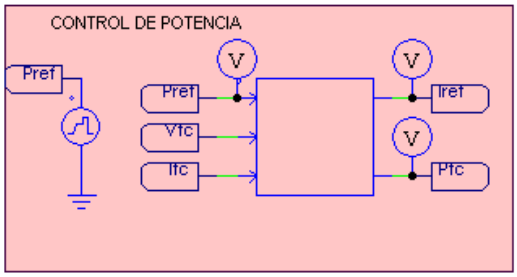

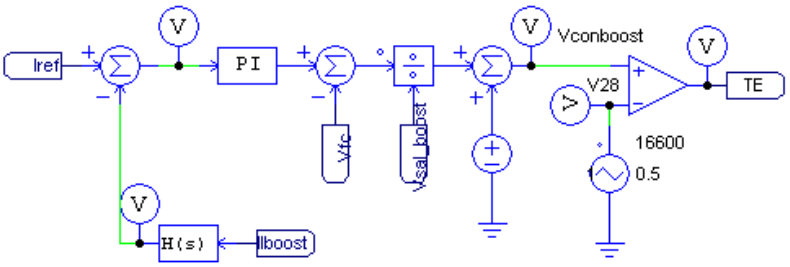

Figure 5.14. *Closed Control Loop*

Analyzing the behavior of the fuel cell power and current for an optimal temperature of 55 ℃, it can be noted that their curve can be approximated to 4 linear regions, as done in Figure 5.15. This approximation will enable an initial value for the reference current, depending on the reference power introduced in the control loop.

Power is dependant to the fuel cell operation temperature. Therefore, the proposed approximation will have some error when the working temperature is different to 55 ℃. That is the reason why, once a first Iref value is achieved, the program compares the reference power with the real power generated with the initial reference current. If the powers are different, the reference current will increase or decrease until the fuel cell power and the reference power are very similar.

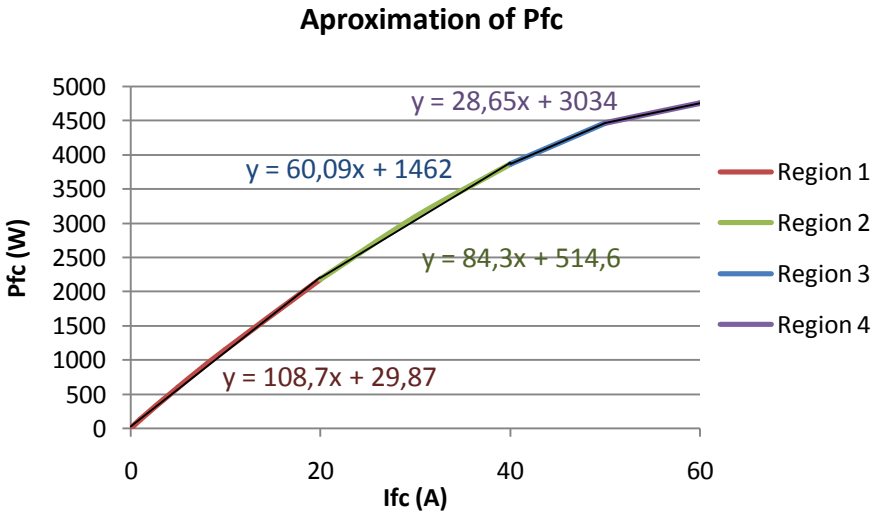

Figure 5.15. *Approximation of the Power Curve to 4 linear regions*

Therefore, the code implemented must do the following:

I. Read the reference power, Pref.

II. Choose the region correspondent to that power reference.

III. Calculate the initial reference current, Iref, correct for a T=55ºC.

IV. Obtain the fuel cell power Pfc reading the voltage Vfc and current Ifc from the model.

V. Compare Pfc and Pref, and evaluate their difference. If this difference is bigger than 50W, the program will generate a new reference current.

VI. Calculate the new reference current Iref:

- If $Pref > Pfc \rightarrow Iref,new = 1.02 \cdot Iref$
- If $Pref < Pfc \rightarrow Iref,new = 0.98 \cdot Iref$

The mentioned code is included in Annex 1.

In order to understand better the behavior of this program, the curves for an operation temperature of 25 ºC have been shown in Figure 5.16.

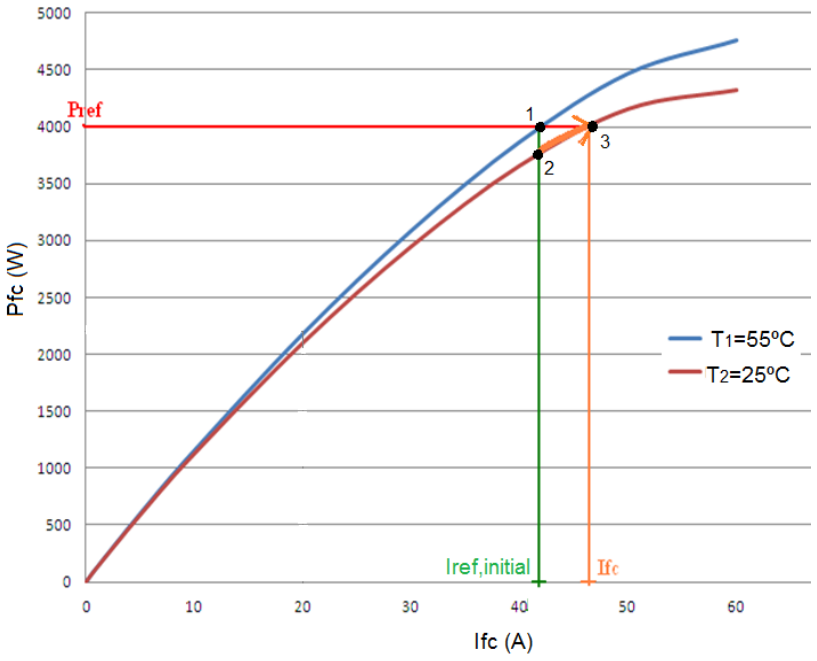

Figure 5.16. *Operation of the program when T=25* ºC

- Point 1: First approach.

With the Pref introduced, a first value of Iref is obtained from the 55ºC power curve.

- Point 2: Real Power given by the fuel cell at Iref.

This value is different to the Pref demanded since the operation temperature of the stacks is different to the optimal one.

- Point 3: Pfc=Pref

The Iref must be increased until the power given by the cells is equal to the reference demanded.

For instance, in order to show the behavior of the previous program, we have simulated a change of the reference power from 3000W to 2000W, for two different temperatures: 55ºC and 25ºC. In the following figure the curves obtained for the fuel cell power and current, as well as the reference power and current, are shown in Figure 5.17.

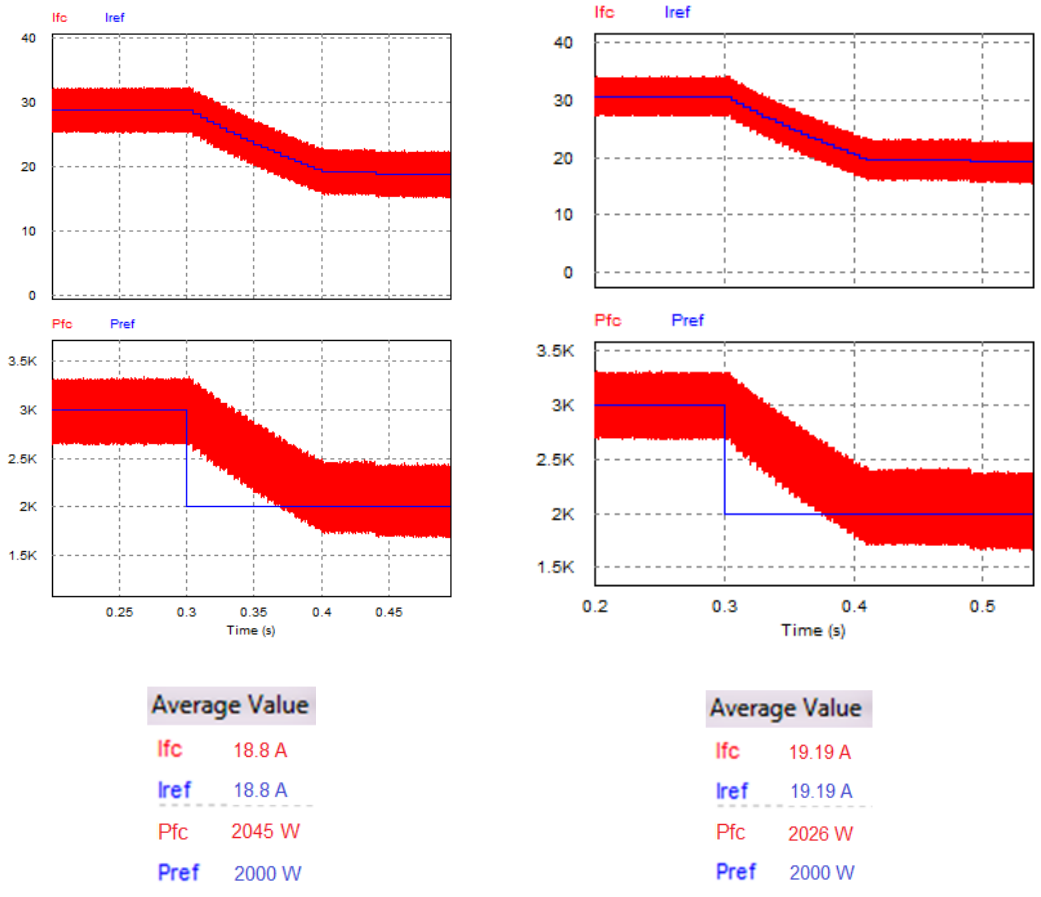

a) T=55ºC *b) T=25ºC*

Figure 5.17. *Simulation of the reference current and power for different temperatures*

It can be noted that the reference current to obtain 2000 W with a temperature of 25℃ is bigger than the one needed for 55℃. This difference will increase as the reference power is augmented.

5.4.3. MAXIMUM EFFICIENCY POINT TRACKING (MEPT)

In Chapter 3, the FC efficiency and the connection of one to four FCs in series were evaluated. The conclusions that can be taken from that study are:

- If the turned-off fuel cells have fuel consumption in the peripherals, the most efficient configuration consists on having the four fuel cells operating all the time. Therefore, the closed loop implemented in the previous section could be use.
- On the other hand, when the turned-off fuel cells are invisible to the rest of the system, as their consumption is zero, it is optimal, from the point of view of the efficiency, to decrease the number of fuel cells connected for low power.

Based on this last affirmation, in the present section we are going to implement a control loop that decides the number of fuel cells connected at any moment, depending on the power asked by the system. This control is called “Maximum Efficiency Point Tracking”, since it makes the system work at the highest efficiency all the time.

As the fuel cell operating point is determined using a certain current consign, the current that must be asked to obtain a certain power has been plotted in Figure 5.18. This plot has been created from the empirical data used in Chapter 2 and 3. The current value differs depending on the number of fuel cells that are working at the selected moment and the operation temperature.

It is visible that for the effect of temperature on the electrochemical reaction, at higher temperatures the needed current is smaller for a certain power. Furthermore it can be noted that to deliver a certain power, the current needed will decrease as more FCs are connected.

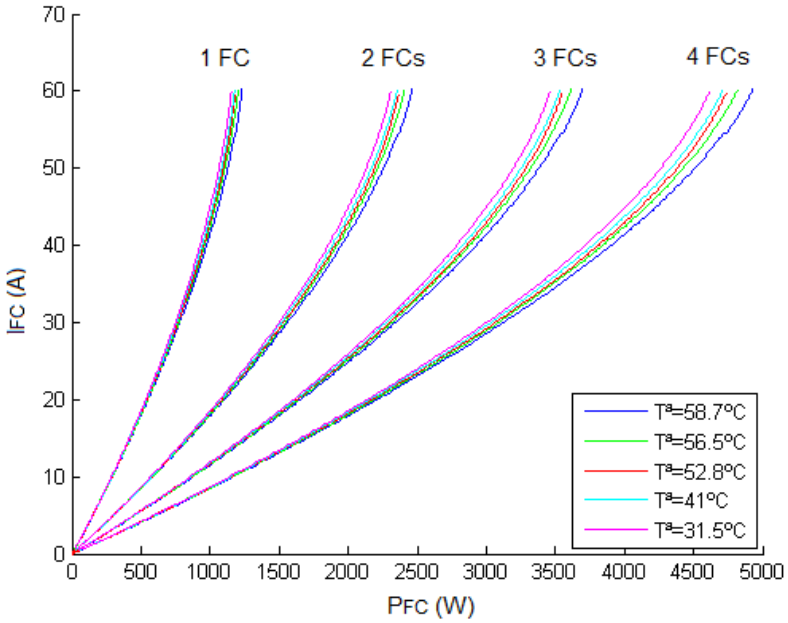

Figure 5.18. *Fuel cell current needed to deliver certain power*

In this case, provided that in the simulation performed before the nominal operation temperature was 55℃, the plots corresponding to the measures done at 56.5℃ are used, since it is the closest value available

The inductor and diode of the Boost have been supposed ideal in the simulation. However, the real system presents some losses due to their internal resistance. The minimum voltage with which the Boost can be fed is approximately 40 V, since for lower voltages the duty cycle would be excessively high. In conclusion, the minimum number of fuel cells that must be connected are two.

Therefore, three different configurations can be used:

- 2 FCs operating
- 3 FCs operating
- 4 FCs operating

Finally, taken from Figure 3.13, the power ranges for which each configuration can work to respect the maximum efficiency purpose are:

Number of FCs operating	Power (W)
2	0 - 1182
3	1182 - 1668.5
4	1668.5 - 4800

Table 5.2. *Power ranges for the different number of FCs connected*

In order to implement this efficiency control in PSIM, we use the element "C-Block", where the needed code for the control is introduced. The input of this block are the current and voltage generated in the system, that can be used to obtain the power delivered; and the asked reference power Pref, which is the one wanted to be delivered. On the other hand, the output signals from the block are the reference current Iref, that will be introduced in the Boost control loop; the power delivered by the system; and the switching commands for the different cells.

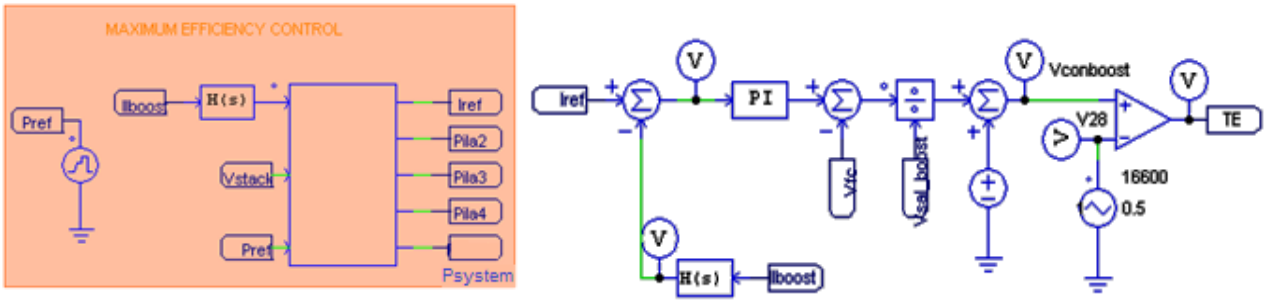

Figure 5.19. *Maximum efficiency control in PSIM*

Until this part, all the fuel cells were operating all the time, having identical properties. However, in this last control, a new way of connecting and disconnecting the fuel cells must be implemented. For that, we used switches. We must take into account that voltage sources cannot operate in short-cirtuit and current sources cannot be left in an open circuit.

Furthermore, as explained in Chapter 3, a problem of the series-connection is that if one module operates in different conditions than the rest, this may affect decreasing the efficiency of the whole system. In this simulation, the turned-off fuel cells will affect to the rest of the system, and therefore one diode has been introduced in anti-parallel to each fuel cell.

The code written in the "C-Block", included in Annex 1, must do the following:

I. Assign configuration and Iref depending on the asked power Pref

After reading the reference power and the delivered power, every time the asked power changes, the control evaluates which is the optimal configuration for the system (that is, the better number of FCs connected) and calculates the needed Iref to achieve the reference power.

II. Reference current variation

When the reference power is constant, the control checks if the power delivered by the fuel cells is the same than the asked one. If it is not, normally due to having operating temperatures different from 56.5 ºC, the reference current will increase or decrease until the powers are similar.

5.4.3.1. Flow diagram

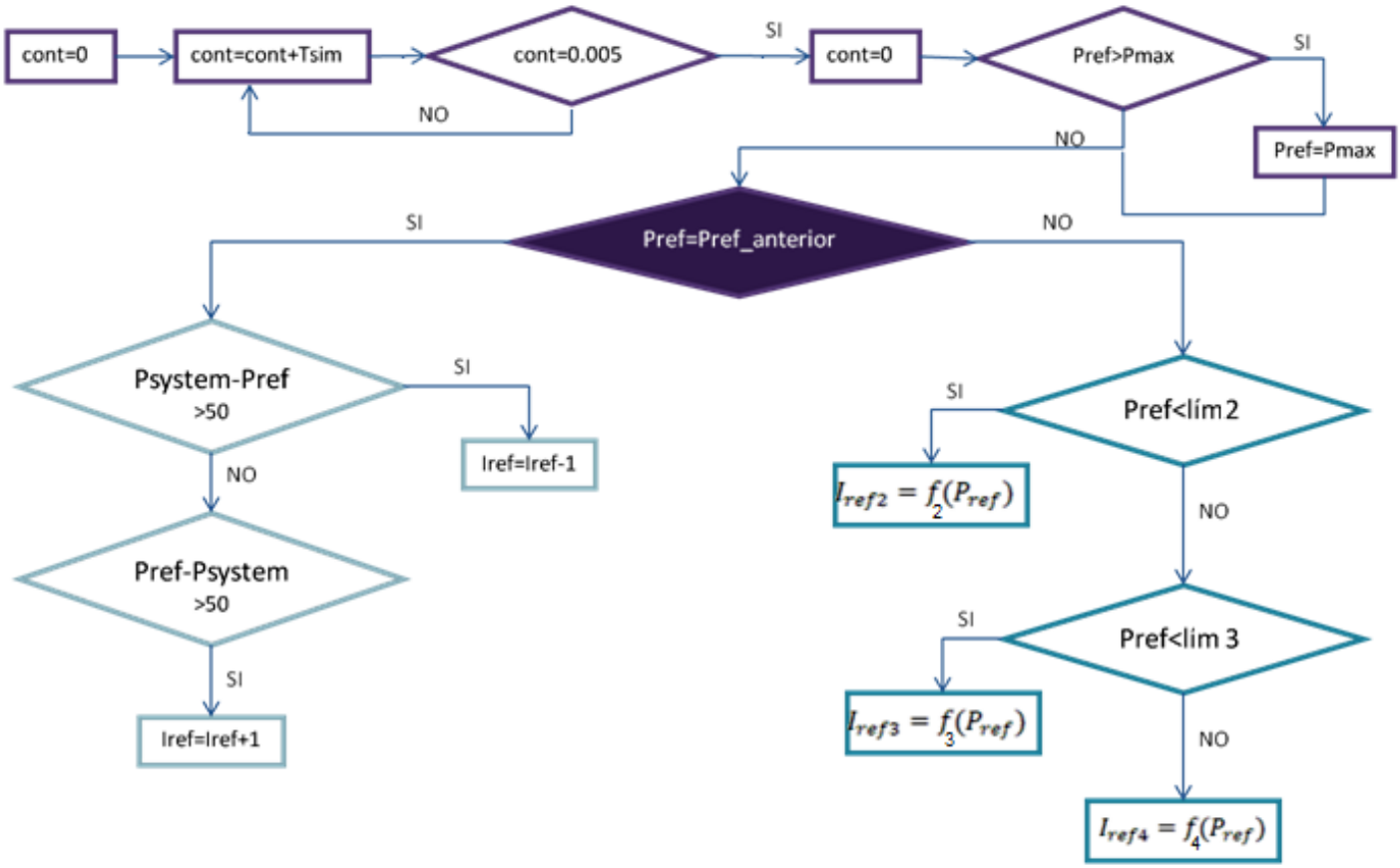

Figure 5.20. *Flow diagram of the FCs connection control*

5.4.3.2. Simulation results

In order to check the correct operation of this control, a reference power has been introduced. This power varies in time, to check if the control is right when the reference is a ramp or a step. Basically, it is aimed to see how fast and accurate is the control when a different reference power is asked.

First of all, we have simulated the system for an increasing ramped reference, and the results obtained are shown in the following Figure 5.21:

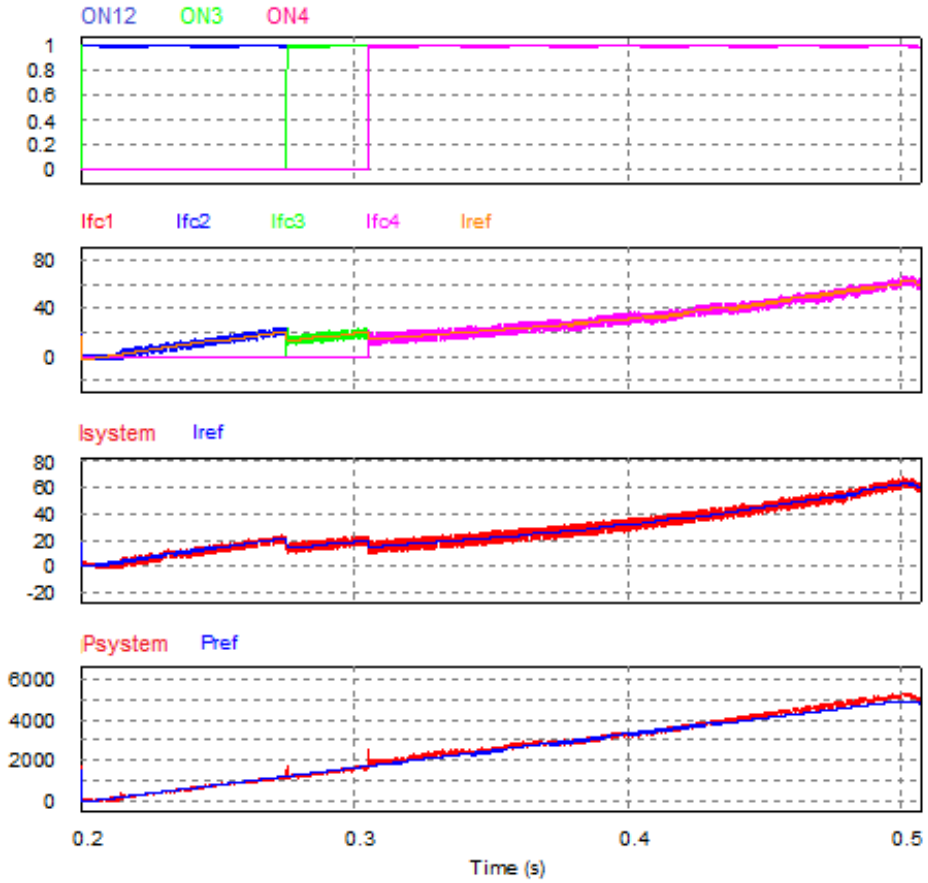

Figure 5.21. *Simulation of the system for an increasing ramped reference*

It can be seen that when the reference power increases, the reference current does too, and so the fuel cells current and power.

At the beginning, just two fuel cells are operating. However, when the reference power reaches the fist limit of 1182 W (stored in table 5.1), the control connects a third fuel cell. Afterwards, when the reference power reaches the second limit of 1668.5 W, a fourth fuel cell starts operating.

It can also be noted how when a new fuel cell is connected, the current given by the cells decreases, and so less fuel will be fed to each of them.

In the following Figure 5.22, the system has been simulated for a decreasing ramped reference. In this case, instead of seeing how the fuel cells are connecting, it can be appreciated how they are disconnecting.

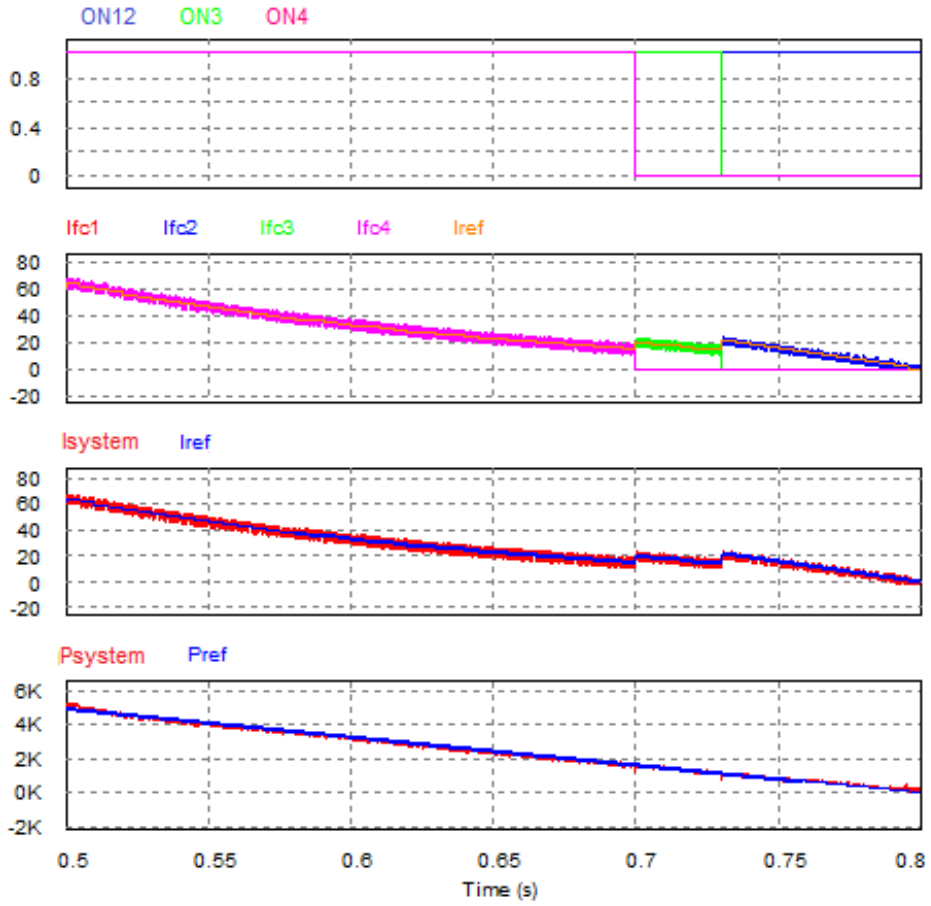

Figure 5.22. *Simulation of the system for decreasing ramped reference*

Finally, in Figure 5.23, the behavior of the system has been tested for very fast changes in the reference. Particularly, a step power reference from 0 to 3000 W has been introduced, and therefore the working number of fuel cells must pass from 2 to 4.

It can be seen that when the reference power changes the control starts compensating it with some delay. This is produced by the C-Block, since it has been programmed to operate with a frequency of 200 Hz.

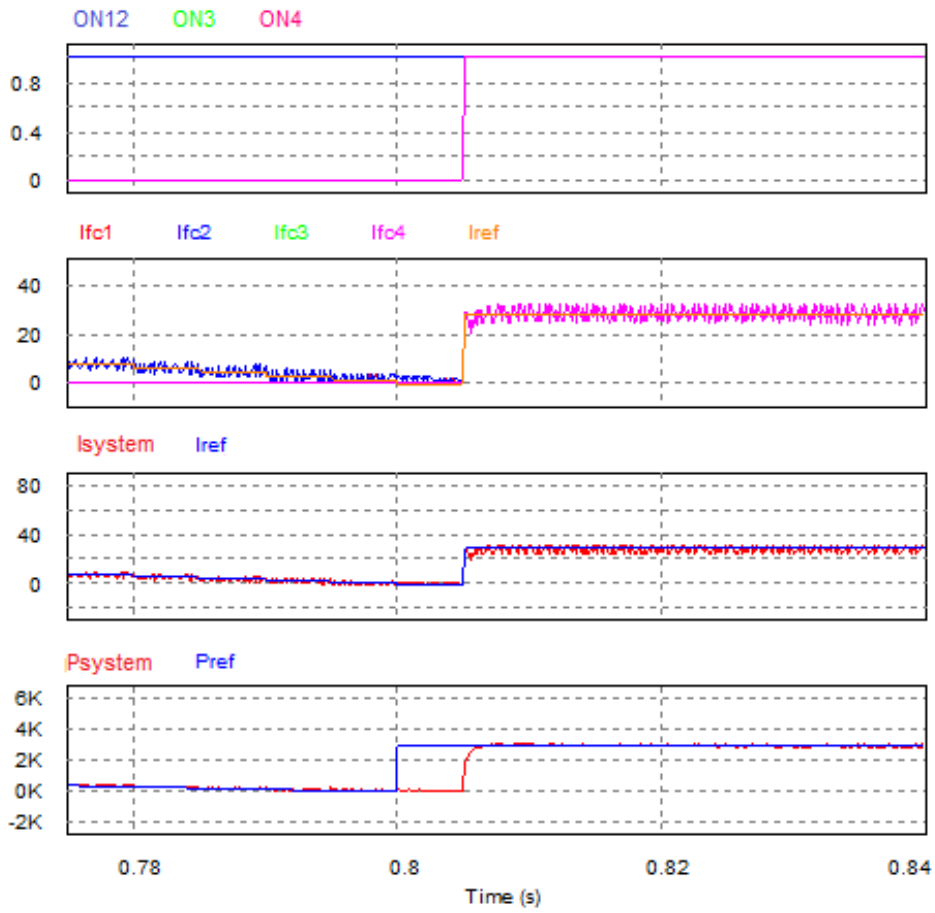

Figure 5.23. *Simulation of the system for an upwards step reference*

As an example, the efficiency curves and the operating point of the fuel cells, for a reference power change from 1000 W to 3000 W, have been shown in Figure 5.24.

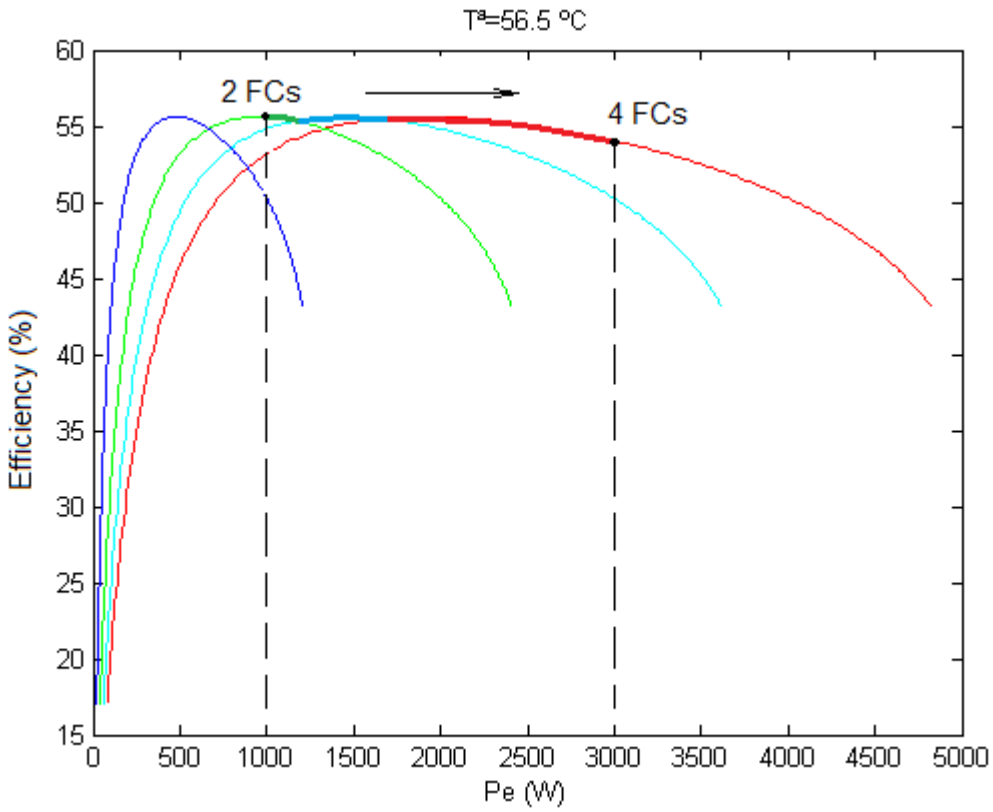

Figure 5.24. *Example of number of fuel cells connected*

CHAPTER 6

CONCLUSIONS AND FUTURE WORK LINES

The theoretical analysis of a generation system compound by fuel cells and an inversion stage has been accomplished.

The fuel cells have been deeply analyzed from the electricity point of view. For that, the electric model of a PEM fuel cell has been presented, to be simulated afterwards. It has been noted that the power generated by the fuel cells depends on the current delivered and the operating temperature.

A study about the possible power conversion stages that can be used to inject the power generated into the electricity grid has been developed. It has been concluded with the selection of the most adequate converter. This comprises a boost converter to increase the output voltage from the fuel cells; a resonant DC/DC converter with HF transformer that enables galvanic isolation and commutation with minimum losses; and an H-Bridge inverter to adapt the generated DC wave to the grid characteristics.

A study about the elements comprising the inversion stage has been developed. It has been noted that implementing a power control loop for them, the point of operation of the fuel cells can be determined.

The possible interaction that takes place between the fuel cells and the converter has been analyzed. Special attention has been paid to the effects of the converter's current ripples on the fuel cell. These ripples are generated in the Boost with a frequency of 16.6 kHz, in the resonant converter of 100 kHz and in the H-Bridge of 100 Hz.

Furthermore a control algorithm has been created to achieve the maximum efficiency point tracking for any delivered power. This control is based on the connection and

disconnection of the fuel cells comprising the system. The number of cells operating is determined after obtaining the power ranges for which the efficiency is maximized.

As future work lines, the photovoltaic inverter provided by Ingeteam could be adapted to fulfill the conversion stage properties presented in this paper.

Furthermore, the series connection of the fuel cells could be done in the university's system, including the AP diode for protection against unpredicted faults.

The presented MEPT control could be implemented, but before it would be necessary to perform an evaluation of the cost of the saved hydrogen versus the cost of the control and connection system, to see if it is profitable.

Finally, it would be interesting to validate this project empirically in the Renewable Energies Laboratory in the UPNA.

REFERENCES

[1] Petr Moldrik, Roman Chvalek, *"PEM Fuel Cells - The Basic Characteristics"*, Department of Electrical Power Engineering, VSB - Technical University of Ostrava, Czech Republic.

[2] Vincenzo Naso, Marco Lucentini, Marco Aresti, *"Evaluation of the overall efficiency of a low pressure Proton-Exchange Membrane Fuel Cell power unit"*, 2000, Department of Mechanical and Aeronautical Engineering.

[3] J. Larminie and A. Dicks*, "Fuel Cell Systems Explained – Second Edition"*, 2003, Wiley, Oxford, England.

[4] K. Kordesh and G. Simander, *"Fuel Cells and Their Applications"*, 1996, VCH, Publishers, Inc., New York, USA.

[5] Idoia San Martín, Alfredo Ursúa, Pablo Sanchis, *"Modeling of PEM Fuel Cell Performance: Steady-State and Dynamic Experimental Validation"*, Energies 2014.

[6] Alberto Berrueta, *"Caracterización de sistemas electroquímicos para su aplicación en una microrred"*, 2013, UPNA.

[7] Petr Moldrik, Roman Chvalek, ‘‘*PEM Fuel Cells - The Effect of Fuel Parameters on Efficiency and Quality of Electric Power Supply*", Department of Electrical Power Engineering VSB - Technical University of Ostrava, Ostrava, Czech Republic.

[8] Carlos Andrés Ramos-Paja, Carlos Bordons, Alfonso Romero, Roberto Giral and Luis Martínez-Salamero *, "Minimum Fuel Consumption Strategy for PEM Fuel Cells"*, IEEE.

[9] Burak Ozpineci, Zhong Du, Leon M. Tolbert, Donald J. Adams, Donald Collings, *"Integrating multiple solid oxide fuel cell modules"*, Department of Electrical and Computer Engineering, Tennessee.

[10] Gérard Coquery, Alexandre De Bernandinis, *"First Approach for a Fault Tolerant Power Converter Interface for Multi-Stack PEM Fuel Cell Generator in Transportation Systems"*.

[11] Hendrik Dohle, *"Current source with series connected cells",* 2000, Patent number: CA 2 398727 (A1).

[12] Denis Candusso, Alexandre De Bernardinis, Marie-Cécile Péra, Fabien Harel, Xavier François, Daniel Hissel, Gérard Coquery, Jean-Marie Kauffmann, *"Fuel cell operation*

under degraded working modes and study of diode by-pass dedicated to multi-stack association", 2007, Elsevier.

[13] Denis Candusso, Alexandre De Bernardinis, Fabien Harel, Xavier François, Gérard Coquery, *"Experiments of a 20 cell PEFC opetating under fault conditions with diode by-pass circuit for uninterrupted power delivery"*, 2009.

[14] Josef Lersch, Arno Mattejat, *"Direct-current power supply device comprising a number of series-connected fuel cell blocks"*, Siemens, 2001, Patent number: WO 02/045197 (A3).

[15] Victor W. Logan, James W. Dandaliedes, *"System stack contingency and efficiency switching",* General Motors Corporation, 2007, Patent number: US 7247398.

[16] Timothy LaBreche, *"Fuel cell including bypass circuit for interconnecting fuel cell"*, 2010, Adaptive Materials Inc, Patent number: US 7799481 (B2).

[17] Shanna D. Knights, Jacob W. De Vaal, Michael V. Lauritzen, David P. Wilkinson, *"Electrochemical fuel cell stack having a plurality of integrated voltage reversal protection diodes"*, Ballard Power Systems Inc, 2005, Patent number: US 7235315 (B2)

[18] I. Sánchez, *"Integración de sistemas de producción de hidrógeno en parques eólicos conectados a la red: configuraciones, estrategias de gestión y topologías de conversión electrónica"*, UPNA, España, 2013.

[19] Datasheet of the Boost IGBT: IGW50N60H3, 600 V high speed switching series third edition, Infeneon.

[20] Datasheet of the Boost diode: PCFF30S65W, 650 V, 30 A, Stealth™ .

ANNEX 1

POWER CONTROL PROGRAMS

In order to implement the power control explained in Chapter 5, a code is introduced in a “C-Block”.

1. BASIC POWER CONTROL

```
//POWER CONTROL

//Definition of parameters

        double Pref;
        double Ifc,Vfc,Pfc;
        static double counter=0;
        static double i=0;
        static double Iref;

        #define lim0 2179.6
        #define lim1 3865.6
        #define lim2 4466.5
        #define lim3 4778

        #define m0 108.7
        #define n0 29.87

        #define m1 84.3
        #define n1 519.6

        #define m2 60.09
        #define n2 1462

        #define m3 28.65
        #define n3 3034

//Input
```

```
        Pref=in[0];
        Vfc=in[1];
        Ifc=in[2];

//Control algorithm

        Pfc=Ifc*Vfc;
        if (Pref>lim3)
                Pref=lim3;
        counter=counter+delt;

//Initial value of Iref

        if (counter>0.005){
                counter=0;
                i=i+1;

                if (i<10){
                if (Pref<lim0){
                        Iref=(Pref-n0)/m0;}
                else
                        if (Pref<lim1){
                        Iref=(Pref-n1)/m1;}
                        else
                        if (Pref<lim2){
                                Iref=(Pref-n2)/m2;}
                        else
                                Iref=(Pref-n3)/m3;
                }
                Else
                if ((Pfc-Pref)>50)
                        Iref=Iref*0.98;
                if ((Pref-Pfc)>50)
                        Iref=Iref*1.02
        }

//Output
        out[0]=Iref;
        out[1]=Pfc;
```

2. MAXIMUM EFFICIENCY TRACKING CONTROL

```
// CONTROL ALGORITHM FOR FUEL CELLS CONNECTION

//Definition of Parameters

        double Pref,Pref_anterior=0;
        double Ifc,Vsystem,Psystem;
        static double contador=0;
        static double Iref;
        int Pila2=0,Pila3=0,Pila4=0;
        int num_pilas;
        static double i=0;


        //Maximum power that the system can give
                #define Pmax 5000

        //Powe limit for which the operating FCs pass of being 2 to 3
                #define lim2 1182

        //Powe limit for which the operating FCs pass of being 3 to 4
                #define lim3 1668.5

        //Iref generation when 2 FCs are operating
                #define m11 (3.141E-9)
                #define m12 (-6.2416E-6)
                #define m13 0.021681
                #define m14 (-0.69679)

        //Iref generation when 3 FCs are operating
                #define m21 (9.367E-10)
                #define m22 (-2.774E-6)
                #define m23 0.01445
                #define m24 (-0.69679)

        //Iref generation when 3 FCs are operating
                #define m31 (3.9263E-10)
                #define m32 (-1.56E-6)
                #define m33 0.01084
                #define m34 (-0.69679)

//Inputs

        Ifc=in[0];
        Vsystem=in[1];
```

```
        Pref=in[2];


//Control Algorithm

        Psystem=Ifc*Vsystem;
        if (Pref>Pmax){
                Pref=Pmax;}

        contador=contador+delt;

        if (contador>0.005){
                contador=0;

                   if (Pref==Pref_anterior){
                                if ((Psystem-Pref)>200)
                                        Iref=Iref-1;
                                if ((Pref-Psystem)>200)
                                        Iref=Iref+1;}

                   else{
                        if (Pref<lim2){
                          num_pilas=2;
                          Pila2=1;
                          Pila3=0;
                          Pila4=0;
                          Iref=(m11*(Pref*Pref*Pref))+(m12*(Pref*Pref))+(m13*Pref)+m14;}

                       else{
                          if (Pref<lim3){
                              num_pilas=3;
                              Pila2=1;
                              Pila3=1;
                              Pila4=0
                             Iref=(m21*(Pref*Pref*Pref))+(m22*(Pref*Pref))+(m23*Pref)+m24;}

                          else{
                              num_pilas=4;
                              Pila2=1;
                              Pila3=1;
                              Pila4=1;
                              Iref=(m31*(Pref*Pref*Pref))+(m32*(Pref*Pref))+(m33*Pref)+m34;}}

                Pref_anterior=Pref;}


//Output
        out[0]=Iref;
        out[1]=Pila2;
        out[2]=Pila3;
        out[3]=Pila4;
        out[4]=Psystem;
```

ANNEX 2

MATLAB PROGRAMATION

```
%% POTENCIAS Y RENDIMIENTOS
%% Datos reales
        load ('datos_IV')
        load ('datos_H2')
        load('ecuaciones') %(ecuaciones que aproximan la curva de potencia de hidrógeno y periféricos)

%% Potencia eléctrica
        Pe1=I1.*V1;
        Pe2=I2.*V2;
        Pe3=I3.*V3;
        Pe4=I4.*V4;
        Pe5=I5.*V5;

%% Potencia hidrógeno
        PCI=3;% Poder calorifico inferior del hidrogeno [kWh/Nm3]

        Ph2_1=f1*(60/1000)*PCI*1000;
        Ph2_2=f2*(60/1000)*PCI*1000;
        Ph2_3=f3*(60/1000)*PCI*1000;
        Ph2_4=f4*(60/1000)*PCI*1000;
        Ph2_5=f5*(60/1000)*PCI*1000;

        %Cálculo Ph2 para I1,I2,I3,I4,I5
                for i=1:length(I1)
                Ph21(i)=ecuacion1.coeff(1)*I1(i)+ecuacion1.coeff(2);%potencia hidrógeno para I1
                end
                for i=1:length(I2)
                Ph22(i)=ecuacion2.coeff(1)*I2(i)+ecuacion2.coeff(2);%potencia hidrógeno para I2
                end
                for i=1:length(I3)
                Ph23(i)=ecuacion3.coeff(1)*I3(i)+ecuacion3.coeff(2);%potencia hidrógeno para I3
                end
                for i=1:length(I4)
                Ph24(i)=ecuacion4.coeff(1)*I4(i)+ecuacion4.coeff(2);%potencia hidrógeno para I4
                end
                for i=1:length(I5)
                Ph25(i)=ecuacion5.coeff(1)*I5(i)+ecuacion5.coeff(2);%potencia hidrógeno para I5
                end

        %Función de I que aproxima la potencia de hidrógeno
                pendientepH2=[ecuacion1.coeff(1),ecuacion2.coeff(1),ecuacion3.coeff(1),ecuacion4.coeff(1),ecu
                acion5.coeff(1)];
                ordenadaspH2=[ecuacion1.coeff(2),ecuacion2.coeff(2),ecuacion3.coeff(2),ecuacion4.coeff(2),ec
                uacion5.coeff(2)];

                m_media=mean(pendientepH2);
                n_media=mean(ordenadaspH2);
```

```
for i=1:length(I1)
Ph2_med1(i)=m_media*I1(i)+n_media;%potencia hidrógeno para I1
end
for i=1:length(I2)
Ph2_med2(i)=m_media*I2(i)+n_media;%potencia hidrógeno para I5
end
for i=1:length(I3)
Ph2_med3(i)=m_media*I3(i)+n_media;%potencia hidrógeno para I5
end
for i=1:length(I4)
Ph2_med4(i)=m_media*I4(i)+n_media;%potencia hidrógeno para I5
end
for i=1:length(I5)
Ph2_med5(i)=m_media*I5(i)+n_media;%potencia hidrógeno para I5
end

%Cálculo de Ph2 TOTAL (suma de la potencia de hidrógeno de las pilas on)
pilas_total=4;
for i=1:length(I1)%Tª1
for pilas_conectadas=1:pilas_total
   Ph2total1(pilas_conectadas,i)=pilas_conectadas*Ph21(i);
end
end
for i=1:length(I2)%Tª2
for pilas_conectadas=1:4
   Ph2total2(pilas_conectadas,i)=pilas_conectadas*Ph22(i);
end
end
for i=1:length(I3)%Tª3
for pilas_conectadas=1:4
   Ph2total3(pilas_conectadas,i)=pilas_conectadas*Ph23(i);
end
end
for i=1:length(I4)%Tª4
for pilas_conectadas=1:4
   Ph2total4(pilas_conectadas,i)=pilas_conectadas*Ph24(i);
end
end
for i=1:length(I5)%Tª5
for pilas_conectadas=1:4
   Ph2total5(pilas_conectadas,i)=pilas_conectadas*Ph25(i);
end
end

%% Rendimiento
%Cálculo rendimiento para I1,I2,I3,I4,I5 SIN PERIFERICOS
for i=1:length(I1)
rend_pila1(i)=(Pe1(i)/Ph2_med1(i)*100);
end
for i=1:length(I2)
rend_pila2(i)=(Pe2(i)/Ph2_med2(i)*100);
end
for i=1:length(I3)
rend_pila3(i)=(Pe3(i)/Ph2_med3(i)*100);
end
for i=1:length(I4)
rend_pila4(i)=(Pe4(i)/Ph2_med4(i)*100);
end
for i=1:length(I5)
rend_pila5(i)=(Pe5(i)/Ph2_med5(i)*100);
end
```

```
%Cálculo del rendimiento TOTAL, CON PERIFERICOS
        pilas_total=4;
        for i=1:length(I1)%Tª1
        for pilas_conectadas=1:4
            rendimientototal1(pilas_conectadas,i)=100*(pilas_conectadas*Pe1(i)-(4-
        pilas_conectadas)*Pper(1))/(Ph2_med1(i)*pilas_conectadas);
        end
        end
        for i=1:length(I2)%Tª2
        for pilas_conectadas=1:4
            rendimientototal2(pilas_conectadas,i)=100*(pilas_conectadas*Pe2(i)-(4-
        pilas_conectadas)*Pper(1))/(Ph2_med2(i)*pilas_conectadas);
        end
        end
        for i=1:length(I3)%Tª3
        for pilas_conectadas=1:4
            rendimientototal3(pilas_conectadas,i)=100*(pilas_conectadas*Pe3(i)-(4-
        pilas_conectadas)*Pper(1))/(Ph2_med3(i)*pilas_conectadas);
        end
        end
        for i=1:length(I4)%Tª4
        for pilas_conectadas=1:4
            rendimientototal4(pilas_conectadas,i)=100*(pilas_conectadas*Pe4(i)-(4-
        pilas_conectadas)*Pper(1))/(Ph2_med4(i)*pilas_conectadas);
        end
        end
        for i=1:length(I5)%Tª5
        for pilas_conectadas=1:4
            rendimientototal5(pilas_conectadas,i)=100*(pilas_conectadas*Pe5(i)-(4-
        pilas_conectadas)*Pper(1))/(Ph2_med5(i)*pilas_conectadas);
        end
        end

%% Potencia periféricos
    %Cálculo Iper real
        ko=1.524;
        k1=-1.208*(10^-3);
        k2=4.118*(10^-4);
        for i=1:length(I1)
          Iper1(i)=k2*I1(i)^2+k1*I1(i)+ko;
        end
        for i=1:length(I2)
          Iper2(i)=k2*I2(i)^2+k1*I2(i)+ko;
        end
        for i=1:length(I3)
          Iper3(i)=k2*I3(i)^2+k1*I3(i)+ko;
        end
        for i=4:length(I4)
          Iper4(i)=k2*I4(i)^2+k1*I4(i)+ko;
        end
        for i=1:length(I5)
          Iper5(i)=k2*I5(i)^2+k1*I5(i)+ko;
        end

    %toma de datos manual(figura 9 articulo)
        Vfcper=[31,29.5,28.3,27.5,27,25.5,23.9,22.5,21];
        Ifcper=[0,5,10,15,20,30,40,50,60];

        for i=1:length(Ifcper)
          Iper(i)=k2*Ifcper(i)^2+k1*Ifcper(i)+ko;
          Pper(i)=Iper(i)*Vfcper(i);
        end
```

```
%Cálculo de la Pper para I1,I2,I3,I4,I5
        for i=1:length(I1)
        Pper1(i)=ecuacionper.coeff(1)*(I1(i))^3+ecuacionper.coeff(2)*(I1(i))^2+ecuacionper.coeff(3)*I1(i
        )+ecuacionper.coeff(4);
        end
        for i=1:length(I2)
        Pper2(i)=ecuacionper.coeff(1)*(I2(i))^3+ecuacionper.coeff(2)*(I2(i))^2+ecuacionper.coeff(3)*I2(i
        )+ecuacionper.coeff(4);
        end
        for i=1:length(I3)
        Pper3(i)=ecuacionper.coeff(1)*(I3(i))^3+ecuacionper.coeff(2)*(I3(i))^2+ecuacionper.coeff(3)*I3(i
        )+ecuacionper.coeff(4);
        end
        for i=1:length(I4)
        Pper4(i)=ecuacionper.coeff(1)*(I4(i))^3+ecuacionper.coeff(2)*(I4(i))^2+ecuacionper.coeff(3)*I4(i
        )+ecuacionper.coeff(4);
        end
        for i=1:length(I5)
        Pper5(i)=ecuacionper.coeff(1)*(I5(i))^3+ecuacionper.coeff(2)*(I5(i))^2+ecuacionper.coeff(3)*I5(i
        )+ecuacionper.coeff(4);
        end

%% Balance de pérdidas
    %Cálculo de Ppérdidas para I1,I2,I3,I4,I5
        for i=1:length(I1)
        Pperdidas1(i)=Ph21(i)-Pe1(i)-Pper1(i);
        end
        for i=1:length(I2)
        Pperdidas2(i)=Ph22(i)-Pe2(i)-Pper2(i);
        end
        for i=1:length(I3)
        Pperdidas3(i)=Ph23(i)-Pe3(i)-Pper3(i);
        end
        for i=1:length(I4)
        Pperdidas4(i)=Ph24(i)-Pe4(i)-Pper4(i);
        end
        for i=1:length(I5)
        Pperdidas5(i)=Ph25(i)-Pe5(i)-Pper5(i);
        end

%% GRÁFICA CURVA I-V MAS CONSUMO H2
    figure
    title('Curva I-V')
    hold all %gráfica de la tensión y corriente de la pila (Ifc,Vfc)
    plotyy(I1,V1,I1f,f1), xlabel('Ifc (A)'), ylabel('Vfc (V)')%Tª=58.7
    plotyy(I2,V2,I2f,f2)%Tª=56.5
    plotyy(I3,V3,I3f,f3)%Tª=52.8
    plotyy(I4,V4,I4f,f4)%Tª=41
    plotyy(I5,V5,I5f,f5)%Tª=31.5
    legend('Tª=58.7ºC','Tª=56.5ºC','Tª=52.8ºC','Tª=41ºC','Tª=31.5ºC')

    plot(I1f,f1)%gráfica del consumo de hidrógeno(NL min^-1) y la corriente
    plot(I2f,f2)
    plot(I3f,f3)
    plot(I4f,f4)
    plot(I5f,f5)

%% GRÁFICA RENDIMIENTO RESPECTO I
    figure %gráfica del rendimiento de la pila
    title ('1 PILA')
    hold all
    plot(I1,rend_pila1),xlabel('Ifc (A)'), ylabel('rendimiento')
    plot(I2,rend_pila2)
```

```
        plot(I3,rend_pila3)
        plot(I4,rend_pila4)
        plot(I5,rend_pila5,'r')

%% GRÁFICA POTENCIA ELÉCTRICA,HIDRÓGENO Y RENDIMIENTO
        figure
        title ('1 PILA')
        hold all
        plotyy(I1,Ph2_med1,I1,rend_pila1)%potencia de hidrógeno y rendimiento
        plotyy(I1,Ph2_med1,I2,rend_pila2)
        plotyy(I1,Ph2_med1,I3,rend_pila3)
        plotyy(I1,Ph2_med1,I4,rend_pila4)
        plotyy(I1,Ph2_med1,I5,rend_pila5)
        legend('Tª=58.7ºC','Tª=56.5ºC','Tª=52.8ºC','Tª=41ºC','Tª=31.5ºC')
%% GRÁFICA POTENCIA ELÉCTRICA, HIDRÓGENO, PER, PÉRDIDAS
        figure
        title ('1 PILA, POTENCIAS')
        hold all
        plotyy(I1,Ph2,Ifcper,Pper), xlabel('Corriente (A)'),ylabel('Potencia (W)')%potencia de hidrógeno

        plot(I1,Pe1,('b'))%potencia eléctrica
        plot(I2,Pe2,('g'))
        plot(I3,Pe3,('r'))
        plot(I4,Pe4,('c'))
        plot(I5,Pe5,('m'))

        plot(I1,Pperdidas1,('b'))%potencia pérdidas
        plot(I2,Pperdidas2,('g'))
        plot(I3,Pperdidas3,('r'))
        plot(I4,Pperdidas4,('c'))
        plot(I5,Pperdidas5,('m'))
        legend('Tª=58.7ºC','Tª=56.5ºC','Tª=52.8ºC','Tª=41ºC','Tª=31.5ºC')

%%%%%%%%%%%%%%%%%%%%%%%%%%%%%%%%%%%%%%%%%%%%%%%%%%%%%%%%%%%%%%%%%%%%%%%%%%%%%%%
%% CONEXIÓN DE PILAS
%%%%%%%%%%%%%%%%%%%%%%%%%%%%%%%%%%%%%%%%%%%%%%%%%%%%%%%%%%%%%%%%%%%%%%%%%%%%%%%
%% 1 PILA
%GRÁFICA pH2 y rendimiento frente a potencia eléctrica
        figure
        hold all
        plotyy(Pe1,rend_pila1,Pe1,Ph2), xlabel('Pe (W)'), ylabel('Rendimiento (%)')
        plotyy(Pe2,rend_pila2,Pe1,Ph2)
        plotyy(Pe3,rend_pila3,Pe1,Ph2)
        plotyy(Pe4,rend_pila4,Pe1,Ph2)
        plotyy(Pe5,rend_pila5,Pe1,Ph2)
        legend('Tª=58.7ºC','Tª=56.5ºC','Tª=52.8ºC','Tª=41ºC','Tª=31.5ºC')
        title('1 PILA')

%% 4 EN SERIE
        figure
        hold all
        plotyy(Pe1*4,Ph2_med1*4,Pe1*4,rend_pila1)
        plotyy(Pe1*4,Ph2_med1*4,4*Pe2,rend_pila2)
        plotyy(Pe1*4,Ph2_med1*4,4*Pe3,rend_pila3)
        plotyy(Pe1*4,Ph2_med1*4,4*Pe4,rend_pila4)
        plot(Pe1*4,Ph2_med1*4,Pe5*4,rend_pila5)
        xlabel('Pe (W)'),ylabel('Ph2')
        title('4PILAS')

%% 4PILAS SIN CONSIDERAR CONSUMO PERIFERICOS en las pilas en off
        %Rendimiento
                figure
                title('RENDIMIENTO sin considerar el consumo de perifericos en pilas off')
```

```
hold all
legend('Tª=58.7ºC','Tª=56.5ºC','Tª=52.8ºC','Tª=41ºC','Tª=31.5ºC')
plot(Pe1*4,rend_pila1,('b'))%T1
plot(3*Pe1,rend_pila1,('b'))
plot(2*Pe1,rend_pila1,('b'))
plot(1*Pe1,rend_pila1,('b'))

plot(Pe2*4,rend_pila2,('g'))%T2
plot(3*Pe2,rend_pila2,('g'))
plot(2*Pe2,rend_pila2,('g'))
plot(1*Pe2,rend_pila2,('g'))

plot(Pe3*4,rend_pila3,('r'))%T3
plot(3*Pe3,rend_pila3,('r'))
plot(2*Pe3,rend_pila3,('r'))
plot(1*Pe3,rend_pila3,('r'))
plot(Pe4*4,rend_pila4,('c'))%T4
plot(3*Pe4,rend_pila4,('c'))
plot(2*Pe4,rend_pila4,('c'))
plot(1*Pe4,rend_pila4,('c'))
plot(Pe5*4,rend_pila5,('m'))%T5
plot(3*Pe5,rend_pila5,('m'))
plot(2*Pe5,rend_pila5,('m'))
plot(1*Pe5,rend_pila5,('m'))
xlabel('Pe (w)'), ylabel('Rendimiento (%)')

figure
title('RENDIMIENTO sin considerar el consumo de perifericos en pilas off')
subplot(1,5,1),plot(Pe1*4,rend_pila1,'-r'),hold on, plot(Pe1*3,rend_pila1,'-
c'),plot(Pe1*2,rend_pila1,'-g'),plot(Pe1,rend_pila1,'-b'), title(' Tª=58.7 ºC' ), xlabel('Pe
(W)'),ylabel('Rendimiento (%)')
axis([0 5000 0 60])
subplot(1,5,2),plot(Pe2*4,rend_pila2,'-r'),hold on, plot(Pe2*3,rend_pila2,'-
c'),plot(Pe2*2,rend_pila2,'-g'),plot(Pe2,rend_pila2,'-b'), title(' Tª=56.5 ºC ' ), xlabel('Pe (W)')
axis([0 5000 0 60])
subplot(1,5,3),plot(Pe3*4,rend_pila3,'-r'),hold on, plot(Pe3*3,rend_pila3,'-
c'),plot(Pe3*2,rend_pila3,'-g'),plot(Pe3,rend_pila3,'-b') ,title(' Tª=52.8 ºC ' ), xlabel('Pe (W)')
axis([0 5000 0 60])
subplot(1,5,4),plot(Pe4*4,rend_pila4,'-r'),hold on, plot(Pe4*3,rend_pila4,'-
c'),plot(Pe4*2,rend_pila4,'-g'),plot(Pe4,rend_pila4,'-b'), title(' Tª=41 ºC' ), xlabel('Pe (W)')
axis([0 5000 0 60])
subplot(1,5,5),plot(Pe5*4,rend_pila5,'-r'),hold on, plot(Pe5*3,rend_pila5,'-
c'),plot(Pe5*2,rend_pila5,'-g'),plot(Pe5,rend_pila5,'-b'), title(' Tª=31.5 ºC' ), xlabel('Pe (W)')
axis([0 5000 0 60])
legend('4pilas','3pilas','2pilas','1pila')

%Potencia hidrógeno
figure
title('POTENCIA HIDRÓGENO sin pper')
plot(Pe1*4,Ph2*4,'-r'),hold on, plot(Pe1*3,Ph2*3,'-c'),plot(Pe1*2,Ph2*2,'-g'),plot(Pe1,Ph2,'-b'),
xlabel('Pe (W)'), ylabel('Potencia Hidrógeno(W)')
legend('4pilas','3pilas','2pilas','1pila')

%% 4PILAS CONSIDERANDO CONSUMO PERIFERICOS
%Rendimiento
figure
title('RENDIMIENTO  consumo de perifericos en pilas off')
for pilas_conectadas=1:4
hold all
plot(Pe1*pilas_conectadas,rendimientototal1(pilas_conectadas,:),('b')),
plot(Pe2*pilas_conectadas,rendimientototal2(pilas_conectadas,:),('g')),
plot(Pe3*pilas_conectadas,rendimientototal3(pilas_conectadas,:),('r')),
plot(Pe4*pilas_conectadas,rendimientototal4(pilas_conectadas,:),('c')),
```

```
        plot(Pe5*pilas_conectadas,rendimientototal5(pilas_conectadas,:),('m')),legend(),xlabel('Pfc
        (W)'), ylabel('Rendimiento (%)')
        legend('Tª=58.7ºC','Tª=56.5ºC','Tª=52.8ºC','Tª=41ºC','Tª=31.5ºC')
        end

        figure
        title('RENDIMIENTO 4 PILAS considerando consumo de perifericos en pilas off')
        subplot(1,5,1),plot(Pe1*4,rendimientototal1(4,:),'-r'),hold on,
        plot(Pe1*3,rendimientototal1(3,:),'-c'),plot(Pe1*2,rendimientototal1(2,:),'-
        g'),plot(Pe1,rendimientototal1(1,:),'-b'), title(' Tª=58.7 ºC' ), xlabel('Pe (W)'), ylabel('Rendimiento
        (%)')
        axis([0 5000 0 60])
        subplot(1,5,2),plot(Pe2*4,rendimientototal2(4,:),'-r'),hold on,
        plot(Pe2*3,rendimientototal2(3,:),'-c'),plot(Pe2*2,rendimientototal2(2,:),'-
        g'),plot(Pe2,rendimientototal2(1,:),'-b'), title(' Tª=56.5 ºC ' ), xlabel('Pe (W)')
        axis([0 5000 0 60])
        subplot(1,5,3),plot(Pe3*4,rendimientototal3(4,:),'-r'),hold on,
        plot(Pe3*3,rendimientototal3(3,:),'-c'),plot(Pe3*2,rendimientototal3(2,:),'-
        g'),plot(Pe3,rendimientototal3(1,:),'-b') ,title(' Tª=52.8 ºC ' ), xlabel('Pe (W)')
        axis([0 5000 0 60])
        subplot(1,5,4),plot(Pe4*4,rendimientototal4(4,:),'-r'),hold on,
        plot(Pe4*3,rendimientototal4(3,:),'-c'),plot(Pe4*2,rendimientototal4(2,:),'-
        g'),plot(Pe4,rendimientototal4(1,:),'-b'), title(' Tª=41 ºC' ), xlabel('Pe (W)')
        axis([0 5000 0 60])
        subplot(1,5,5),plot(Pe5*4,rendimientototal5(4,:),'-r'),hold on,
        plot(Pe5*3,rendimientototal5(3,:),'-c'),plot(Pe5*2,rendimientototal5(2,:),'-
        g'),plot(Pe5,rendimientototal5(1,:),'-b'), title(' Tª=31.5 ºC' ), xlabel('Pe (W)')
        axis([0 5000 0 60])

    %Potencia hidrogeno
        title('POTENCIA HIDRÓGENO con pper')
        figure
        for pilas_conectadas=1:4
        hold all
        plot(Pe1*pilas_conectadas-(4-
        pilas_conectadas)*Pper(1),Ph2total1(pilas_conectadas,:)),xlabel('Pfc (W)'), ylabel('Ph2 (W)')
        end
        legend('1pila','2pilas','3pilas','4pilas')

%% GRÁFICO CORRIENTE IFC REFERENCIA
    figure
    for pilas_conectadas=1:4
    hold all
    plot(Pe1*pilas_conectadas,I1,('b'))
    plot(Pe2*pilas_conectadas,I2,('g'))
    plot(Pe3*pilas_conectadas,I3,('r'))
    plot(Pe4*pilas_conectadas,I4,('c'))
    plot(Pe5*pilas_conectadas,I5,('m')),xlabel('Pe (W)'), ylabel('Corriente pila(A)')
    legend('Tª=58.7ºC','Tª=56.5ºC','Tª=52.8ºC','Tª=41ºC','Tª=31.5ºC')
    end

%%GRÁFICO 3D
    %Vectores de Ifc y Vfc
        Ifc=[0,5,10,20,30,40,50,55,60];
        Vfc=[32,30.3,29.25,27.6,26.05,24.4,22.56,21.62,20.54;
        32,30.23,29.1,27.35,25.7,24,22.1,21.15,20.06;
        32,30.04,28.87,27.14,25.57,23.82,21.9,20.86,19.6;
        32,29.98,28.8,26.94,25.29,23.59,21.67,20.67,19.3;
        32,29.76,28.54,26.73,25.03,23.22,21.29,20.29,18.8];


    Temperature=[58.7,56.5,52.8,41,31.5];
```

```
for i=1:5
   for j=1:length(Ifc)
      Pfc(i,j)=Ifc(1,j)*Vfc(i,j);
   end
end

%Función de I que aproxima la potencia de hidrógeno
pendientepH2=[ecuacion1.coeff(1),ecuacion2.coeff(1),ecuacion3.coeff(1),ecuacion4.coeff(1),ecu
acion5.coeff(1)];
ordenadaspH2=[ecuacion1.coeff(2),ecuacion2.coeff(2),ecuacion3.coeff(2),ecuacion4.coeff(2),ec
uacion5.coeff(2)];


m_media=mean(pendientepH2);
n_media=mean(ordenadaspH2);


for i=1:length(Ifc)
Ph2(i)=m_media*Ifc(i)+n_media;
end

%% Rendimiento
%Cálculo rendimiento, apagando pilas(SIN PERIFERICOS)
%Para 1, 2, 3 y 4 pilas

   for i=1:5
      for j=1:length(Ifc)
         rend1(i,j)=(Pfc(i,j)/Ph2(1,j)*100);
         rend2(i,j)=(2*Pfc(i,j)/(2*Ph2(1,j))*100);
         rend3(i,j)=(3*Pfc(i,j)/(3*Ph2(1,j))*100);
         rend4(i,j)=(4*Pfc(i,j)/(4*Ph2(1,j))*100);
      end
   end


figure
hold on
 surf(1*Pfc,Temperature,rend1)
 surf(2*Pfc,Temperature,rend2)
 surf(3*Pfc,Temperature,rend3)
 surf(4*Pfc,Temperature,rend4)
```

ANNEX 3

FINAL STRUCTURE SIMULATION

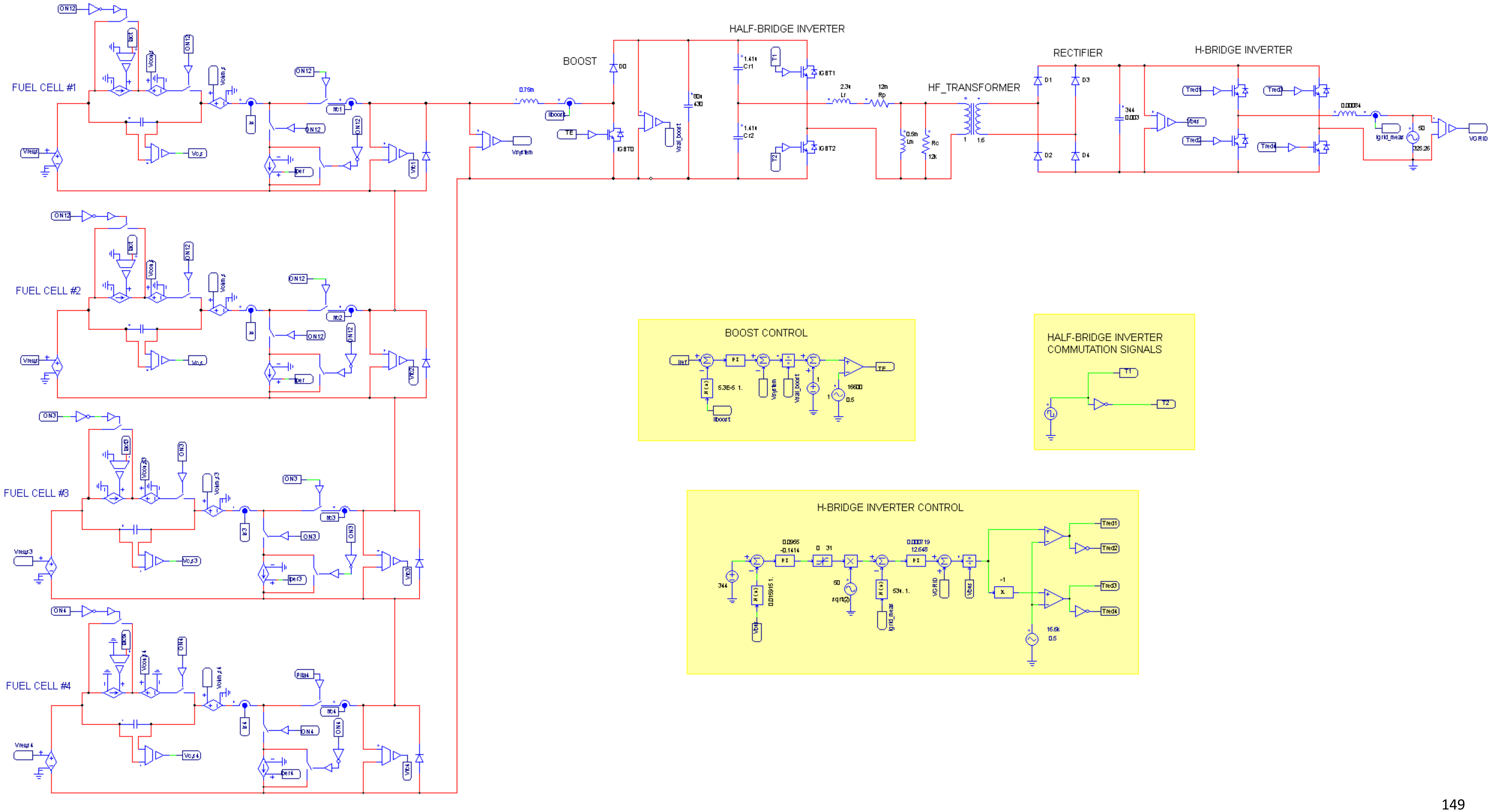

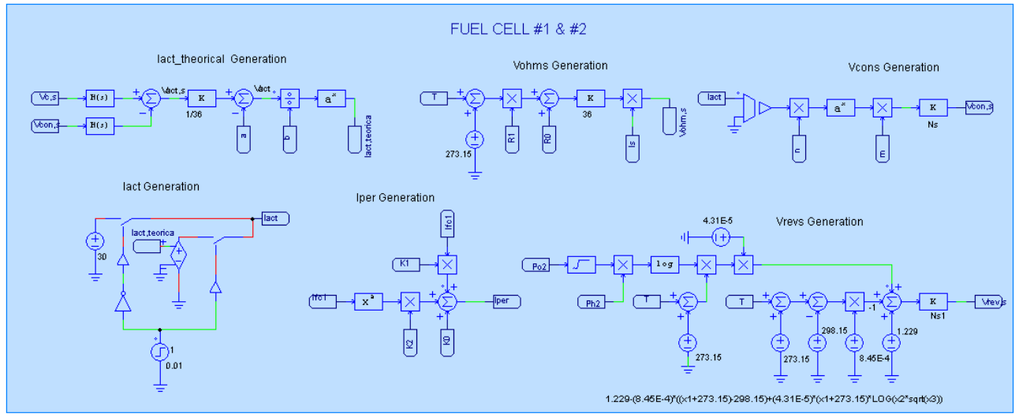
FUEL CELL #1 & #2
Iact_theorical Generation
Vohms Generation
Vcons Generation
Iact Generation
Iper Generation
Vrevs Generation
1.229-(8.45E-4)*((x1+273.15)-298.15)+(4.31E-5)*(x1+273.15)*LOG(x2*sqrt(x3))

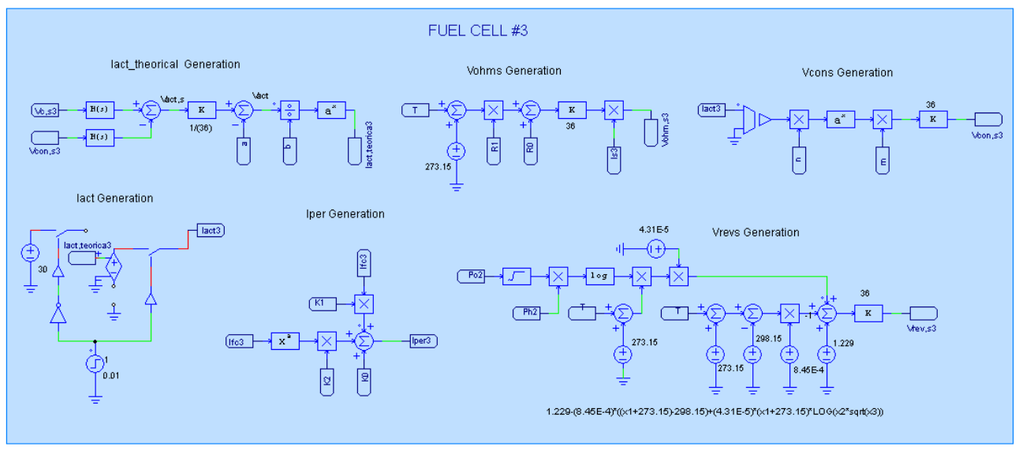
FUEL CELL #3
Iact_theorical Generation
Vohms Generation
Vcons Generation
Iact Generation
Iper Generation
Vrevs Generation
1.229-(8.45E-4)*((x1+273.15)-298.15)+(4.31E-5)*(x1+273.15)*LOG(x2*sqrt(x3))

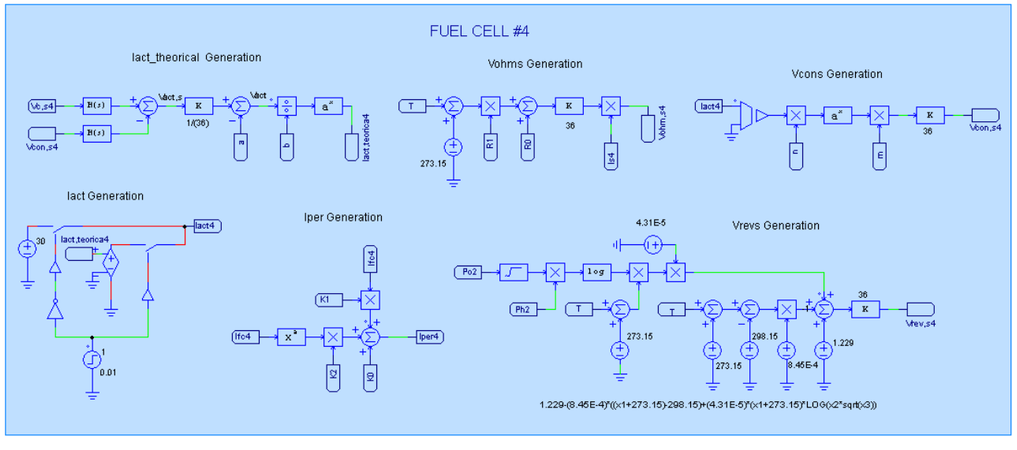
FUEL CELL #4
Iact_theorical Generation
Vohms Generation
Vcons Generation
Iact Generation
Iper Generation
Vrevs Generation
1.229-(8.45E-4)*((x1+273.15)-298.15)+(4.31E-5)*(x1+273.15)*LOG(x2*sqrt(x3))

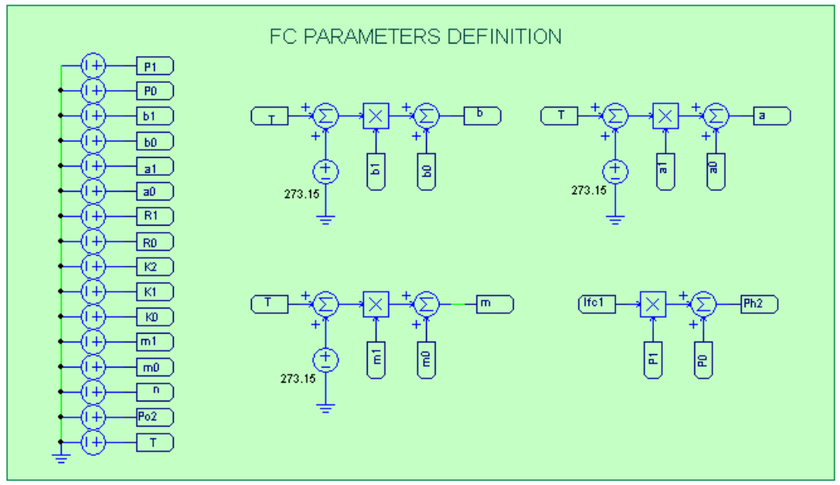
FC PARAMETERS DEFINITION
P1
P0
b1
b0
a1
a0
R1
R0
K2
K1
K0
m1
m0
n
Po2
T

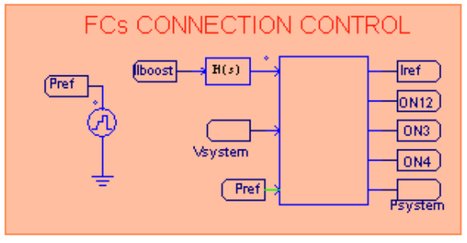
FCs CONNECTION CONTROL
Pref
Iboost
H(s)
Vsystem
Pref
Iref
ON12
ON3
ON4
Psystem